Asia-Pacific
Economic Cooperation

Proceedings of SAKE-2 Workshop

The Second APEC SAKE Workshop on
Satellite Application on Fishery and Coastal Ecosystem (SAFE)

Jakarta, November 5~8, 2007

Sponsors

Asia-Pacific Economic Cooperation, Marine Resource Conservation Working Group
Agency for the Assessment and Application of Technology (BPPT), Indonesia
Agency for Marine and Fisheries Research (BRKP), Indonesia
Environment Protection Administration, Chinese Taipei

Co-organized by

Agency for the Assessment and Application of Technology (BPPT), Indonesia
Agency for Marine and Fisheries Research (BRKP), Indonesia
Institute of Oceanography, National Taiwan University

Hosted by

Agency for the Assessment and Application of Technology (BPPT), Indonesia

SAKE is APEC-sponsored project "Satellite Applications on Knowledge-based Economy"

October 2008

Proceedings of SAKE-2 Workshop
The Second APEC SAKE Workshop on "Satellite Application on Fishery and Coastal Ecosystem (SAFE)"
SAKE is APEC-sponsored project "Satellite Applications on Knowledge-based Economy"

Published for APEC Marine Resource Conservation Working Group
APEC Project No.: MRC 05/2007

Prepared by
Prof. Chia Chuen Kao
Coastal Ocean Monitoring Center (COMC)
National Cheng Kung University
Tainan, Chinese Taipei
Tel/Fax: +886-6-209-8850 / +886-209-8853
http:/sol.oc.ntu.edu.tw/sake/index.htm

Produced for
Asia-Pacific Economic Cooperation Secretariat
35 Heng Mul Keng Terrace Singapore 119616
Tel:(65)6891-9600; Fax:(65)6891-9690
e-mail:info@apec.org website:www.apec.org

©(2008) APEC Secretart

APEC#208-MR-04.2

Proceedings of SAKE-2 Workshop

The Second APEC SAKE Workshop on
Satellite Application on Fishery and Coastal Ecosystem (SAFE)

Jakarta, November 5~8, 2007

APEC Marine Resource Conservation Working Group Project:
Satellite Applications on Knowledge-based Economy

Project Overseer

Dr. Y. F. Liang

Advisor to International Affairs
Environmental Protection Administration
Chinese Taipei

Organizing Committee

Co-Chairs

Dr. NANI Hendiarti

Agency for the Assessment and Application of Technology (BPPT).
Bldg. II, 18th Floor, Jl. M.H. Thamrin No. 8
Jakarta 10340, Indonesia.
Tel:+ 62-21-3169690
hendiarti@webmail.bppt.go.id

Prof. Cho-Teng LIU

Institute of Oceanography
National Taiwan University
Taipei, POB 23-13
work: +886-2-2362-0624
fax: +886-945-864-043
mobile: +886-915-003-185
ctliu@ntu.edu.tw

Mr. Berny A. Subki, MSc

Research Center for Marine Technology
Agency for Marine and Fisheries Research (BRKP)
Ministry of Marine Affairs and Fisheries (DKP)
Jl. M.T. Haryono Kav. 52-53
Jakarta 12770, Indonesia
bernysubki@hotmail.com

Opening Speech

Dear Chairman of Agency for Marine and Fisheries Research; Friends and Colleagues, Ladies and Gentlemen, Good morning!

It is a great pleasure for us to host this "second **APEC SAKE** (Satellite Applications on Knowledge-based Economy)". I would like to express our warm welcome to all of you, especially to the Delegation from National Taiwan University, National Cheng Kung University, Vietnam National University, University of the Philippines, Tokyo University, Nagoya University, Collect Localisation Satellite, ITB, and LIPI.

SAKE project started since 2006, it is the continuation of OMISAR project. The objective of this workshop is to give the opportunity to draw together the researches and stakeholders of the Asia Pacific countries and to promote application of satellite remote sensing for marine conservation and ocean resources sustainability. This program consists of 2 workshop days and 2 days of technical tour to Banten area. This workshop is in cooperation of BRKP –DKP.

I have been informed that SAKE project will continue until 2008 with the focus of activity in the Derawan Island in South Kalimantan and Pangkajene Islands in South Sulawesi. The objective is to develop algorithm for coral reef and seaweed mapping using the Formosat-2 satellite and hyperspectral images. These activities will be beneficial for efforts in monitoring the coastal ecosystem, identification of marine resources and support the local community in preserving the habitat.

In this opportunity, I would like to thank to all organizer committee members from BPPT, to all organizations and all sponsors who have provided their effort to make this workshop become a success. I hope this workshop will help greatly increase the capability and knowledge of the scientists on very high resolution images and to expose the capability of hyperspectral technology to support natural resources management in Indonesia.

I also hope the cooperation between BPPT and Institutions of Chinese Taipei does not stop here, but will continue in the next coming year.

Finally, I wish this workshop a great success and wish you a good time in Jakarta. And with saying Bismillahirahmanirahim, the second APEC Satellite Applications on Knowledge-based Economy workshop is officially opened.

Thank you.

Prof. Ir. Said D. Jenie, Sc.D.
Head of Agency For the Assessment and Application of Technology (BPPT)
Republic of Indonesia
Jakarta, 5 November 2007

Welcome Speech

Dr. Indroyono Soesilo
Lead Shepherd, APEC Marine Resources Working Group

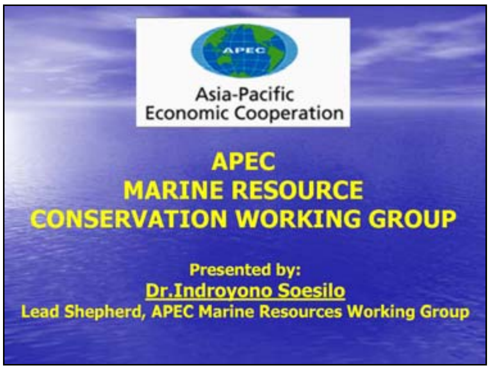

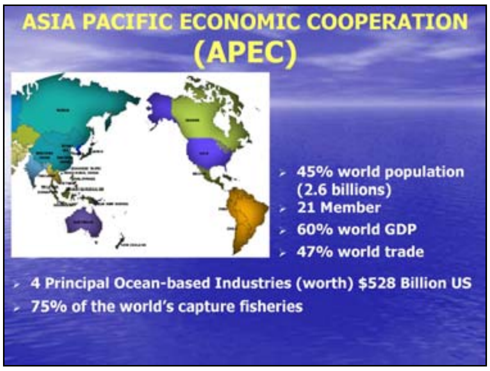

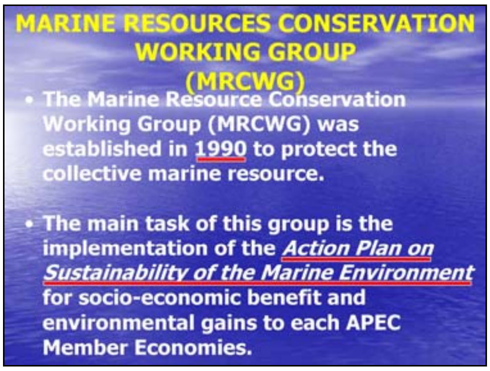

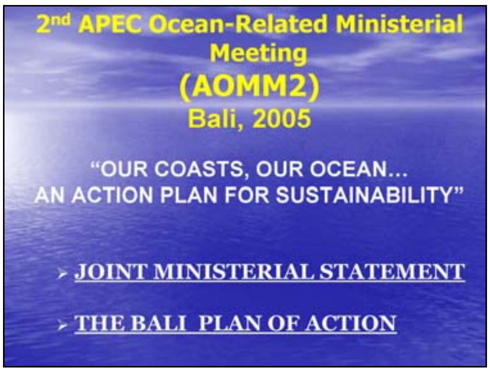

2007 APEC-MRCWG Projects

No	Description	Proposing Economy
1	Tsunami Preparedness and Resilience through Research, Extension, Education and Training.	Indonesia
2	Understanding the economic benefits and costs of controlling marine debris in the APEC region.	Australia
3	Marine Ecosystem Identification and Mapping in the Asia-Pacific Region	USA
4	Capacity Building Workshops on Marine Environmental Conservation and Sustainability for Developing Economies of APEC	Republic of Korea
5	Satellite Application in Knowledge-based Economies (SAKE 2007)	Chinese Taipei
6	Development of an APEC Strategy on Sustainable Aquaculture	Chile

Coral Triangle "Amazon of the Seas": 75.000 Sq-Kilometer, 6 Countries approx. 500 coral reef species, approx. 3000 fish species, 120 million peopole, US$2.3 Billions Economy/Year

APEC-MRCWG NUMBERS OF PROJECTS 2005 – 2008

2005 : 3 Projects,

2006 : 3 Projects,

2007 : 6 Projects,

2008 : 2 Projects (Korea & Chinese Taipei)

What are MRCWG Expectation from SAKE Project ?

- ✓Implement THE BALI PLAN OF ACTION,
- ✓Implement The APEC Leader's Declaration on Coral Triangle Initative,
- ✓Implement the SAKE Project to support the Climate Change Program (Global Warming, Sea Level Rise, El Nino, La Nina)

GLOBAL DISTRIBUTION OF CORAL

The Pacific Ocean, particulary the Southwest Pacific Ocean, is the place of the highest coralreef diversity in the world. "The Amazon of the Seas". It must be rehabilitate, manage, conserve and preserve.

✓MRCWG Lead Shepherd Contact Address

Lead Shepherd
Dr. Indroyono Soesilo
Jl. Pasir Putih 1
Jakarta Utara
Phone: +62 21 647 115 83
Fax: +62 21 647 116 85

Contact Person
Dr. Tonny Wagey
Jl. Pasir Putih 1,
Jakarta Utara
Phone: +62 21 647 115 83
Fax: +62 21 647 116 85
Email: t.wagey@fisheries.ubc.ca

APEC
Asia-Pacific Economic Cooperation

SYDNEY APEC LEADERS' DECLARATION ON CLIMATE CHANGE, ENERGY SECURITY AND CLEAN DEVELOPMENT

Sydney, Australia, 9 September 2007

Marine and coastal resources

Sustainable marine and coastal resources are an integral part of the carbon cycle. We therefore:

- welcome the Coral Triangle Initiative on Coral Reefs, Fisheries and Food Security which is aimed at enhancing the conservation of marine biological resources.

THANK YOU

A Strategic Approach to Oceans Management For Sustainability Together

Contents

Mapping of Inland and Underwater Habitats with Satellite Images

Tu Tuyet Hong, Nguyen Phi Khu
University Technical Education, HCMC

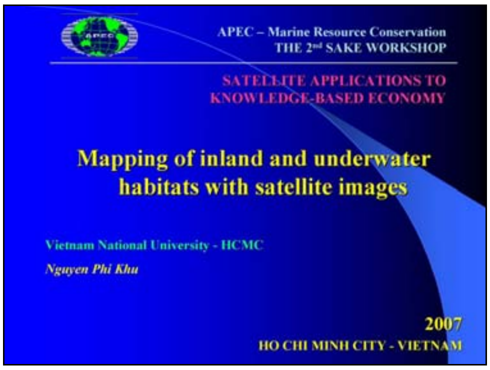

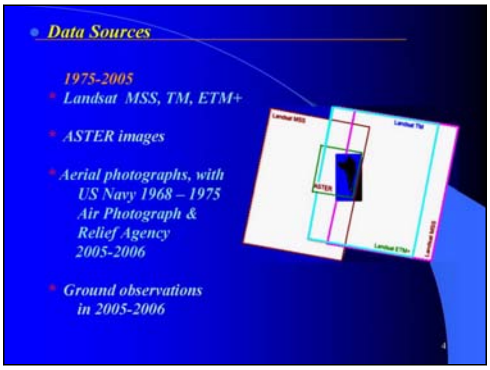

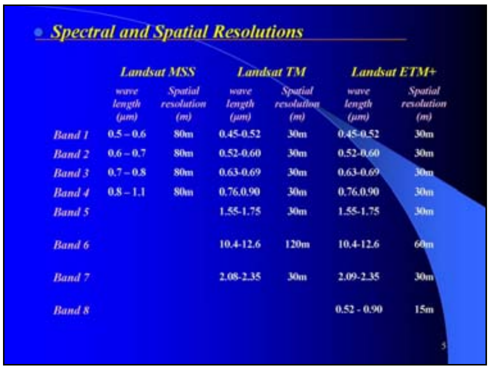

	Landsat MSS		Landsat TM		Landsat ETM+	
	wave length (μm)	Spatial resolution (m)	wave length (μm)	Spatial resolution (m)	wave length (μm)	Spatial resolution (m)
Band 1	0.5 – 0.6	80m	0.45-0.52	30m	0.45-0.52	30m
Band 2	0.6 – 0.7	80m	0.52-0.60	30m	0.52-0.60	30m
Band 3	0.7 – 0.8	80m	0.63-0.69	30m	0.63-0.69	30m
Band 4	0.8 – 1.1	80m	0.76.0.90	30m	0.76.0.90	30m
Band 5			1.55-1.75	30m	1.55-1.75	30m
Band 6			10.4-12.6	120m	10.4-12.6	60m
Band 7			2.08-2.35	30m	2.09-2.35	30m
Band 8					0.52 - 0.90	15m

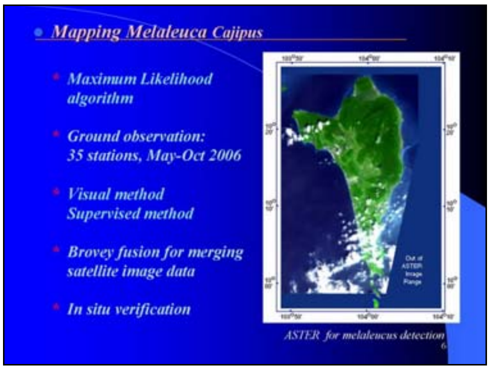

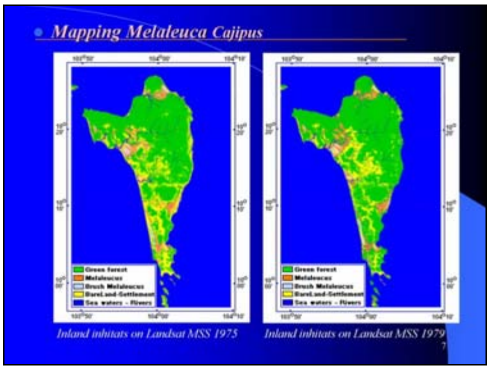

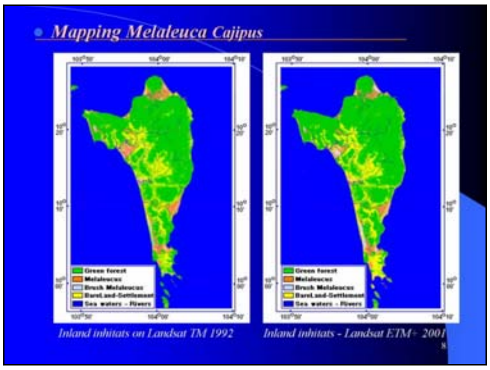

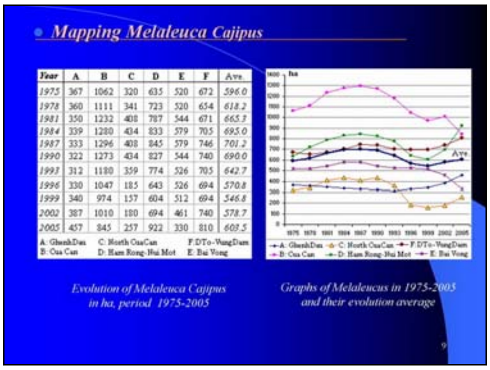

Year	A	B	C	D	E	F	Ave.
1975	367	1062	320	635	520	672	596.0
1978	360	1111	341	723	520	654	618.2
1981	350	1232	408	787	544	671	665.3
1984	339	1280	434	833	579	705	695.0
1987	333	1296	408	845	579	746	701.2
1990	322	1273	434	827	544	740	690.0
1993	312	1180	359	774	526	705	642.7
1996	330	1047	185	643	526	694	570.8
1999	340	974	157	604	512	694	546.8
2002	387	1010	180	694	461	740	578.7
2005	457	845	257	922	330	810	603.5

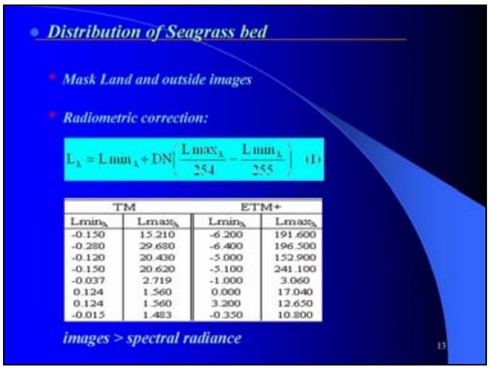

$$L_\lambda = L\min_\lambda + DN\left(\frac{L\max_\lambda}{254} - \frac{L\min_\lambda}{255}\right) \quad (1)$$

TM		ETM+	
$Lmin_\lambda$	$Lmax_\lambda$	$Lmin_\lambda$	$Lmax_\lambda$
-0.150	15.210	-6.200	191.600
-0.280	29.680	-6.400	196.500
-0.120	20.430	-5.000	152.900
-0.150	20.620	-5.100	241.100
-0.037	2.719	-1.000	3.060
0.124	1.560	0.000	17.040
0.124	1.560	3.200	12.650
-0.015	1.483	-0.350	10.800

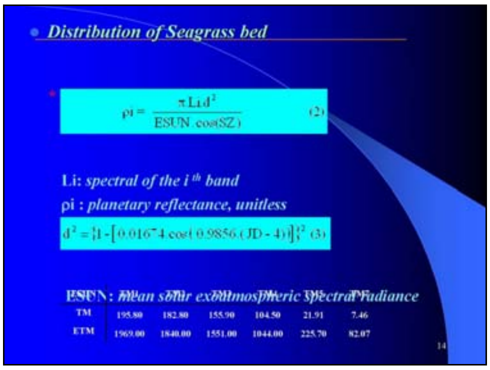

$$\rho i = \frac{\pi Li d^2}{ESUN \cos(SZ)} \quad (2)$$

$$d^2 = \{1 - [0.01674 \cos(0.9856(JD - 4))]\}^2 \quad (3)$$

TM	195.80	182.80	155.90	104.50	21.91	7.46
ETM	1969.00	1840.00	1551.00	1044.00	225.70	82.07

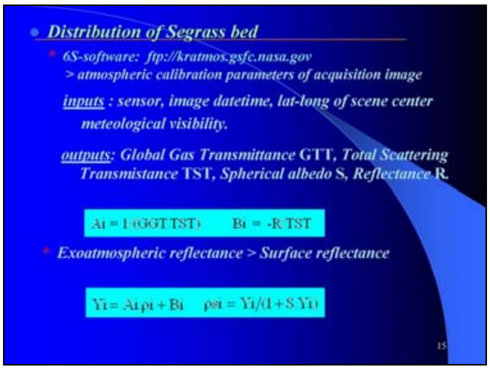
Distribution of Segrass bed
6S-software: ftp://kratmos.gsfc.nasa.gov
> atmospheric calibration parameters of acquisition image
inputs : sensor, image datetime, lat-long of scene center meteological visibility.
outputs: Global Gas Transmittance GTT, Total Scattering Transmistance TST, Spherical albedo S, Reflectance R.
Ai = 1/(GGT.TST)   Bi = -R.TST
Exoatmospheric reflectance > Surface reflectance
Yi = Ai ρi + Bi   ρsi = Yi/(1+S.Yi)
15

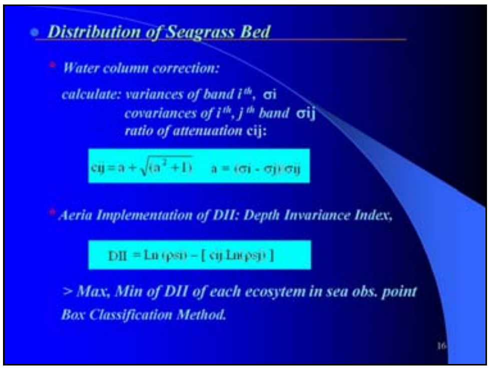
Distribution of Seagrass Bed
Water column correction:
calculate: variances of band i th, σi
covariances of i th, j th band σij
ratio of attenuation cij:
cij = a + √(a² + 1)   a = (σi - σj)/σij
Aeria Implementation of DII: Depth Invariance Index,
DII = Ln (ρsi) – [cij.Ln(ρsj)]
> Max, Min of DII of each ecosytem in sea obs. point
Box Classification Method.
16

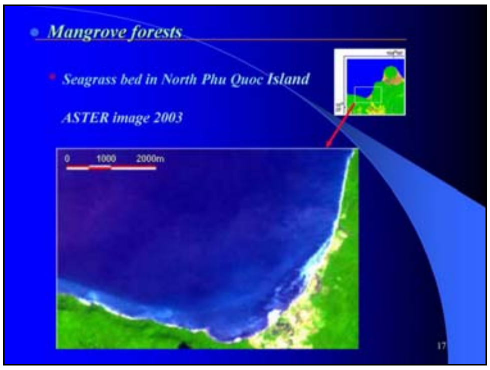
Mangrove forests
Seagrass bed in North Phu Quoc Island
ASTER image 2003
0 1000 2000m
17

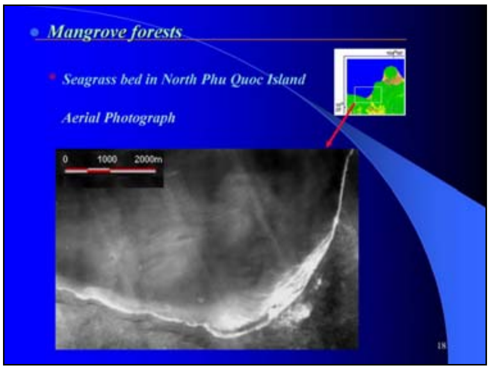
Mangrove forests
Seagrass bed in North Phu Quoc Island
Aerial Photograph
0 1000 2000m
18

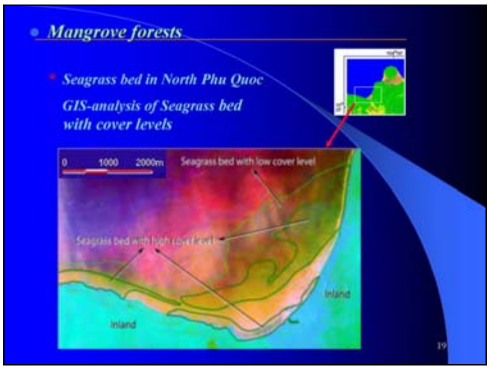
Mangrove forests
Seagrass bed in North Phu Quoc
GIS-analysis of Seagrass bed with cover levels
0 1000 2000m
Seagrass bed with low cover level
Seagrass bed with high cover level
Inland
Inland
19


Mangrove forests
Seagrass bed and Coral reef in North Phu Quoc
Regions | Distributed area (ha)
East of Ghenh dau | 1120
North of Ham Rong | 1045
Nui Mot | 520
Ham Ninh | 6010
Bai Vong | 827
North of Ong Doi Cape | 80
South of Ong Doi Cape | 195
Total: | 9797
A Distribution of Seagrass bed aeras in costal zones
20

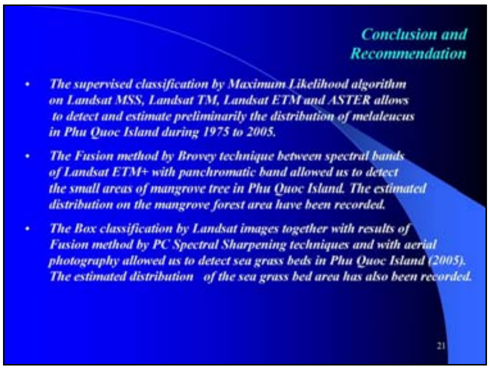
Conclusion and Recommendation
The supervised classification by Maximum Likelihood algorithm on Landsat MSS, Landsat TM, Landsat ETM and ASTER allows to detect and estimate preliminarily the distribution of melaleucus in Phu Quoc Island during 1975 to 2005.
The Fusion method by Brovey technique between spectral bands of Landsat ETM+ with panchromatic band allowed us to detect the small areas of mangrove tree in Phu Quoc Island. The estimated distribution on the mangrove forest area have been recorded.
The Box classification by Landsat images together with results of Fusion method by PC Spectral Sharpening techniques and with aerial photography allowed us to detect sea grass beds in Phu Quoc Island (2005). The estimated distribution of the sea grass bed area has also been recorded.
21

Reef Connectivity: A Study of Larval Dispersal in Sulu Sea

Marites M. Magno-Canto[1], Cesar L. Villanoy[1], Olivia C. Cabrera[1], Wilfredo L. Campos[2], Pacifico D. Beldia[2] and Laura David[1]
[1]The Marine Science Institute, University of the Philippines, Diliman, Quezon City 1101
[2]Oceanbio Laboratory, Division of Biological Sciences, University of the Philippines in the Visayas, Miagao, Iloilo

Reef connectivity: a study of larval dispersal in Sulu Sea

Marites M. Magno-Canto[1], Cesar L. Villanoy[1], Olivia C. Cabrera[1], Wilfredo L. Campos[2], Pacifico D. Beldia[2] and Laura David[1]
[1]The Marine Science Institute, University of the Philippines, Diliman, Quezon City 1101
[2]Oceanbio Laboratory, Division of Biological Sciences, College of Arts and Science, University of the Philippines in the Visayas, Miagao, Iloilo

Objectives

- To quantify potential exchange of larvae between Sulu Sea and neighboring areas and between areas within Sulu Sea
- Compare patterns of larval dispersal between particles with (active) and without (passive) swimming ability
- Compare and assess settlement success between larvae with short (15 days) and long (30 days) pelagic larval duration (PLD)
- Estimate the degree of local settlement based on dispersal simulations

Sulu Sea Dynamics

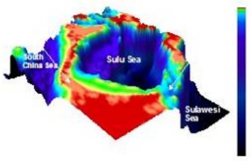

➢Semi-enclosed basin

➢Connections considered as important "marine corridors"

Questions:

•How much connection does Sulu Sea has with neighboring basins (e.g., KIG in SCS)?

Methodology

Hydrodynamic Circulation for Sulu Sea

- Surface velocities derived from HYbrid Coordinate Ocean Model (HYCOM, http://hycom.rsmas.miami.edu/hycom-model/index.html)
  - Hybrid coordinate is one that is isopycnal in the open, stratified ocean, but smoothly reverts to a terrain-following coordinate in shallow coastal regions, and to z-level coordinates in the mixed layer and/or unstratified seas
- Grid size is 5 minute (9km x 9km) resolution
- Vectors for January, April, August and October

What is connectivity?

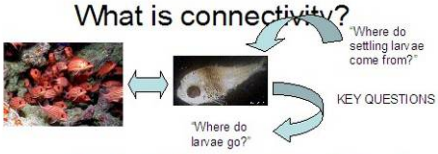

...successful exchange of individuals between marine populations mainly through dispersal

Why is it important?

...design and management of marine protected areas depend on knowledge of the connectivity relationships of the local populations of targeted species

Methodology – Dispersal simulation

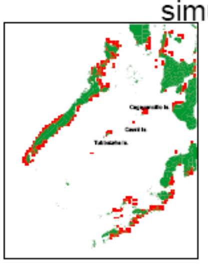

- Particle-tracking dispersal model driven by velocity fields from HYCOM
- Includes scenarios for passive larvae and active larvae
- Virtual larvae originate from each of 446 "reef cells" (9 x 9 km)
- 1000 virtual larvae are released per "reef cell" (=446,000 larvae per model run)
- Model ran monthly for the four different seasons
- Virtual larvae are alive if they are found within a reef cell at the end of their pelagic larval period (otherwise, dead)

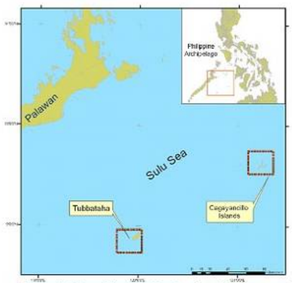

Figure 1. Map of the Sulu Sea showing the box areas of the satellite imagery

Methodology – Dispersal simulation

Parameter	Passive larvae	Active larvae
SHORT		
Pelagic larval duration (PLD)	15 days	15 days
Age when swimming ability is attained	Never	7.5 days
Age when competency to settle is attained	11.25 days	11.25 days
Swimming speed	0 m sec^{-1}	0.2 m sec^{-1}
Sensory range	N/A	18 km
LONG		
Pelagic larval duration (PLD)	30 days	30 days
Age when swimming ability is attained	Never	15 days
Age when competency to settle is attained	22.5 days	22.5 days
Swimming speed	0 m sec^{-1}	0.2 m sec^{-1}
Sensory range	N/A	18 km

* based on the active larval simulation framework for MARINE RESERVES AND REEF CONNECTIVITY IN THE BOHOL SEA by Garry Russ, Angel Alcala, Rene Abesamis, Brian Stockwell,Cesar Villanoy, Charina Repollo

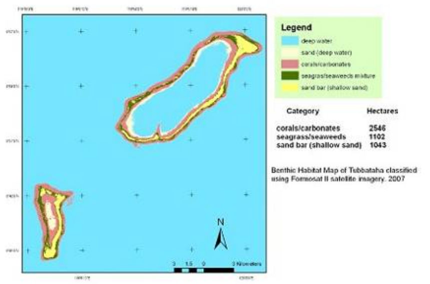

Results - Hydrodynamic Circulation

- HYCOM derived surface velocities

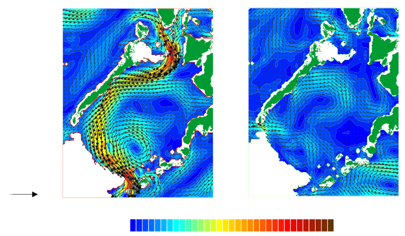

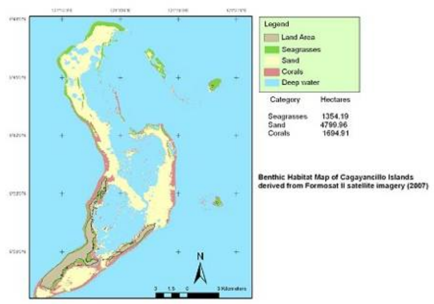

Hydrodynamic Circulation

- HYCOM derived surface velocities

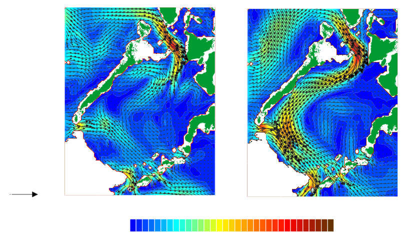

Methodology – Dispersal simulation

position of passive larvae in two-dimensional space

$$x_{t+\Delta t} = x_t + (u_{x,y,t}\Delta t + \varepsilon\sqrt{D\Delta t})$$
$$y_{t+\Delta t} = y_t + (v_{x,y,t}\Delta t + \varepsilon\sqrt{D\Delta t})$$

Where:
x, y = coordinates of a particle
u,v = components of velocities
t = the integration time step
ε = randomly generated number (–1 to 1)
D = the eddy diffusion rate (m^2s^{-1})

position of active larvae incorporating swimming and orienting ability

$$x_{t+\Delta t} = x_t + (u_{x,y,t}\Delta t + \varepsilon\sqrt{D\Delta t} + Sa)$$
$$y_{t+\Delta t} = y_t + (v_{x,y,t}\Delta t + \varepsilon\sqrt{D\Delta t} + Sa)$$

Sa = swimming ability
0m/s if age is < 50% PLD
0.2m/s if age is $\geq$ 50% PLD

Results: SHORT versus LONG PLD

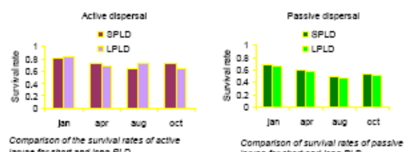

Comparison of the survival rates of active larvae for short and long PLD.

Comparison of survival rates of passive larvae for short and long PLD

- Survival rates (or settlement success) of virtual larvae did not vary significantly with the length of their PLD

Results: ACTIVE versus PASSIVE

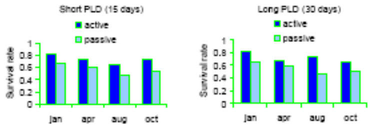

Survival rates between passive and active larvae

- Survival rates are relatively higher for larvae with swimming and orienting ability compared to passive larvae

Dispersal distance - Active

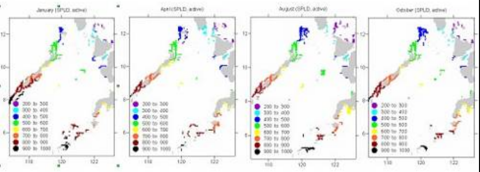

- Dots represents all the virtual larvae that settled to a reef successfully (in kilometers)
- Color of dots signify distance traveled relative to source grid

Dispersal distance - passive

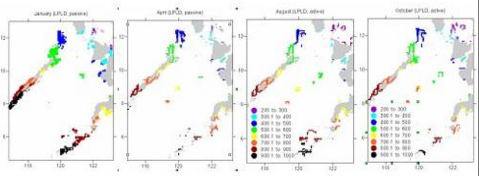

Results: SETTLEMENT SCALE

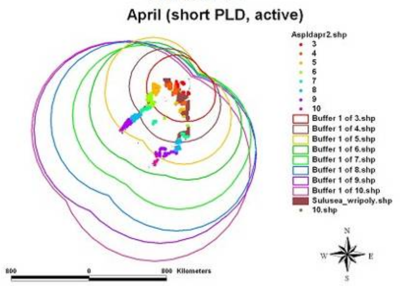

Summary and conclusion

- Survival rates are relatively higher for larvae with swimming and orienting ability
- Survival rate does not differ significantly between PLDs except for August
- There is a net southward advection of larvae based on the computed distance traveled by the particles

Acknowledgements

- Conservation International
- Bohol Sea Connectivity Project
- Francis Friere
- SAKE Project

Thank you!!!

Mapping of Coastal Ecosystem Condition around Thousand Island of North Jakarta

Yudi Wahyudi, Nani Hendiart and Marina CG Frederik
Agency for the Assessment and Application of Technology, M.H. Thamrin 8,
Jakarta 10340, Indonesia

ABSTRACT

Kepulauan Seribu (Thousand Islands) is located north of Jakarta Bay. In addition to the threats of human activities and temperature rise, Kepulauan Seribu suffers from the sewage from city of Jakarta. The focus of this study is to map current condition of the land cover and bathymetry of 3 islands in the Kepulauan Seribu, namely the Pari, Pramuka and Harapan/Kelapa Islands.

Base on Lyzenga algorithm that classification of landcover and underwater substrate type of study area was classified into 5 classes. These classes are land and settlement, mangrove (inland area), mix substrate 1 (rubble and sand), mix substrate 2 (sand, dead coral reef, seagrass), mix substrate 3 (sand and seaweed/seagrass), coral reef condition, and deep water. The largest distribution of coral reef and mangrove ecosystem was found in the Pari Islands. This island is suitable place for conservation of coastal ecosystem such as mangrove, coral reef and seagrass or seaweeds farming. Mangrove species at Pari Islands dominated by *Rhizophora stylosa* dan *Rhizophora mucronata*. Other type can be found such as *Avicennia alba*, *Sonneratia alba*, *Hibiscus tilliaceus* and *Bruguiera gymnorrhiza*. However, according to early study of Fishery and Marine Science of Bogor Agriculture University at 1999 using Landsat ETM that coverage area for density class of mangrove was decreasing caused by growth local population and direct use on mangrove wood.

However, Pramuka and Kelapa/Harapan Islands are not suitable seaweed farming or conservation area caused by centre of economic and human activity in Thousand Islands. Coastal ecosystem around thousand islands is still under threatening by human activity and biophysics degradation.

The advantage of Lyzenga algorithm besides could be used to indentify sub bottom profile also to derive depth chart class. Based on algorithm was resulted 5 classes of depth chart range are (1) 0 -1 m; (2) 1 - 3 m; (3) 3 - 5 m; (4) 5 - 10 m and (1) > 10 m. Whereas, DOP method utilization resulted 4 depth classes range namely (1) 0 - 3 m; (2) 3 - 15 m; (3) 15 - 25 m; and (4) > 25 m.

Keyword: *coastal ecosystem, coral reef, mangrove, seaweed/seagrass, depth chart, shallow water mapping, depth of penetration.*

1. INTRODUCTION

The high biological diversity of coastal and marine ecosystem such as coral reef, seagrass, seaweed and mangrove forest make them valuable resources that sustain local and national economies through fisheries, coastal protection, and tourism. In spite of these important benefits, it has been estimated that 58% of coral reefs globally are threatened by human activities (Bryant et al., 1998). Lack of scientific data about the locations, spatial extent, and health of reefs has hindered responses to these threats. There have been a number of international calls from non-governmental organizations and groups of scientists to improve the mapping of coral reef environments (Center for Marine Conservation, 1999).

As one of the highest biological diversity of coral reef ecosystem in the world, Indonesia's coral reefs and mangrove forest ecosystem are currently undergoing rapid destruction from human activities including at Kepulauan Seribu (Thousand Islands, North of Jakarta Bay). These activities are such as the poison fishing; blast fishing; coral mining; sedimentation; pollution, overfishing, land utilization of mangrove forest for residences and brackish water aquaculture. These forces vary from high risk, high payoff poison fishing to poverty-trap activities such as coral mining.

Kepulauan Seribu (Thousand islands) is a group of small island part of administrative region of Jakarta province as a capital of Indonesia. Kepulauan Seribu is north of Jakarta Bay or Java

Sea. Recently, Kepulauan Seribu just has been new Municipal that separated to main city of North Jakarta Municipal. (Figure 1)

Figure 1: Situation of Thousand Island location at north of Jakarta Bay, Province of Jakarta

Kepulauan Seribu has the misfortune to lie immediately offshore from a society scum of 20 million people and the combined effects of land-based pollution and sedimentation are wreaking havoc in the fragile reef ecosystem of Jakarta Bay. Between 1996 – 2003, the research result of collaboration among UNESCO, Indonesian Institute for Sciences (LIPI) and many universities (University of Indonesia, Bogor Agricultural University, and Nasional University) had reported that the condition of the coral reefs in Kepuluan Seribu was continuing to decline, to the point that some islands have totally disappeared (Figure 2) (UNESCO electronic press released, 2003) .

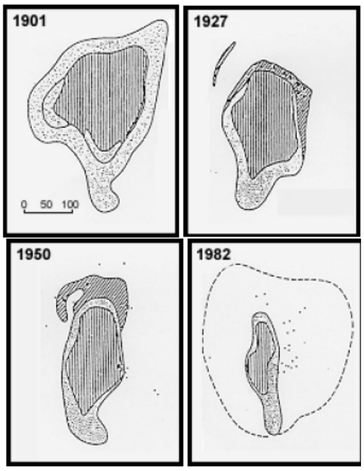

Figure 2: The vast evolution of Ubi Besar island map from 1901 – 1982 (Economic and Business Review Indonesia, 1997).

Part of the problem of coral reef degradation is the global warming and the El Nino effect have led to changed rainfall and runoff patterns and longer "dry-seasons" in Indonesia. Another part of the problem is ‘anthropogenic perturbations’ that affect the structure and health of the coral reef ‘community’. They include archaic waste disposal systems and unsustainable resource management practices which lead to:

- Deposition of rubbish and sedimentation on the reefs,
- Physical destruction of reefs by fish bombing, cyanide fishing, coral mining, and dredging, and
- Decreasing water quality through industrial pollution and nutrient enrichment.

The worsening condition of coral reefs thus goes hand in hand with the unsustainable utilization of resources by local fishermen and specimen collectors and by the developers of private resorts, as well as the improper or inadequate disposal of waste by industry and local government authorities. The spiraling economic cost of reef degradation suggests that the improved management of coral reefs may be in Indonesia’s best economic interest in the long term.

Protection of coral reefs is often presumed to conflict with economic development. However an economic study by the World Bank on the economic value of Indonesian Coral Reefs (1996) clearly indicates that the unsustainable exploitation and management of coral reef leads directly to considerable economic losses in the longer term. The divergence between short-term profits to private individuals and long-term costs to society can reach a ratio of 50:1 (The World Bank Report, *in* H. Cesar 1996).

Base on the vary problem ongoing in Kepuluan Seribu and Jakarta Bay, this research would be focused on 2 topics interest that are:

- Identification of mangrove, seaweeds and coral reef ecosystem condition.
- Shallow water mapping in Pari Islands

Kepulauan Seribu consist more than 100 islands, and due to the limitation of time and cost so the more detail study of coastal ecosystem will be carried out only on 2 islands as sample that represent problem and condition interest namely Pramuka as a municipal city of Thousands Islands and Pari islands as research island (Figure 3).

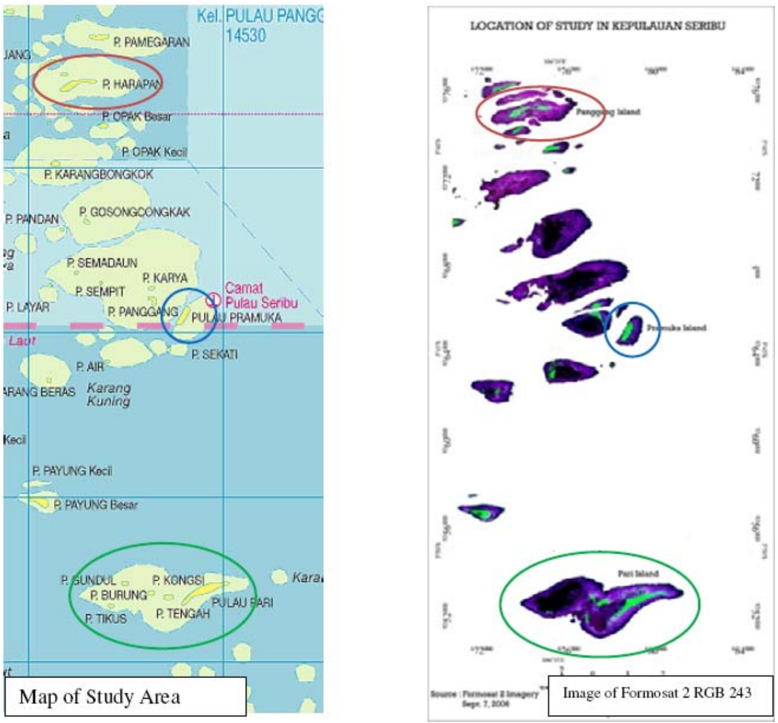

Figure 3: Harapan (red circle), Pramuka (blue circle) and Pari Islands (green circle) as Study area on Kepulauan Seribu, Province of Jakarta

2. DATASETS AND METHODS

2.1Identification Coastal And Marine

Since there are 2 datasets covering the area of study, the first step is to do a mosaic and balance of the histograms of the images. Classification for land cover of the three islands (Pari, Pramuka and Kelapa/Harapan) started with calculation principal component of the 4 bands and then calculates the classification. The classification method used was isodata unsupervised (before field survey) and supervised (after field survey).

A 3x3 majority filter was applied twice to the classified images to reduce speckle appearance. Field survey was done on both terrestrial landcover (vegetation and settlement) and underwater substrate using snorkeling, Line Transect (LIT) and square meter method.

2.2 Shallow Water Mapping

Using the algorithms of Lyzenga (1978) and Depth of Penetration (DOP) by Jupp (1988) to identify the Shallow Water Mapping can identify both a benthic form and water bathymetry. Navigation map and Field survey of water depth was carried out around Pari Island using echosounder (Garmin GPSMAP 178c) to compare between depth classification using Lyzenga and Jupp method and real depth of shallow water.

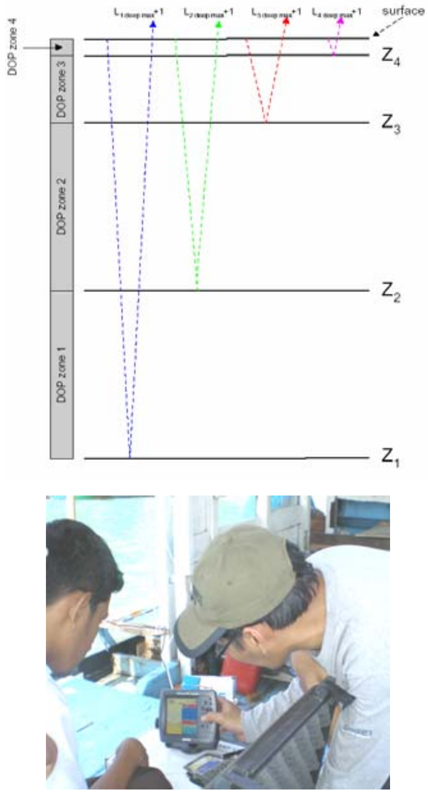

Figure 4: Illustration of Depth of Penetration (DOP) of wavelength characteristics for InfraRed, Red, Green and Blue channel in water column, Jupp (1988) and GPSMAP Garmin 178c.

Figure 5: Small Boat for survey depth and under water substrate type

3. RESULT AND DISCUSSION

3.1 Identification of Coastal Ecosystem

Classification result is presented in the following figures (Figures 6). Landcover and underwater substrate type of study area was classified into 5 classes. These classes are land and settlement, mangrove (inland area), mix substrate 1 (rubble and sand), mix substrate 2 (sand, dead coral reef, seagrass), mix substrate 3 (sand and seaweed/seagrass), coral reef condition, and deep water.

According to data on Table 1 showed that coral reef area and mangrove is found largest in the Pari Island. It is a good place as conservation for coastal ecosystem such as mangrove, coral reef and seagrass or seaweeds farming. Pari Island was dominated by mangrove species such as *Rhizophora stylosa* dan *Rhizophora mucronata*. Other type can be found such as *Avicennia alba*, *Sonneratia alba*, *Hibiscus tilliaceus* and *Bruguiera gymnorrhiza*.

Table 1. Area of class in 3 islands of study area (Pari, Pramuka and Kelapa)

	Percentage of Coverage		
Class	Pari	Pramuka	Kelapa
Coral reef (good & poor)	12	9	15
Sand and Seagrass	40	7	5
Sand, coral, and seagrass	30	33	20
Rubble and Sand	8	24	36
Mangrove	3	1	1
Land & settlement	7	23	23
	100	100	100

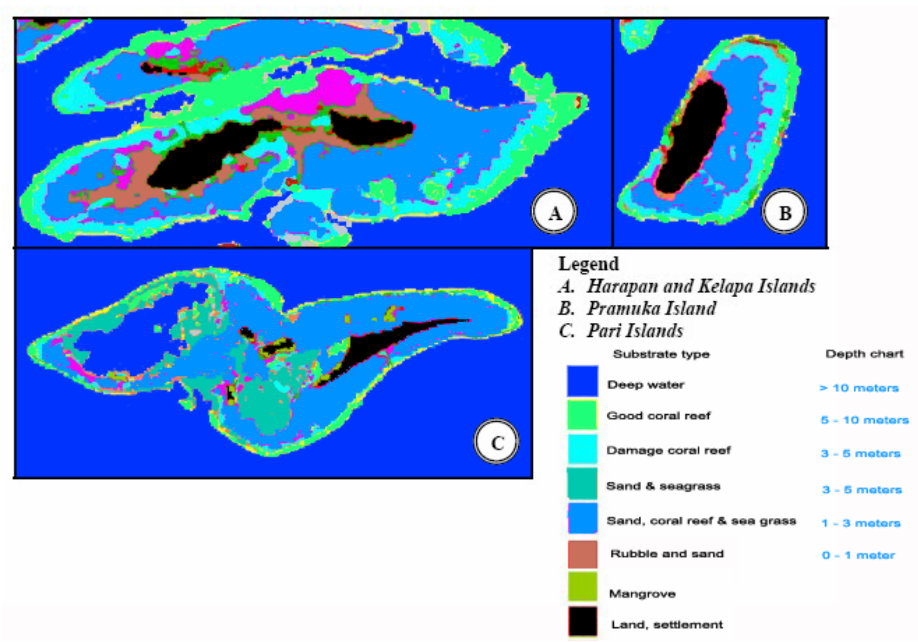

Figure 6: Result of landcover and underwater substrate type of three location study sample area at Kelapa/Harapan Islands, Pramuka Island and Pari Islands and compared to the Depth chart (Using Lyzenga Algorithm).

Harapan/kelapa and Pramuka Island are very dense population and centre of activity than Pari islands. According to the information from the local government, Pramuka island is the location for turtle conservation and one of place for Mangrove seedling. There are only 200 m2 classified as mangrove ecosystem that dominated by *Rhizhopora stylosa*. More detail about distribution and coverage of mangrove and seaweeds farming at Pari Islands as showed at table 2 and figure 7.

Table 2. Mangrove coverage at Pari Islands (in hectare)

Mangrove Class	ETM 1999	F2 2006	LC change	+/-
Rare	7.65	0.15	7.50	Decrease
Moderate	13.96	8.17	5.79	Decrease
Dense	8.32	6.08	2.24	Decrease
Land/Settlement	67.77	83.30	24.47	Increase
	97.7	97.7		

IPB survey in Ganjar (2007)

Mangrove Seedling at Pramuka Island

Mangrove ecosystem at Kongsi Island of Pari Islands

Seaweeds Farming near Kongsi Island of Pari Islands

Figure 7: Condition and Distribution of Mangrove Ecosystem and seaweeds farming around Study Location (Pramuka and Pari Islands)

According to early study of Fisheries Faculty of Bogor of Agriculture University using Landsat ETM at 1999, there are a difference of wide area of mangrove ecosystem at Pari Islands between Landsat ETM 1999 with survey and Formosat 2 2006 classification result. During 5 years, mangrove coverage in all class using (rare, moderate and dense) in decreasing condition, and the other side the land and settlement was increasing. This condition correlated to population growth and mangrove product direct using was increasing as socio-economic activity at Pari Islands.

Generally, Pari Peoples used mangrove wood as boat anchor pole, firewood, and pole of seaweeds farming. Existence of ecosystem mangrove very supported on nutrient supply and suitable habitat for fish and crab economical that gave beneficiary for socio-economic activity in this island. For instant, grouper fish has economic value ranging from 80.000 ~ 120.000 rupiah per kilo, crab has value ranging from 20.000 ~ 25.000 rupiah per kilo, and for seaweeds has value ranging from 5.000 ~ 15.000 rupiah per kilo.

To support mangrove conservation area at Penjaliran Island north of Kelapa/Harapan Islands, the forest local official has collaborate with local people to make seedling location at Pramuka and Pari Island (Figure 7). The institution gave a price about 1.500 rupiah per seed of mangrove tree. Other than, this island is managed by is LIPI (Indonesian Scientific Institute) as a research island since 1980’s. This island will also become the location for seaweed mariculture research. But considering the location of this island to be nearest to Jakarta, the water and environment may not be conducive for healthy coral growth. Pari Island is a good study area for bathymetry because of the size of shallow water area.

Due to the limitation of time and seawater transportation support, detail coverage and distribution of coral reef ecosystem survey only carried out at Pari Islands. The percentage of coral reef coverage at Pari Islands showed at the following table 3. Line transect 1 and 2 was done at south of Pari Island (Figure 8) with 10 sample square plot where is in the LIT 2 that coral reef condition relative good that LIT 1. Refer to the TERANGI foundation (NGO of coral reef conservation activity) suggestion this location is quiet good for coral reef conservation area at Pari Islands.

Table 3. Percentage of Coral coverage at Pari Island

Station No		Hard Coral (%)	Dead Coral (%)
LIT 1	1	8.92	0
	2	40.07	26.04
	3	87.68	0
	4	24.19	0
	5	71.08	9.18
	6	13.32	5.77
Average		40.88	6.83
LIT 2	1	89.87	1.04
	2	83.51	11.07
	3	100	0
	4	46.74	26.30
Average		80.03	9.6

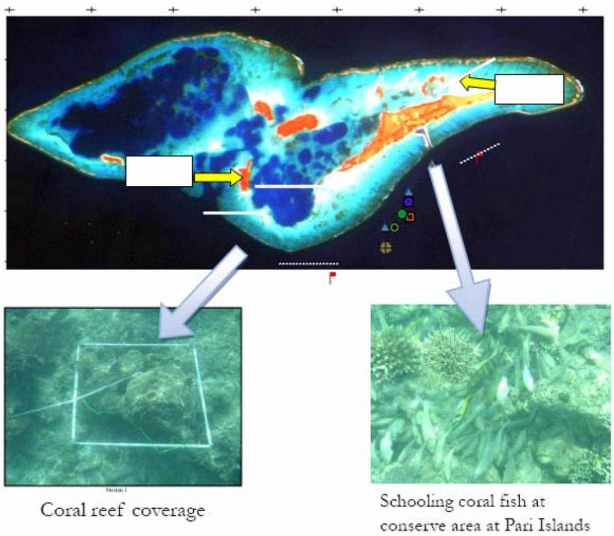

Figure 8: Line Transect (LIT 1 and LIT2) of coral reef coverage location at Pari Islands and sample of coral reef coverage using square meter transect.

4. Shallow Water Mapping

The Shallow Water Mapping Analysis derived from Formosat 2 images was carried out at Pari Islands. In this study algorithm of Lyzenga and DOP method of Jupp used to indicate depth chart in shallow water area mapping. Refer to Lyzenga analysis (Figure 9) was resulted 5 classes of depth chart range are (1) 0 -1 m; (2) 1 - 3 m; (3) 3 - 5 m; (4) 5 - 10 m and (1) > 10 m. And the other side, the depth chart of DOP method resulted 4 depth classes range namely (1) 0 - 3 m; (2) 3 - 15 m; (3) 15 - 25 m; and (4) > 25 m (Figure 10). The difference both

Lyzenga and DOP method based on initial approach. Lyzenga algorithm used green and blue channel in his linier interpolation formula to classify not only underwater substrate identification but also can used for shallow water mapping.

Whereas, DOP method was only focused on depth penetration based on the wave length characteristic of each channel using. For instants, blue is the far penetration in underwater column, than green, red and infrared channel. So we can

describe that the composition of depth penetration of 4 differences channel are blue (0 – 25 m) > green (0 – 15 m) > red (0 – 3 m) > infrared (0 – 1 m).

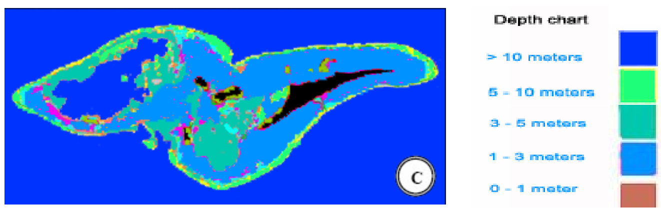

Figure 9: Result of depth chart using lyzenga Algorithm (1978) has resulted 5 depth classes.

Figure 10: Result of depth chart using DOP of Jupp (1988) has resulted 4 depth classes.

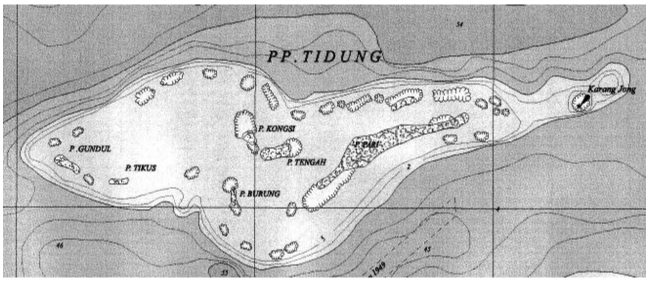

Figure 11: Bathymetry Map of Indonesia Seawater at Pari Islands at 1999, Bakosurtanal scale map 1 : 50.000.

Table 4. Zone of DOP division based on Pixel Digital Number.

Formosat 2 band	1	2	3	Zone DOP
DN of Maximum Depth	136	121	12	
If DN value (L_i) of pixel	≤136	≤121	≤12	then depth > 25.02 m
If DN value (L_i) of pixel	>136	≤121	≤12	then depth = 15.64-25.02 m (zone 1)
If DN value (L_i) of pixel	>136	>121	≤12	then depth = 3.32-15.64 m (zone 2)
If DN value (L_i) of pixel	>136	>121	>12	then depth = 0-3.32 m (zone 3)

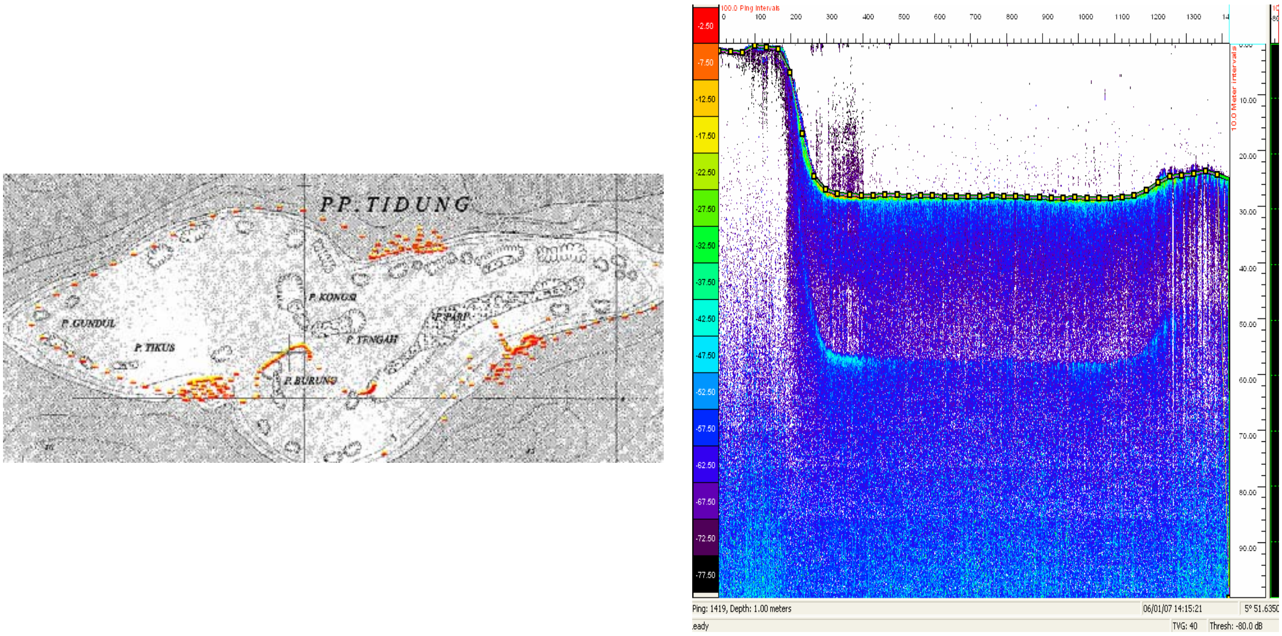

Figure 12: 293 points sample data and depth echogram data around Pari Islands.

Using confusion matrix to test the truth level between DOP zone range class and ground truth data from 293 points of depth sample data (Figure 12) indicated that the overall accuracy value is 99,87% (Table 5).

Table 5. Matrix Confusion to test the truth level of depth classification based on ground truth data.

Classification	Depth Reference					Total Row	UA (%)
	Land	Zona DOP 3	Zona DOP 2	Zona DOP 1	Depth Water		
Land	448	0	0	1	0	449	99.777
Zona DOP 3	0	1400	0	0	0	1400	100
Zona DOP 2	0	0	623	2	0	625	99.680
Zona DOP 1	1	0	2	683	3	689	99.129
Depth Water	0	0	0	3	6618	6621	99.455
Total Column	449	1400	625	689	6621	9784	
PA (%)	99.777	100	99.680	99.129	99.455		
Overall Accuracy (%)	99.877%						
Kappa coeff.	0.998						

5.CONCLUSION AND SUGGESTION

According to the study and final result about mapping of coastal ecosystem condition around thousands island at north Jakarta could be concluded that:

- Utilization FORMOSAT 2 satellite image data in this study very useful especially to identify coastal ecosystem condition in remote and small islands likes Thousand Islands Municipal at the North of Jakarta.
- Coral reef ecosystem condition at surrounding area of Pramuka and Harapan/Kelapa Islands has been threatening not only by local people activity such as coral mining and illegal fish but also by water quality degradation.
- Coverage area of mangrove and coral reef at Pari Islands is 3% and 12% of total coverage area. This condition is quiet good compare to mangrove and Coral reef ecosystem coverage at Pramuka and Harapan/Kelapa Islands.
- Mangrove coverage in Pari Islands was decreasing in all class (rare, moderate, and dense) due to the local population growth and direct use of mangrove wood by local people.
- Both Lyzenga Algorithm and DOP of Jupp method can use to indentify
- depth chart in shallow water mapping is very worthwhile.

For the next study to get a good reason which the main factor that caused coastal ecosystem degradation whether human socio-economic condition, biophysics factor or both, we suggest that economic valuation and socio-economic must be carried out. Whereas, to get the sub bottom profile, we could be used hyperspectral data (imagery or radiometer data) and high resolution image data such Quick bird (0,6 m) or IKONOS (1 m) to derive sub bottom substrate characteristic profile or spectral profile.

REFERENCES

Center for Marine Conservation, "Technical Issues Related to Coral Reef Remote Sensing and Workshop Recommendations," Center for Marine Conservation, Washington, D. C., June, 1999.

Bryant, D., L. Burke, J. McManus, and M. Spalding, Reefs at Risk: A Map-based Indicator of Threats to the World's Coral Reefs, World Resources Institute, International Center for Living Aquatic Resources Management, World Conservation Monitoring Centre, and United Nations Environment Programme, Washington D. C., 1998.

Economic and Business Review Indonesia.. “One by one the real Thousand Islands (Kepulauan Seribu) in Jakarta Bay are disappearing!”. Article. No. 262, April 23, 1997 pp.38 – 39.

Ganjar, Sebaran dan Tutupan Mangrove di Gugusan Pulau Pari, Kepulauan Seribu. Skripsi. Fakultas Perikanan dan Ilmu Kelautan. Institut Pertanian Bogor. 2007. (Unpublished)

Cesar H., 1996. The Economic Value of Indonesian Coral Reefs. World Bank Environmental Economics Series.

Jupp, D.L.B., 1988, Background and extensions to depth of penetration (DOP) mapping in shallow coastal waters. Proceedings of the Symposium on Remote Sensing of the Coastal Zone, Gold Coast, Queensland, September 1988, IV.2.1-IV.2.19.

Kurniadhi, 2006. Pemetaan dengan Citra Satelit Resolusi Tinggi dan Perancangan Sistem Informasi Sebaran Terumbu Karang di Kepulauan Seribu (High Resolution Imagery Mapping and Information System Design of Coral Reef Distribution at Kepulauan Seribu). Bogor Agricultural University. Unpublished.

Lyzenga, D.R., 1978, Passive remote sensing techniques for mapping water depth and bottom features. Applied Optics 17: 379-383.

UNESCO Electronic Press Released,

2003.http://www.unesco.or.id/prog/science/jkbay/index.htm

World Resources Institute.
http://www.wri.org/biodiv/project_description2.cfm

A Remote Sensing Investigation on River Discharges and Their Influences to Marine Environmental Changes over Jakarta Bay

N. Hendiarti, E. Aldrian,,M.Sadly, M.C.G.Frederik
Agency for the Assessment and Application of Technology,
M.H. Thamrin 8, Jakarta 10340, Indonesia

A Remote sensing investigation on river discharges and their influences to marine environmental changes over Jakarta Bay

N. Hendiarti, E. Aldrian,, M. Sadly, M.C.G. Frederik

Agency for the Assessment and Application of Technology,
M.H. Thamrin 8, Jakarta 10340, Indonesia

River discharge nearby Jakarta Bay

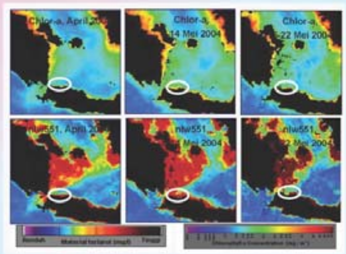

Chlorophyll (upper) and *nlw* 551nm (lower) images derived from MODIS Aqua data between March and Mei 2004, when thousand fish were killed in and near Jakarta Bay.

Why Jakarta Bay?

Parameters	Characteristics		
	Coastal: S. Citarum	**Estuary: S. Siak**	**Lagoon: Segaraanakan**
Residence time	Short	medium	longer
River plume	Obviously observed		
Discharged materials	chlorophyll-a conc.: $\geq$ 2.5 mg/m^3 TSM cons.: $\geq$ 10 mg/l slightly higher of SST		
Duration of peak event	Wet season and transition phase (Feb., Mar., Apr., Nov.)		
Sedimentation	Low	medium	high
Water exchange	Good	enough	limited
Key environmental driven	freshwater inflows		sea-level rise, wind-driven shelf circ.
Ecological management issues	nutrient enrichment, algae bloom, water pollution		sedimentation

Mapping, monitoring and possibly prediction.

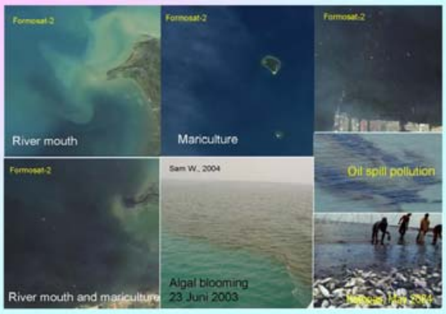

What we have?

DATA archives:
- Satellite remote sensing data to monitor the distribution of chlorophyll *a* and suspended matter concentration near the river mouth.
- Satellite high resolution images i.e. Formosat for mapping the coastal ecosystem
- Precipitation data (long term & near real time) from the meteorological station.
- Water discharge (long term & near real time) from the hydrological station.

→ Subset areas for satellite images analysis

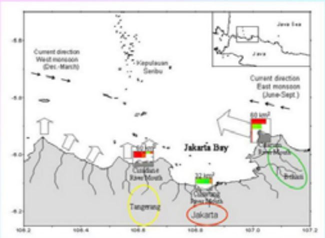

River Mouth - City	Coverage (km²)	Geographic Location
Cisadane - Tangerang	54 - 80	5.92 - 6.06° S ; 106.50 - 106.70° E
Ciliwung - Jakarta	36 - 48	6.02 - 6.12° S ; 106.76 - 106.90°E
Citarum - Bekasi	108 - 120	5.82 - 6.00° S ; 106.95 - 107.12° E

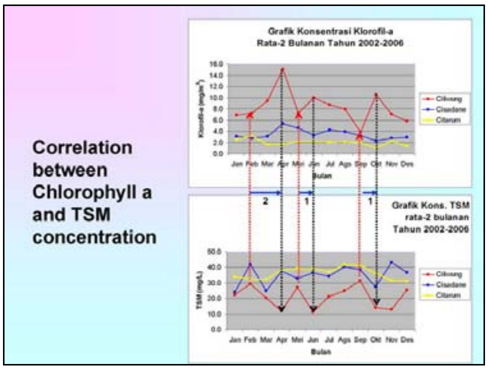

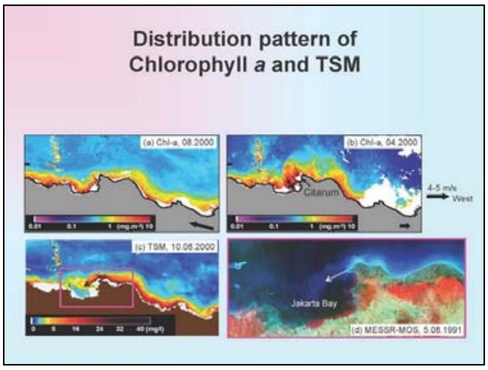

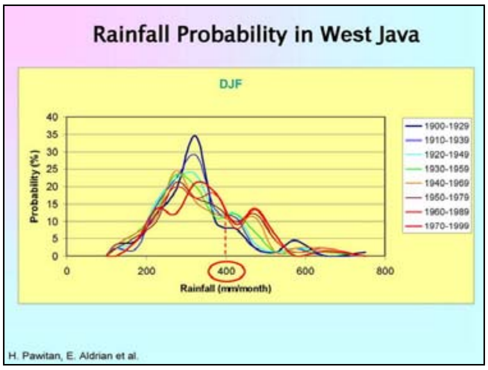

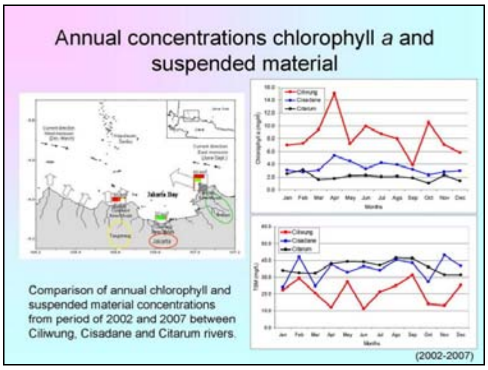

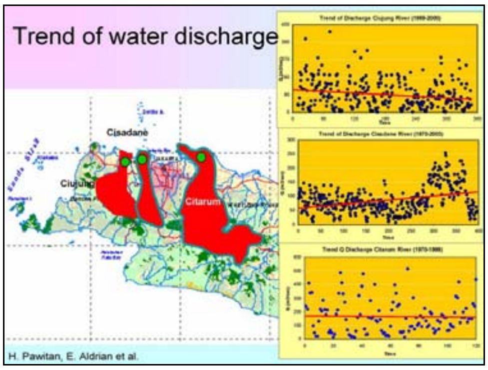

General characteristics of discharged waters near the river mouth from images

River Name	Suspended Material		Chlorophyll *a*		Distribu-tion Pattern	Land use cover	Water Classifi cation	Potential problem
	Range Conc. (mg/L)	Peak months	Range Conc. (mg/ m³)	Peak months				
Citarum (Eastern)	30 – 40	Slightly Apr. – Sept.	1 – 3	Slightly in Feb.	**No seasonal influence**	Bekasi city	Very turbid	Accretion
Ciliwung (Middle)	10 - 30	Feb., May, Sept.	4 - 15	Apr., Jun., Oct.	**Seasonal influence**	Jakarta city	turbid	**Algae blooming**
Cisadane (Western)	25 - 45	Feb., Apr.- Sept., Nov.	2 – 5,5	Apr., Jul.	**Small seasonal influence**	Tangerang city	Very turbid	Accretion

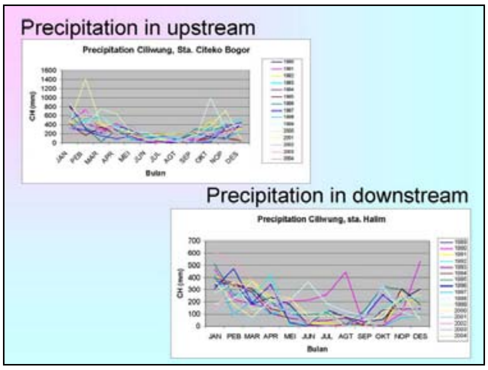

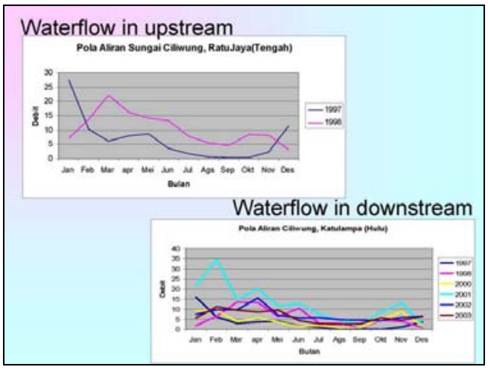
Waterflow in upstream
Pola Aliran Sungai Ciliwung, RatuJaya(Tengah)
Debit
Jan Feb Mar apr Mei Jun Jul Ags Sep Okt Nov Des
Bulan
1997
1998
Waterflow in downstream
Pola Aliran Ciliwung, Katulampa (Hulu)
Bulan

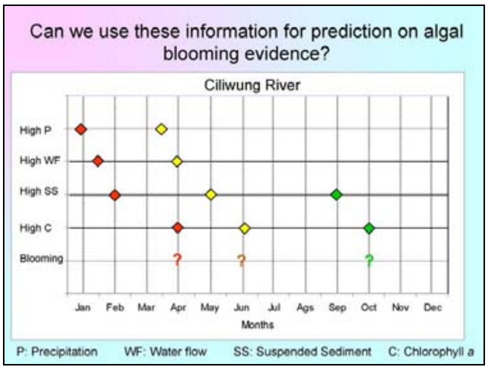
Can we use these information for prediction on algal blooming evidence?
Ciliwung River
High P
High WF
High SS
High C
Blooming
Jan Feb Mar Apr May Jun Jul Ags Sep Oct Nov Dec
Months
P: Precipitation
WF: Water flow
SS: Suspended Sediment
C: Chlorophyll a


Thank you

Application of Ocean Color Remote Sensing for Monitoring and Mapping Total Suspended Matter: A Case Study in East China Sea

Eko Siswanto, *Hydrospheric Atmospheric Research Center, Nagoya University, Japan*
Agency for the Assessment and Application of Technology, Indonesia
Joji Ishizaka, *Faculty of Fisheries, Nagasaki University, Japan*
Yu-Hwan Ahn, *Korean Ocean Research and Development Institute, Korea*
Sinjae Yoo, *Korean Ocean Research and Development Institute, Korea*
Sang-Woo Kim, *National Fisheries Research and Development Institute, Korea*
Junwu Tang, *National Satellite Ocean Application Service, China*
Akihiko Tanaka, *School of Marine Science and Technology, Tokai University, Japan*
Yoko Kiyomoto, *Seikai National Fisheries Research Institute, Fisheries Research Agency, Japan*
Hiroshi Kawamura, *Graduated School of Science, Tohoku University, Japan*

ABSTRACT

In situ total suspended matter concentration (TSM) and the Sea-viewing Wide Field-of-view Sensor (SeaWiFS)-derived normalized water leaving radiance (nlw) data were used to examine to what degree the current SeaWiFS ocean color data in conjunction with TSM algorithms can be used to assess TSM in the East China Sea (ECS). In general, current SeaWiFS ocean color data combined with local TSM algorithms could explain the variability of in situ TSM by < 80% with a single band algorithm at 555 nm seemed to be an optimal algorithm for retrieving TSM from the SeaWiFS ocean color sensor. Estimated TSM showed a clear seasonal variation in the ECS. A remarkable high TSM was observed over the shallow region during the prevailing strong wind in winter and disappeared during the calm condition in summer, suggesting that the seasonal variation of TSM in the ECS was modulated by the East Asian monsoon wind systems and bottom topographic feature. Flow pattern of the Yangtze River diluted water during the severe summer flood in 1998 could also be traced from the summer TSM image. This study showed the potency of using SeaWiFS ocean color data to monitor both spatial and temporal variations of TSM in the ECS, the variability of which seemed to be largely influenced by monsoon system, bottom topography, and the Yangtze River discharge.

1. BACKGROUND

The Asia's longest Yangtze River is the main source of freshwater discharge, by which nutrients and sediment are transported into the East China Sea (ECS), one of the most productive waters in the world's ocean. The Yangtze River has been undergoing long-term ecosystem modifications due to anthropogenic perturbations such as the increase in nitrogen fertilizer application and the long-term dam constructions in the Yangtze River basin. More than 50,000 dams, including the world's largest hydroelectric dam, Three Gorges Dam, have been built since 1950 in the Yangtze River basin.

It has been reported that due to the dam constructions since 1950s in the Yangtze River basin, sediment discharged into the ECS has decreased more than 40% compared to that in the 1950s – 1960s period despite an increase in the Yangtze River discharge (e.g., Yang et al., 2006;Xu et al., 2006). The transport of sediment from river into the marine ecosystem is of critical important because of its co-occurrence with nutrients, carbon materials, and pollutants. Suspended sediment also influences light availability in the water column that in turn will influence biological production. This may have a further impact on the biogeochemical processes in the ECS (e.g., Jiao et al., 2007).

It is thus crucial to routinely monitor temporal variation and map spatial extent of biogeochemical variable than can be directly influenced by changes in sediment load, such as total suspended matter concentration (TSM). Ship-borne TSM observation however is not feasible especially when deals with the high spatial and temporal resolutions.

Satellite remote sensing with its synoptic observation capability is the only reasonable tool for monitoring TSM variation with the high spatial and temporal resolutions. The long-wavelength bands (e.g., 555 nm and 670 nm) in the visible spectrum from the Sea-viewing Wide Field-of-view Sensor (SeaWiFS) ocean color sensor are commonly used as an index of TSM and thus to map its spatial extent, as well as its temporal variation (e.g., Salisbury et al., 2004; Thomas and Weatherbee, 2006). This is because water reflectance from the long-wavelength bands can be obviously enhanced from the water with high TSM.

With the use of bio-optical datasets shared under the research collaboration between Korea, China and Japan, and supported by UNDP/GEF Yellow Sea Large Marine Ecosystem (YSLME) Project, this preliminary study is therefore to investigate the relationship between TSM and the SeaWiFS normalized water leaving radiance bands 555 nm and 670 nm (hereinafter referred to as nlw 555 and nlw 670, respectively). The study merely aims at investigating to what degree current SeaWiFS ocean color data in conjunction with TSM algorithms can be used to monitor spatial and temporal variations of TSM in the ECS.

2. MATERIALS AND METHODS

2.1. In situ and satellite data

In situ TSM data from the bio-optical data sharing used in this study were collected within the period from 1998 through 2006 covering all seasons. Despite more than 750 in situ TSM data are available from the shared bio-optical datasets, we only analyzed 160 pairs of in situ TSM and satellite data for match-up due to the cloud coverage. The region where the 160 in situ TSM data were collected encompassing both deep clear open ocean and shallow turbid coastal water and thus optically encompassing both Case 1 and Case 2 waters (Fig.1). In situ TSM used in this study were within the range of 0.04 – 22.86 mg l^{-1}.

With the use of SeaWiFS Data Analysis System (SeaDAS) version 5, nlw 555 and nlw 670 were derived from the SeaWiFS level 2 products. For the periods of 1997 – 2004 and 2005 – 2006 we used respectively, SeaWiFS daily merged local area coverage (MLAC) with 1 km resolution and daily global area coverage (GAC) with 4 km resolution.

2.2. Data match-up

SeaWiFS-derived nlw 555 and nlw 670 to be compared with the in situ TSM are defined as the median values from 3 x 3 boxes the center of which is the in situ TSM sampling point. Rather than the mean value, the use of median value has an advantage as it is less sensitive to the outlier value than the mean one.

The relations between nlw 555, nlw 670 versus in situ TSM are then plotted. The least squares fittings are applied to obtain the equation that best fits to the emerged relationships. TSM is then computed to be compared with in situ TSM. The capabilities of previous local and SeaWiFS standard TSM algorithms in assessing TSM in the ECS are also investigated.

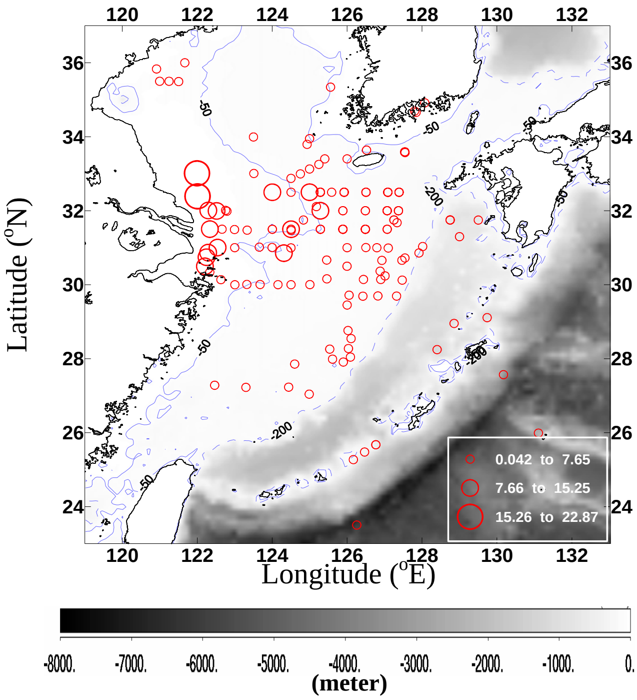

Fig. 1: Bathymetric map of the ECS over which the sampling points (red circles) for TSM are overlaid. The size of the red circles represents the magnitude of TSM as indicated in the legend. Solid and dashed blue contours indicate 50 m and 100 m isobaths, respectively. The bottom depth is shown as negative values (see the scale bar).

3. RESULTS AND DISCUSSION

3.1. Relationship between SeaWiFS nlw 555, nlw 670 and in situ total suspended matter

With the in situ TSM within the range of 0.04 – 22.86 mg l^{-1}, remarkable increases of both nlw 555 and nlw 670 could be observed with the increase of in situ TSM (Fig. 2). Applying a linear function, the variation of in situ TSM could significantly be explained better by nlw 670 (75%) than that by nlw 555 (68%). But by applying an exponential function, nlw 555 could assess in situ TSM variation better (79%) than nlw 670 (51%).

Applying a multiple linear regression relation expressing TSM as a function of both nlw 555 and nlw 670 (TSM = 0.48 + 0.29 nlw555 + 5.91 nlw670, $R^2 = 0.76$, $p < 0.0001$) could not improve the accuracy in assessing TSM. Ahn et al. (2001) also showed that TSM algorithm using a single band at long-wavelength band provided a better result than that using multiband.

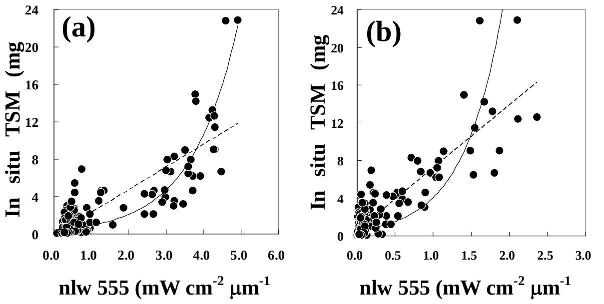

Fig. 2: (a), Scatter plot of nlw 555 versus in situ TSM. The dashed line indicates linear least squares fit to the data (TSM = 2.44 nlw555 - 0.18, $R^2 = 0.68$, $p < 0.0001$). The solid curve indicates the exponential least squares fits to the data (TSM = 0.41 $e^{0.81\,\mathrm{nlw555}}$, $R^2 = 0.79$, $p < 0.0001$). (b), The same as (a), except for nlw 670. Linear least squares and exponential least squares fits to the data are respectively, TSM = 6.62 nlw670 + 0.60 ($R^2 = 0.75$, $p < 0.0001$) and TSM = 0.57 $e^{1.95\,\mathrm{nlw670}}$, $R^2 = 0.51$, $p < 0.0001$).

It has been commonly reported that the water reflectance of long-wavelength band is non-linearly or exponentially correlated to TSM (e.g., Nechad et al., 2003; Salisbury et al., 2004). It is therefore in the present state, the exponential function and nlw 555 respectively, seemed to be the effective model and band to be used for estimating TSM in the ECS from the SeaWiFS sensor, at least within the observed TSM range (0.04 – 22.86 mg l^{-1}). Ahn et al. (2001) also suggested the 555 nm band as an alternative band for retrieving TSM from SeaWiFS, as the optimal band (625 nm) he suggested is not available in the SeaWiFS channels.

3.2. Comparison of present study, local and SeaWiFS standard total suspended matter algorithms

In order to know the capability of current SeaWiFS ocean color data in conjunction with TSM algorithms for retrieving TSM in the ECS, we also analyzed several established local TSM algorithms which were also constructed for the ECS region, to be compared with the single band (555 nm) algorithm resulted from the present study.

Among the local algorithms is the multiband ratio proposed by Tang et al. (2004) with the equation of log(TSM) = 0.58 + 23.84 (nlw555 + nlw670) – 0.48 (nlw490/nlw555). The other algorithms to be verified are Ahn et al.'s (2001) single band algorithms from SeaWiFS bands (555 nm and 670 nm) with the formulations of TSM = 3.18 $(\mathrm{nlw555})^{0.95}$ and TSM = 6.38 $(\mathrm{nlw670})^{0.69}$. Standard SeaWiFS TSM algorithm embedded in the SeaDAS msl12 code was also verified.

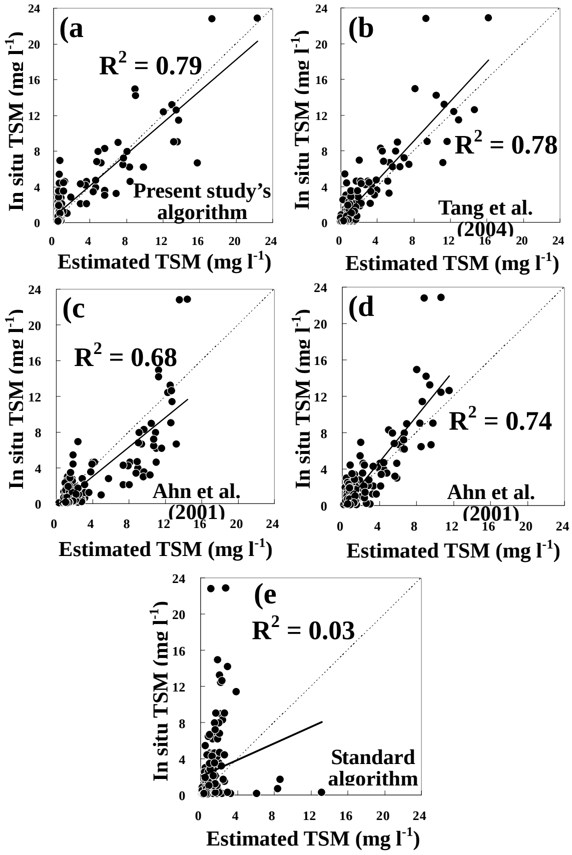

Fig. 3: Scatter plot of estimated versus in situ TSM. The estimated TSM in (a), (b), (c), (d) and (e) were computed based on the present study-derived exponential function of single band algorithm, Tang et al.'s (2004), Ahn et al.'s (2001) nlw555 single band, Ahn et al.'s (2001) nlw670 single band and SeaWiFS standard algorithms, respectively. The variability of the in situ TSM explained by each algorithm is represented by R^2 values. Dashed and solid lines are respectively, the unity and linear regression lines, respectively.

In general, TSM in the ECS could be predicted by the current SeaWiFS ocean color data in conjunction with TSM algorithms both yielded from the present study and previously established ones by less than 80% (Figs.3a - 3d). SeaWiFS standard TSM algorithm however did not work well in the ECS region (Fig. 3e). Such inaccuracy of standard algorithm might be due to the optical property differences between the ECS and the region from which the data were collected to develop standard algorithm (mostly Case 1 waters).

3.3. Seasonal variation of total suspended matter

The ecosystem of the ECS is largely influenced by the East Asian monsoon system with the strong northeasterly wind prevails during winter and weak southwesterly wind prevails during summer. In addition, the feature of bottom topography may also modulate the seasonal variations of physical and biogeochemical variable in the ECS (e.g., Tseng et al., 2000).

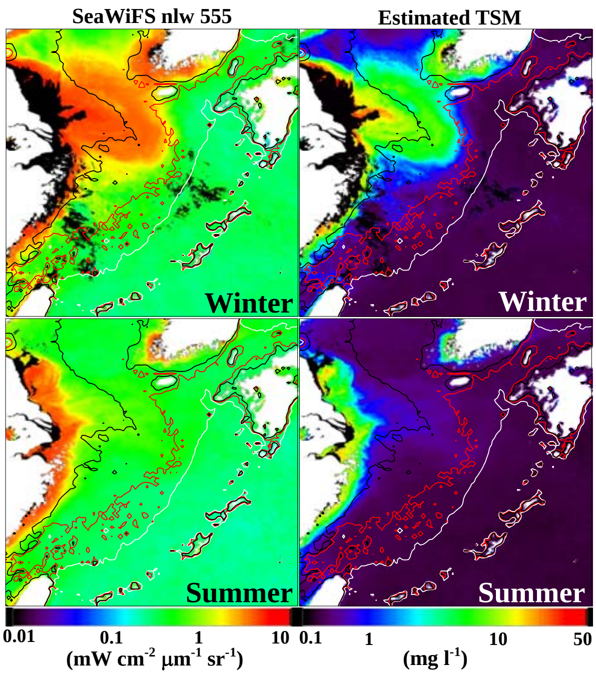

Fig. 4: Images of SeaWiFS-retrieved nlw 555 (left) and TSM estimated using present study's algorithm (right) during winter (upper) and summer (lower) in the ECS. Black, red and white contours are 50 m, 100 m and 200 m isobaths, respectively. The nlw 555 and TSM images are based on the 1998 SeaWiFS data.

The East Asian monsoon wind systems and bottom topographic feature seemed also to influence the seasonal variation of TSM in the ECS. During winter, high nlw 555 and thus TSM were clearly observed in the shallow region of the ECS. The pattern distribution of this high TSM during winter seemed to follow the tongue-like shallow bathymetric feature indicating that the prevailing strong winter wind re-suspended shallow bottom sediment, resulting in high TSM during winter (Fig. 4). The tongue-like high TSM pattern disappeared in summer associated with the less sediment re-suspension due to the weak southwesterly wind during summer.

Summer is flood season in the Yangtze River valley, particularly during the summer 1998 when the catastrophic flood occurred. Based on the ship-borne observations, Wang et al. (2003) showed that during this catastrophic flood period (August 1998) the Yangtze River diluted water flowed to the northeast toward the Cheju Island in a tongue-like shape, and then it diffused southeastward in the area east of 125.5^{o}E, and eastward continually. Such a flow of Yangtze River diluted water could also be traced from the summer TSM image (Fig. 4).

Despite using SeaWiFS standard or dark pixel atmospheric correction which usually fails to retrieve water leaving radiance in the Case 2 waters, this preliminary study indicated that the ocean color data in conjunction with TSM algorithms can be used to assess TSM in the ECS. Conducting atmospheric correction scheme for turbid water (e.g., Lavender et al., 2005) and validating TSM algorithm with more datasets are expected to improve TSM retrieval from SeaWiFS ocean color sensor, and thus allowing us to better understand the spatial and not only the seasonal, but also the interannual variations of TSM, as well as the future scenario of TSM variation related to the completion of the Three Gorges Dam in the middle stream of the Yangtze River in 2009.

4. SUMMARY

Analyzing 160 pairs of in situ TSM and SeaWiFS ocean color data, significant relationships between nlw 555, nlw 670 and in situ TSM emerged. In general, current SeaWiFS data combined with present study's and previously established TSM algorithms could explain the variability of in situ TSM by < 80%, whereas SeaWiFS standard algorithm could not work well in the ECS. A single band algorithm at 555 nm, rather than at 670 nm, seemed to be the effective algorithm for retrieving TSM from the SeaWiFS ocean color sensor.

Applying the present study's single band equation with the SeaWiFS-derived nlw 555, a seasonal variation of TSM was clearly observed. The magnitude and spatial extent of TSM variation seemed to be influenced by the East Asian monsoon wind systems, bottom topographic feature, and the Yangtze River discharge.

Despite using standard atmospheric correction, this preliminary study showed the potency of using ocean color data to monitor both spatial and temporal variations of TSM in the ECS. Improving atmospheric correction and TSM algorithm are expected to obtain a better accuracy in retrieving TSM from the SeaWiFS ocean color sensor.

ACKNOWLEDGEMENT

The bio-optical data sharing is supported by "UNDP/GEF Yellow Sea Project's activity on Developing Ocean Colour Algorithm for the Yellow Sea (CA-E-7-jpn-colour-3334)".

REFERENCES

Ahn Y-H, Moon J-E, Gallegos S (2001), Development of suspended particulate matter algorithms for ocean color remote sensing, Kor J Rem Sen, Vol.17, No.4, pp: 285 - 295.

Jiao N, Zhang Y, Zeng Y, Gardner, Mishonov AV, Richardson MJ, Hong N, Pan D, Yan X-H, Joe Y-H, Chen C-TA, Wang P, Chen Y, Hong H, Bai Y, Chen X, Huang B, Deng H, Shi Y, Yang D (2007), Ecological anomalies in the East China Sea: Impacts of the Three Gorges Dam? Water Res 41: 1287 - 1293.

Lavender SJ, Pinkerton MH, Moore GF, Aiken J, Blondeau-Patissier (2005), Modification to the atmospheric correction of SeaWiFS ocean colour images over turbid waters, Cont Shelf Res 25: 539 - 555.

Nechad B, Cauwer VD, Park Y, Ruddick KG (2003), Suspended Particulate Matter (SPM) mapping from MERIS imagery. Calibration of a regional algorithm for the Belgian coastal waters, ESA Special Publication SP-549.

Salisbury JE, Campbell JW, Linder E, Meeker LD, Muller-Karger FE, Vorosmarty CJ (2004), On the seasonal correlation of surface particle fields with wind stress and Mississippi discharge in the northern Gulf of Mexico, Deep-Sea Res II 51: 1187 - 1203.

Tang J, Wang X, Song Q, Li T, Chen J, Huang H, Ren J (2004), The statistic inversion algorithms of water constituents for the Huanghai Sea and the East China Sea, Act Oceanol Sin, Vol. 23, No. 4, pp: 617 - 626.

Thomas AC, Weatherbee RA (2006), Satellite-measured temporal variability of the Columbia River plume, Rem Sen Env 100: 167 - 178.

Tseng C, Lin C, Chen S, Shyu C (2000), Temporal and spatial variations of sea surface temperature in the East China Sea, Cont Shelf Res 20: 373 - 387.

Wang B-D, Wang X-L, Zhan R (2003), Nutrient conditions in the Yellow Sea and the East China Sea, Est Coast Shelf Sci 58: 127 - 136.

Xu K, Milliman JD, Yang Z, Wang H (2006), Yangtze sediment decline partly from Three Gorges Dam, EOS, 87(19).

Yang Z, Wang H, Saito Y, Milliman JD, Xu K, Qiao S, Shi G (2006), Dam impacts on the Changjiang (Yangtze) River sediment discharge to the sea: The past 55 years and after the Three Gorges Dam, Wat Res Res, Vol. 42, W04407, doi:10.1029/2005WR003970.

Coastal Water Monitoring and Algorithm Development for Hyper-Spectrum Sensor

Ichio ASANUMA, Shinya Odagawa**, Chiaki Kobayashi**, Masaki Kawai**, Masatane Kato**, Genya Saitoh***, and Akihiro Kishima****

**The Tokyo University of Information Sciences, 1200-2, Yato, Wakaba, Chiba, Japan 265-8501*

***The Earth Remote Sensing Data Analysis Center, 3-12-1, Kachidoki, Chuo, Japan 104-0054*

****The University of Tohoku, 1-1, Tsutsumi, Amamiya, Aoba, Sendai, Japan 981-8555*

ABSTRACT

The airborne hyper-spectrum sensor was deployed over the coastal water to monitor bio-optical properties and to develop algorithms to estimate chlorophyll-a concentration, diffuse attenuation coefficient, and colored dissolved organic matter. The hyper-spectrum data will cover the missing information among bands, which are spectrum bands in the traditional satellite borne ocean color remote sensors. The new concept of algorithms using hyper-spectrum information will be discussed for the apparent optical property (AOP) and the inherent optical property (IOP). The test study area includes the coastal water with high turbidity and clear water within a range, and includes biologically damaged coastal floor.

Keywords: hyperspectral imaging, ocean color, CDOM, Kd, chlorophyll

1. INTRODUCTION

In the history of the ocean color remote sensing, the coastal water is the further problem for the alogorthm development including atmospheric correction and/or bio-optical algorithm (Wang et al., 2007, Chami, 2007, O'Reilly et al., 1998). Especially, the colored dissolved organic matter (CDOM) and the suspended particles in the case II water are unavoidable substances to be analyzed so as to obtain the chlorophyll-a concentration from remotely sensed data (IOCCG, 2000). As the case II water, located along the coast or on the continental shelf, exhibits the none-zero upwelling radiance at the red or in the near infra-red bands, it is difficult to remove an atmospheric contribution from the upwelling radiance in the short visible bands like 400 and 500 nm. In contrast, the case I water with only phytoplankton exhibits the zero upwelling radiance in the long wavelength and the current atomospheric correction works very well to remove the atmospheric contribution in the short visible bands. The accuracy of the atmospheric correction restricts the accuracy in the bio-optical algorithm combining the bands in the short visible bands.

Although, there remains an uncertainity in the atmospheric correction in the short visible bands over the case II waters, the bio-optical algorithms were porposed to estimate chlorophyll-a concentration, the CDOM, and the diffused attenuation coefficient at 490 nm (Kd490), where

Kd490 is used to represent the concentration of suspended particles. The chlorophyll-a concentration, CDOM and Kd490 are given by the empirical functions with the ratios among bands, but with the uncertainity in the coastal water. Sometimes, by the exceeding atmospheric correction from red and infra-red bands to the green and blue bands, the negative radiances are observed in the blue and green bands with resulting failers in estimating chlorophyll-a concentration and so on. Among ocean color scientists, there were many efforts to obtain the accurate bio-optical parameters from surface radiances (Siegel et al., 2002, Johannessen et al., 2003, Oliver et al., 2004). Unfortunately, the current discreate bands in the visible and near infra-red restrict the algorithm development to estimate chlorophyll-a, CDOM, and Kd490.

Recently, the hyperspectral imaging system has been implemented to the monitoring of land resources. Kerekes and Baum (2003) proposed the model for the hyperspectral imaging system to forecast remote sensing performance. The hyperspectral images were applied to many field of land remote sensing to identify and classify land objects (Mahesh and Mather, 2003, Haboudane et al., 2004, Thenkabail et al., 2004). Shafri et al. (2007) studied the performance of classification methods for the hyperspectral imaging data among the maximum likelihood classification, the spectral angle mapper, the nural network, and the decision tree classifiers. Plaza (2006) discussed the possibility of the parallel processing for the hyperspectral imaging. These land applications are intended to classify targets and slightly different from the application in the oceanography.

In advance to the application of the hyperspectral sensor to the oceanography, the atmospheric correction was proposed with a spectrum-matching technique (Gao et al., 2000). Base on these studies, the ocean Portable Hyperspectral Image for Low-Light Spectroscopy (ocean PHILLS) was developed and demonstrated a good spectrum measurements as well as in-situ measurements (Davis et al., 2002). The hyperspectral sensors are applied to the coastal region to monitor the benthic habitats (Dierssen et al., 2003, Filippi et al., 2006), and to the coral reef (Mishra et at., 2007). In the oceanography, the coastal water is the strong interest to be studied, because of their sensitivity to the environmental change on the land and human activities like the dam construction in the upstream region of rivers. The coastal water shoud be analyzed from the remote sensor with discreminating substances in the water.

In this study, we discuss a possibility to estimate CDOM as the inherent optical properties as a function of the aparent optical properties from the hyperspectral imaging data. We introduce the in-situ measurements including CTD profiling, water sampling, and following water analysis, which are conducted simultanously with the flight and measurements by the airborne hyperspectrum sensor near Japan.

2. METHOD FOR ALGORITHM DEVELOPMENT

2.1 CTD profiling with PAR sensor

The conductivity, tempeature and depth sensors (CTD, RBR-420) with the photo-synthetically available radiation (PAR) sensor are deployed from a small boat to get the vertical profile of water temperature, salinity, and PAR. This profiler is operated in a logger mode, and data are retrieved after the cruise. The PAR sensor gives the downwelling irradiance integrated from 400 to 700 nm. The profiles given by CTD will provide us the basic physical concept of the water column.

2.2 Irradiance and radiance measurements with on-board spectrum meter

The spectrum irradiance and radiance radiometers (TRIOS) are operated to measure the downwelling irradiance and the surface upwelling radiance with the above water measurement protocol (Hooker and Lazin, 2000). The spectrum coverage of these radiometers are from 350 to 900 nm. Also, the spectrum irradiance radiometer is deployed into the water column to estimate the diffused attenuation coefficient ($Kd(\lambda)$) from the downwelling irradiance measurement at two different depths. The diffused attenuation coefficient at 490 nm is reffered as one parameter to represent the concentration of suspended particles, which absorb and scatter the light penetration in the water column.

2.3 Water sampling

The surface water is sampled with a bucket sampling and the water near the bottom or at 10 m is sampled with the Niskin water sampler. The sampled water is analyzed to know the chlorophyll-a concentration, the nutrients concentration, the CDOM, and the suspended particles.

The chlorophyll-a concentration is determined by the fluorometric determination (Welschmeyer, 1994). The sampled sea water is filtered by the GF/F glass fiber filter. The GF/F filter is soaked with N, N-dimethylformamide for more than 24 hours. The fluorescence of the soaking liquid is measured by the Turner AU-10 to detemine the chlorophyll-a concentration.

A large portion of the CDOM is considered as the terrestrially derived dissolved organic carbon that enters the ocean and some portion of the CDOM is from the fate of phytoplankton and zooplankton in the ocean. As the CDOM is defined by the spectrum absorption at 300 nm, the CDOM exhibits a distinct absorption at the ultra-violet (UV) spectrum. The UV light from the solar irradiation has a function to inhibits a photosynthesis or to destroy the phytoplankton cell in the water. The UV penetration along the water column varies with the concentration of CDOM in the water. The sampled water is measured by the absorption spectrophotometer with 10 cm optical cell from 300 to 800 nm.

Suspended particles within the water are partly inorganic particles from river or ocean floor and organic particles from biogenic activities in the ocean. The chemical comsition of suspended particles vary and its optical properties also different in region. In this study, the sea water is filtered by the membran filter with a pore size of 0.2 μm and its dry weight is computed as the concentration of suspended particles in the unit volume. The concentration of suspended particles is compared with the diffused attenuation coefficient at 490 nm.

2.4 Hyperspectrum sensor measurements

The Airborne Imaging Spectrometer for Applications (AISA) is deployed synchronously with the in-situ measurement. The visible and near infrared sensor called Eagle and the short wave infrared sensor called Hawk are concurrently operated to get the surface radiance from 400 to 2400 nm with 190 channels.

The AISA data are processed for the atmospheric correction by the Fast Line-of-Sight Atmospheric Analysis of Spectral Hyercubes (FLAASH) to estimate the water leaving radiance.

3 DISCUSSION

The Sea Wide Field-of-View Sensor (SeaWiFS) and the Moderate Image Scanning Radiometer (MODIS), which have been used for ocean color monitoring, have the discrete spectrum bands, where a limited combination of spectrum bands are applied to estimate the concentrations of water substances. In contrast, the hyperspectrum sensor provides a continuous spectrum observation in all spectrum region with including a possibility to estimate geophysical parameters in different ways from the traditional ocean color algorithms.

Currently, the inherent optical properties like CDOM or Kd490 are estimated from the limitted number of apparent optical properties. Johannessen et al. (2003) proposed the empirical equation to estiamte the diffused attenuation coefficient at 323 nm, Kd(323), as follows;

$$K_d(323) = 0.781[R_{rs}(412)/R_{rs}(555)]^{-1.07} \quad (1)$$

where Rrs is the remote sensing reflectance that is given from the direct measurement of the remote sensor and the extrateristrial solar irradiation. Then, the spectral absorption coefficient of CDOM, $a_{CDOM}(323)$, is given by;

$$a_{CDOM}(323)=0.904K_d(323)-0.00714 \quad (2).$$

Simillary, Kd490 is given by the empirical equation (Mueller, 2000);

$$K_d(490)=0.016+0.15645[{}_nL_w(490)/{}_nL_w(555)]^{1.5401} \quad (3)$$

These estimates of inherent optical properties from the apparent optical porperties have a freedom of 2 channels only.

In the hyperspectral remote sensing, we are able to increase the freedom of signal variation with more spectral bands. Fig. 1 shows the sample plots of three targets in 2007. One spectrum plot, showing a strong radiance in the near infra-red, is the upwelling radiance from the forest. Other two spectrum plots, exhibiting a low radiance in all spectrum range, are corresponding to the upwelling radiance from two different water mass.

We are currently, validating the hyperspectral data and in-situ data, and constracting a new algorithm to estimate an absorption coefficient for CDOM, a diffused attenuation coefficient of the water, and including chlorophyll-a concentration on the coastal waters.

The hyperspectrum remote sensing over the water is quite different from the target over lands, where the traditional classification does not work and it is required to classify the analogously distributed substances.

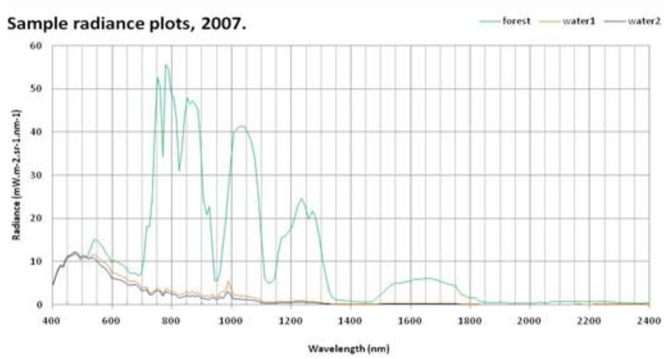

Fig. 1 Sample radiance plots from AISA 2007

REFERENCES

Chami, M. (2007), Importance of the polarization in the retrieval of oceanic constituents from the remote sensing reflectance, *J. G. R.,* 112, C05026, doi:10.1029/2006JC003843.

Davis, C. O., J. Bowles, R. A. Leathers, D. Korwan, T. V. Downes, W. A. Snyder, W. J.

Rhea, W. Chen, J. Fisher, W. P. Bissett, and R. A. Reisse (2002), Ocean PHILLS hyperspecral imager: design, characterization, and calibration, *Optics Express*, 10 (4), 210-221.

Dierssen H. M., R. C. Zimmerman, R. A. Leathers, T. V. Downes, and C. O. Davis (2003), Ocean color remote sensing of seagrass and bathymetry in the Bahamas Banks by high-resolution airborne imagery, *Limnol. Oceanogr.*, 48(1, part 2), 444-4555.

Filippi, A. M., K. L Carder, and C. O. Davis (2006), Vicarious calibration of the Ocean PHILLS hyperspectral sensor using a coastal tree-shadow method, *Geophys. Res. Lett.*, 33, L22605, doi:10.1029/2006GL027073.

Gao, B. C., M. J. Montes, Z. Ahmad, and C. O. Davis (2000), Atmospheric correction algorithm for hyperspectral remote sensing of ocean color from space, *Applied Optics*, 39 (6), 887-896.

Haboudane, D., J. R. Miller, E. Pattey, P. J. Zacro-Tejada, and I. Strachan (2004), Hyperspectral vegetation indices and novel algorithms for predicting green LAI of crop canopies: Modeling and validation in the context of precision agriculture, *Remote Sensing of Environment*, 90 (3): 337-352.

Hooker, S. B., and G. Lazin (2000), The SeaBOARR-99 Field Campaign, SeaWiFS Postlaunch Technical Report Series, NASA Tech Memo 2000-206892, 8, 46pp.

IOCCG (2000), Remote Sensing of Ocean Colour in Coastal, and Other Optically-Complex, Waters, Ed. S. Sathyendranath, 140pp.

Johannessen, S. C., W. L. Miller, and J. J. Cullen (2003), Calculation of UV attenuation and colored dissolved organic matter absorption spectra from measurements of ocean color, *J. G.. R.* 108(C9), 3301, doi:10.1029/2000JC000514.

Kerekes J. P. and J. E. Baum (2003), Hyperspectral Imaging System Modeling, Lincoln Laboratory Journal, 14, 1, 117-130.

Mahesh, P. and P. M. Mather (2003), An assessment of the effectiveness of decision tree methods for land cover classification, *Remote Sensing of Environment*, 86, 554-565.

Mishra, D. R., S. Narumalani, D. Rundquist, M. Lawson, and R. Perk (2007), Enhancing the detection and classification of coral reef and associated benthic habitats: A hyperspectral remote sensing approach, *J. Geophys. Res.*, 112, C08014, doi:10.1029/2006JC003892.

Mueller, J. (2000), SeaWiFS Algorithm for the Diffuse Attenuation Coefficient, K(490), Using Water-Leaving Radiances at 490 and 555 nm, *NASA Technical Memorandum* 2000-206892, (11), 24-27.

O'reilly, J. E., S. Maritorena, B. G. Mitchell, D. A. Siegel, K. L. Carder, S. A. Garver, M. Kahru, and C. McClain (1998), Ocean color chlorophyll algorithms for SeaWiFS, *J. Geophys. Res.,*103, C11, 24,937-24,953.

Oliver, M. J., O. Schofield, T. Bergmann, S. Glenn, C. Orrico. And M. Moline (2004), Deriving in situ phytoplankton absorption for bio-optical productivity models in turbid waters, *J. Geophys. Res.*, 109, C07S11, doi:10.1029/2002JC001627.

Plaza, A. (2006), Parallel processing opens new perspectives for hyperspectral imaging, *SPIE Newsroom*, 10.1117/2.1200606.0275.

Siegel, D. A., S. Maritorena, N. B. Nelson, D. A. Hansell, and M. Lorenzi-Kayser (2002), Global distribution and dynamics of colored dissolved and detrital organic materials, *J. Geophys. Res.*, 107(C12), 3228, doi:10.1029/2001JC000965.

Shafri, H. Z. M., A. Suhaili, and S. Mansor (2007), The Performance of Maximum Likelihood, Spectral Angle Mapper, Neural Network and Decision Tree Classifiers in Hyperspectral Image Analysis, *J. Computer Science*, 3 (6): 419-423.

Thenkabail, P. S., E. A. Enclona, M. S. Ashton, B. Van, D. Meer (2004), Accuracy assessments of hyperspectral waveband performance for vegetation analysis applications, *Remote Sensing of Environment*, 91 (3-4): 354-376.

Wang, M., J. Tang, and W. Shi (2007), MODIS-derived ocean color products along the China east coastal region, *Geo. Res. Lett.*, 34, L06611, doi:10.1029/2006GL028599

Welschmeyer, N. A. (1994), Fluorometric analysis of chlorophyll a in the presence of chlorophyll b and phaeopigments, *Limnol. Oceanogr.* 39, 1985-1992

Development of Mangrove Spectral Library

Hartanto Sanjaya, Ariani Andayani
Center for Natural Resources Inventory (TISDA), Agency for Assessment and Application of Technology (BPPT).
Institute of Marine Research and Observation, Research Center for Marine Technology (PRTK), Agency for Marine and Fisheries Research (BRKP), Ministry of Marine Affairs and Fisheries

Development of mangrove spectral library

Hartanto Sanjaya, Center for Natural Resources Inventory (TISDA), Agency for Assessment and Application of Technology (BPPT).

Ariani Andayani, Institute of Marine Research and Observation, Research Center for Marine Technology (PRTK), Agency for Marine and Fisheries Research (BRKP), Ministry of Marine Affairs and Fisheries

Presented on APEC SAKE Workshop, Jakarta, 5 November 2007

- Introduction
- Methods
  - Study Site, and Survey Design
  - Mangrove Identification
  - Field Data Acquisition
- Result
- References

Introduction

- Spectral Library => finger print of objects => remote sensing data analysis.
- Mangroves => important plants in coastal zones.
- This study is to develop spectral library of Mangroves species.

Methods

- Study Site and Survey Design
- Mangrove Identification
- Field Data Acquisition (Measurement Procedure)

Method: Study Sites and Survey Design

- In September of 2007 reflectance spectra were collected in Mangrove areas, Southern part of Kabupaten Jembrana, Bali:
  - Perancak
  - Delod Brawah
  - Tuwed

Study Sites

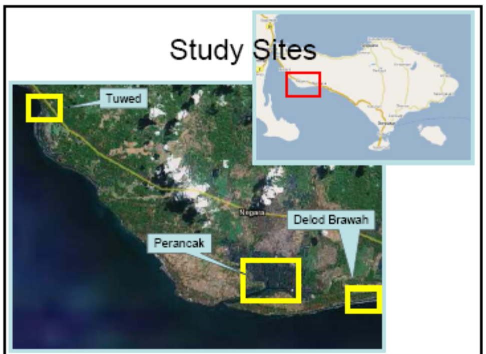

Method:
Survey Design

- Survey Design:
  - mangrove mapping ("roughly")
    - identify the locations,
    - plan the optimum tracks
    - need special day(s)
  - Acquisition timing:
    - effective time range: 10am – 2pm
    - Number of days: depends

Method:
Field Data Acquisition

- Reference and dark spectrum must be measured if at any time any sampling variable changes.
- In order to remove random noise from the spectral reflectance, the three spectra collected for each sample were averaged.

Method:
Mangrove Identification

- "keys" to identify mangrove species:
  - Roots
  - Leaves
  - Flowers and Fruits
  - Tree's shape
- Reference: Handbook of Mangroves

(in actions ☺…)

Tuwed, Jembrana, 2007

Mangrove Identification

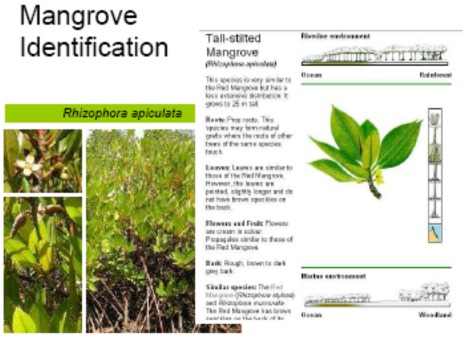

Result

- Perancak Estuary (13 species):
  - *Acanthus ilicifolius, Aegiceras corniculatum, Avicennia alba, Avicennia marina, Bruguiera gymnorrhiza, Ceriops decandra, Hibiscus tiliaceus, Nypa fruticans, Sonneratia alba, Excoecaria agalocha, Xylocarpus granatum, Rhizophora stylosa, Rhizophora apiculata*
- Delod Brawah (2 species):
  - *Pandanus tectorius, Scaevola tacada*
- Tuwed (6 species):
  - *Ceriops decandra, Ceriops tagal, Spinifex littoreus, Osbornia octodonta, Sonneratia alba, Thespesia populnea*

Method:
Field Data Acquisition

- For each tree, 3 spectral measurements were taken of the sunlit side of the tree, at nadir from a distance of approximately 10 - 20 cm using a USB2000 Ocean Optics field spectrometer, equipped with a fiber optic cable of 1.5m.

Rhizophora apiculata

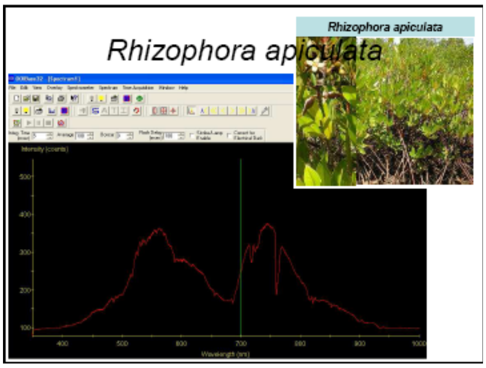

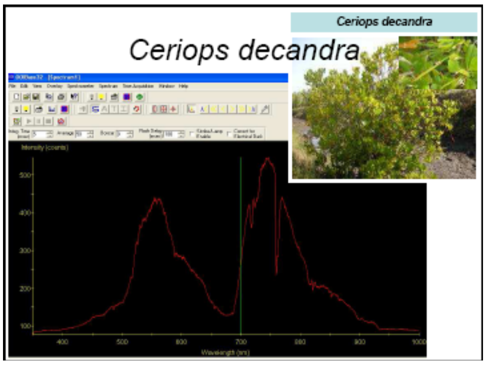

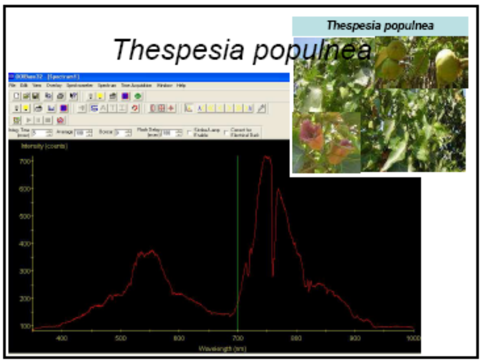

References

- Ferwerda, et.al., 2002, *Field Spectrometry of Leaves for Nutrient Assessment*, ITC The Netherland.
- Kitamura, Sozo et,al., 1997, *Handbook of Mangroves in Indonesia – Bali & Lombok*, Ministry of Forestry Indonesia, Japan International Cooperation Agency (JICA), The International Society of Mangrove Ecosystems (ISME), ISBN:4-906584-04-7.

Land Cover Classification of Fordata Island with Hyperspectral Data

MCG. Frederik, Y. Wahyudi, H. Sanjaya, M. Sadly, D. Yusuf, I. Farahidy
Center for Technology of Natural Resources Inventory (PTISDA)
Agency for Assessment and Application of Technology (BPPT)

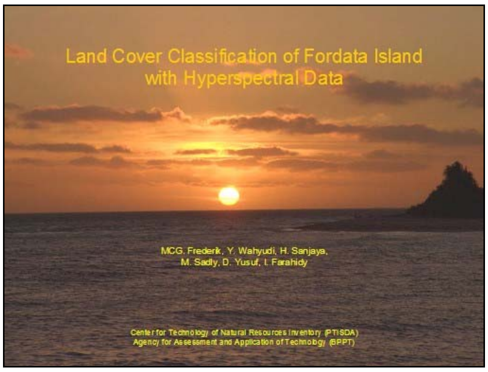

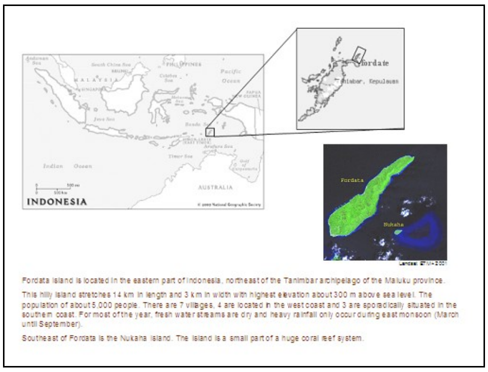

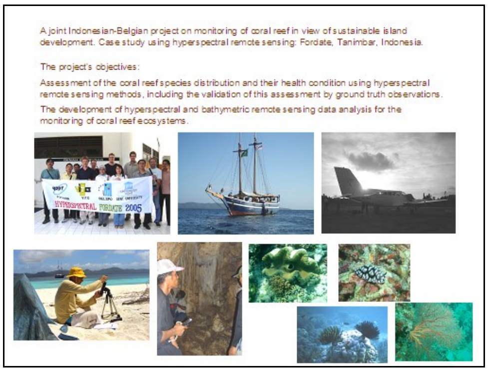

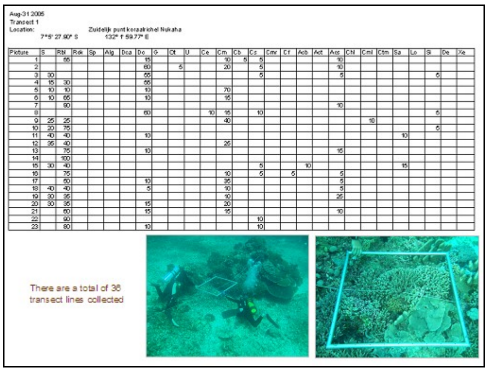

Picture	S	Rbl	Rdk	Sp	Alg	Dca	Dc	G	Ot	U	Ce	Cm	Cb	Cs	Cmr	Cf	Acb	Act	Acs	CN	Cml	Ctm	Sa	Lo	Si	De	Xe
1		55					15					10	5	5					10								
2							60		5			20		5					10								
3	30						65							5					5						5		
4	15	30					55																				
5	10	10					10					70															
6	10	65					10					15															
7		60																	10								
8							60				10	15		10											5		
9	25	25										40									10						
10	20	75																							5		
11	40	40					10																10				
12	35	40										25															
13		75					10												15								
14		100																									
15	30	40												5			10						15				
16		75										10		5		5			5								
17		60					10					35							5								
18	40	40					5					10							5								
19	30	35										10							25								
20	30	35					15					20															
21		60					15					15							10								
22		90												10													
23		80					10							10													

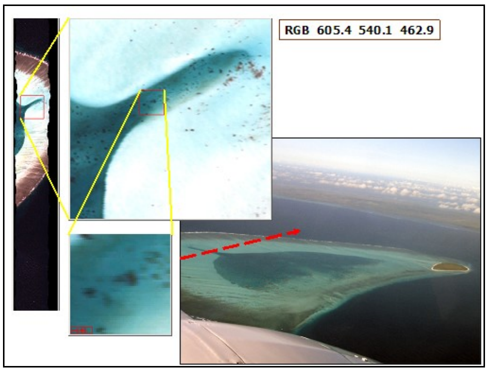
RGB 605.4 540.1 462.9

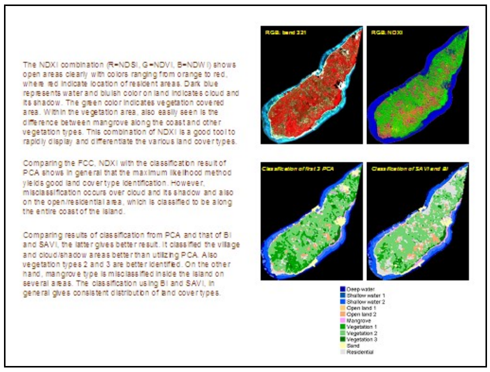
The NDXI combination (R=NDSI, G=NDVI, B=NDWI) shows open areas clearly with colors ranging from orange to red, where red indicate location of resident areas. Dark blue represents water and bluish color on land indicates cloud and its shadow. The green color indicates vegetation covered area. Within the vegetation area, also easily seen is the difference between mangrove along the coast and other vegetation types. This combination of NDXI is a good tool to rapidly display and differentiate the various land cover types.
Comparing the FCC, NDXI with the classification result of PCA shows in general that the maximum likelihood method yields good land cover type identification. However, misclassification occurs over cloud and its shadow and also on the open/residential area, which is classified to be along the entire coast of the island.
Comparing results of classification from PCA and that of BI and SAVI, the latter gives better result. It classified the village and cloud/shadow areas better than utilizing PCA. Also vegetation types 2 and 3 are better identified. On the other hand, mangrove type is misclassified inside the island on several areas. The classification using BI and SAVI, in general gives consistent distribution of land cover types.
RGB: band 321
RGB: NDXI
Classification of first 3 PCA
Classification of SAVI and BI
Deep water
Shallow water 1
Shallow water 2
Open land 1
Open land 2
Mangrove
Vegetation 1
Vegetation 2
Vegetation 3
Sand
Residential

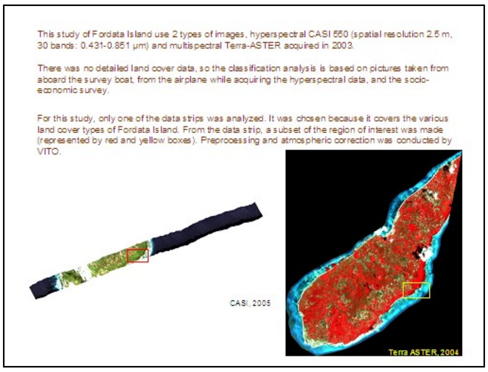
This study of Fordata Island use 2 types of images, hyperspectral CASI 550 (spatial resolution 2.5 m, 30 bands: 0.431-0.851 μm) and multispectral Terra-ASTER acquired in 2003.
There was no detailed land cover data, so the classification analysis is based on pictures taken from aboard the survey boat, from the airplane while acquiring the hyperspectral data, and the socio-economic survey.
For this study, only one of the data strips was analyzed. It was chosen because it covers the various land cover types of Fordata Island. From the data strip, a subset of the region of interest was made (represented by red and yellow boxes). Preprocessing and atmospheric correction was conducted by VITO.
CASI, 2005
Terra ASTER, 2004

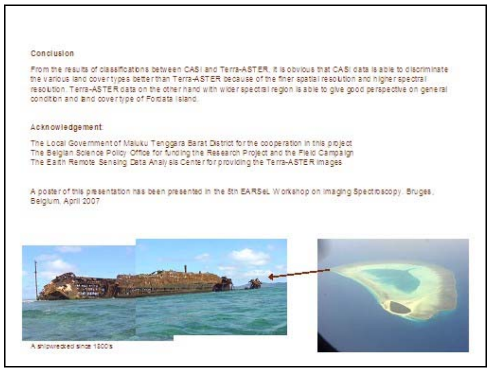
Conclusion
From the results of classifications between CASI and Terra-ASTER, it is obvious that CASI data is able to discriminate the various land cover types better than Terra-ASTER because of the finer spatial resolution and higher spectral resolution. Terra-ASTER data on the other hand with wider spectral region is able to give good perspective on general condition and land cover type of Fordata Island.
Acknowledgement:
The Local Government of Maluku Tenggara Barat District for the cooperation in this project
The Belgian Science Policy Office for funding the Research Project and the Field Campaign
The Earth Remote Sensing Data Analysis Center for providing the Terra-ASTER images
A poster of this presentation has been presented in the 5th EARSeL Workshop on Imaging Spectroscopy. Bruges, Belgium, April 2007
A shipwrecked since 1800's

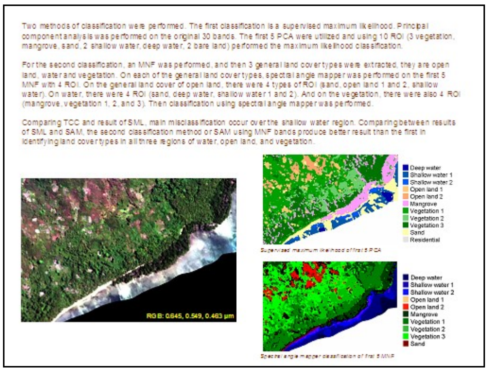
Two methods of classification were performed. The first classification is a supervised maximum likelihood. Principal component analysis was performed on the original 30 bands. The first 5 PCA were utilized and using 10 ROI (3 vegetation, mangrove, sand, 2 shallow water, deep water, 2 bare land) performed the maximum likelihood classification.
For the second classification, an MNF was performed, and then 3 general land cover types were extracted, they are open land, water and vegetation. On each of the general land cover types, spectral angle mapper was performed on the first 5 MNF with 4 ROI. On the general land cover of open land, there were 4 types of ROI (sand, open land 1 and 2, shallow water). On water, there were 4 ROI (sand, deep water, shallow water 1 and 2). And on the vegetation, there were also 4 ROI (mangrove, vegetation 1, 2, and 3). Then classification using spectral angle mapper was performed.
Comparing TCC and result of SML, main misclassification occur over the shallow water region. Comparing between results of SML and SAM, the second classification method or SAM using MNF bands produce better result than the first in identifying land cover types in all three regions of water, open land, and vegetation.
RGB: 0.645, 0.549, 0.463 μm
Deep water
Shallow water 1
Shallow water 2
Open land 1
Open land 2
Mangrove
Vegetation 1
Vegetation 2
Vegetation 3
Sand
Residential
Supervised maximum likelihood of first 5 PCA
Deep water
Shallow water 1
Shallow water 2
Open land 1
Open land 2
Mangrove
Vegetation 1
Vegetation 2
Vegetation 3
Sand
Spectral angle mapper classification of first 5 MNF

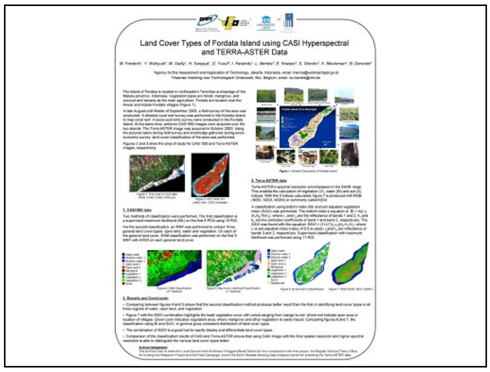
Land Cover Types of Fordata Island using CASI Hyperspectral and TERRA-ASTER Data

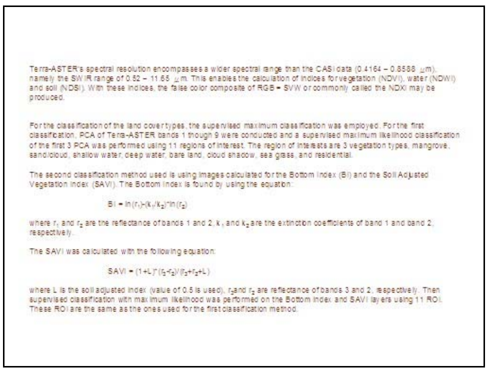
Terra-ASTER's spectral resolution encompasses a wider spectral range than the CASI data (0.4164 – 0.8588 μm), namely the SWIR range of 0.52 – 11.65 μm. This enables the calculation of indices for vegetation (NDVI), water (NDWI) and soil (NDSI). With these indices, the false color composite of RGB = SVW or commonly called the NDXI may be produced.
For the classification of the land cover types, the supervised maximum classification was employed. For the first classification, PCA of Terra-ASTER bands 1 though 9 were conducted and a supervised maximum likelihood classification of the first 3 PCA was performed using 11 regions of interest. The region of interests are 3 vegetation types, mangrove, sand/cloud, shallow water, deep water, bare land, cloud shadow, sea grass, and residential.
The second classification method used is using images calculated for the Bottom Index (BI) and the Soil Adjusted Vegetation Index (SAVI). The Bottom Index is found by using the equation:
$BI = \ln(r_1)-(k_1/k_2)*\ln(r_2)$
where r_1 and r_2 are the reflectance of bands 1 and 2, k_1 and k_2 are the extinction coefficients of band 1 and band 2, respectively.
The SAVI was calculated with the following equation:
$SAVI = (1+L)*(r_3-r_2)/(r_3+r_2+L)$
where L is the soil adjusted index (value of 0.5 is used), r_3 and r_2 are reflectance of bands 3 and 2, respectively. Then supervised classification with maximum likelihood was performed on the Bottom Index and SAVI layers using 11 ROI. These ROI are the same as the ones used for the first classification method.


Thank you!

Observations of SST and Chlorophyll-a Concentration in Coastal Sea of Vietnam Using Ocean Color Remote Sensing

Tu Tuyet Hong and Nguyen Phi Khu
University Technical Education -HCMC
Vietnam National University - HCMC

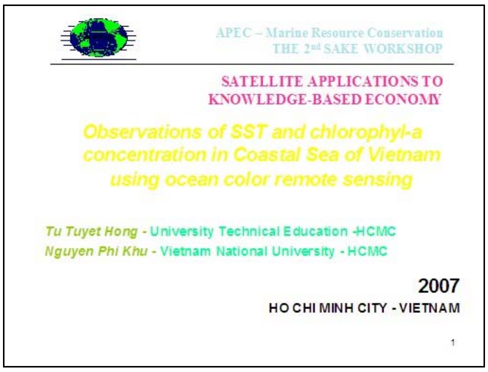

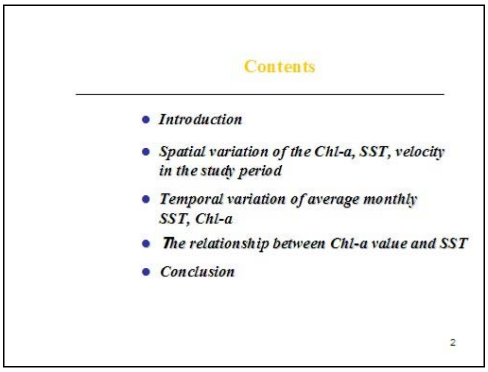

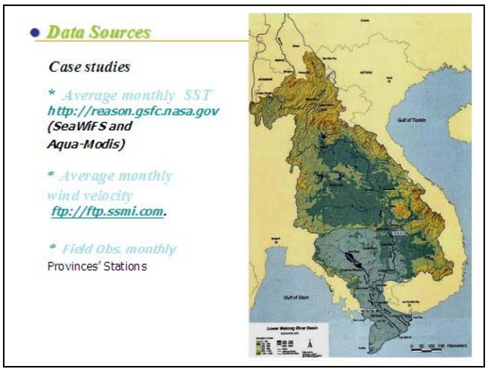

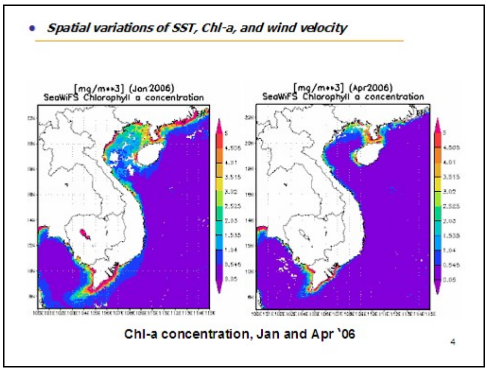

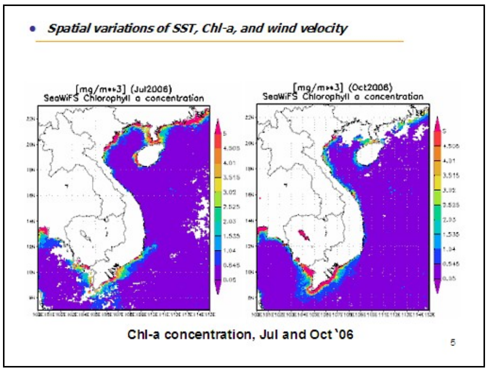

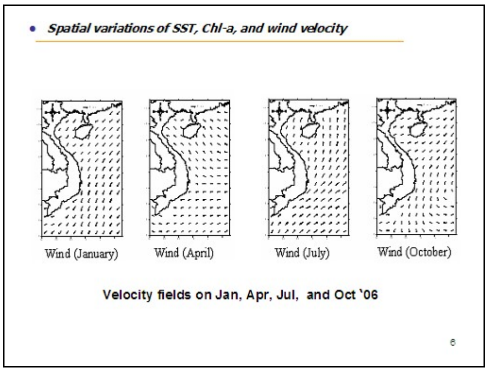

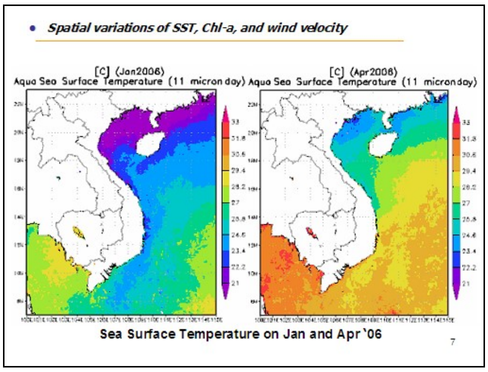

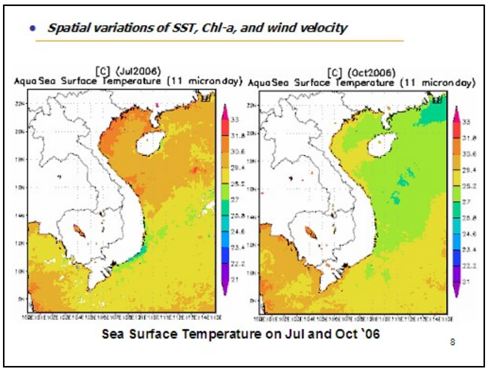

Temporal variation of average monthly SST, Chl-a

Case study: Binh Thuan Province

Time series of Chl-a at Binh Thuan Province in SWM

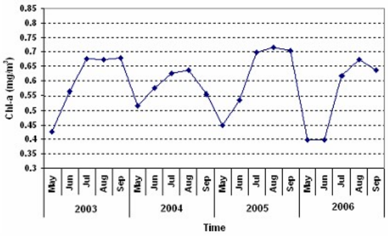

9

- ***Temporal variation of average monthly SST, Chl-a***

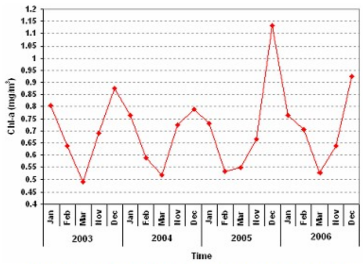

Time series of Chl-a at Binh Thuan Province in NEM

10

- ***The relationship between Chl-a value and SST***

R = 0.907

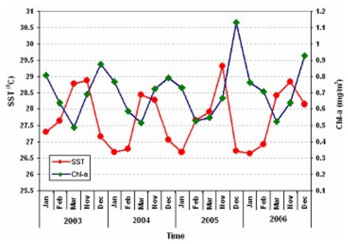

The relationship between SST and Chl-a in NEM season at Binh thuan coastal

11

- ***The relationship between Chl-a value and SST***

	Chl-a			
	2003	2004	2005	2006
Jan	0.805956	0.764605	0.729043	0.764332
Feb	0.638264	0.589655	0.531317	0.707170
Mar	0.490580	0.517036	0.548989	0.526767
Apr	0.398628	0.400108	0.440129	0.388418
May	0.426313	0.516784	0.450032	0.398820
Jun	0.565014	0.575720	0.536319	0.398655
Jul	0.675098	0.625395	0.697992	0.617969
Aug	0.672159	0.636596	0.716033	0.672409
Sep	0.678790	0.556515	0.705443	0.638000
Oct	0.747492	0.673670	0.600371	0.697513
Nov	0.689427	0.723766	0.667040	0.638014
Dec	0.875886	0.790421	1.130850	0.926213

Selected averaging area: lat=[7.0N,12.0N], lon=[100.0E,110.0E]

The relationship between SST and Chl-a in NEM season at Binh thuan coastal

12

- ***The relationship between Chl-a value and SST***

R = 0.879

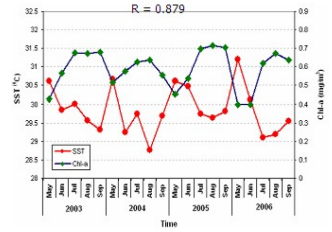

The relationship between SST and Chl-a in SWM season at Binh thuan coastal

13

- ***The relationship between Chl-a value and SST***

	SST			
	2003	2004	2005	2006
Jan	27.303	26.680	26.685	26.651
Feb	27.651	26.777	27.658	26.935
Mar	28.766	28.440	27.936	28.401
Apr	30.359	29.988	29.762	30.483
May	30.611	30.665	30.615	31.208
Jun	29.858	29.254	30.468	30.117
Jul	30.014	29.741	29.737	29.110
Aug	29.574	28.768	29.632	29.190
Sep	29.323	29.683	29.822	29.553
Oct	29.007	29.028	29.798	29.335
Nov	28.871	28.280	29.318	28.841
Dec	27.160	27.068	26.733	28.158

Averaging area: lat=[7.0N,12.0N], lon=[100.0E,110.0E]

The relationship between SST and Chl-a in SWM season at Binh thuan coastal

14

Recommendation

- ***Spatial distribution features of SST and Chl-a in the Vietnam Sea depend up on: monsoons, precipitation, river runoff, upwelling, ect.***
- ***Temporal variation features of SST and Chl-a indicated that there are 4 seasons at Vietnam Sea: NE monsoon, Transition period from Spring to Summer, SW monsoon, and Transition period from Summer to Winter.***
- ***Along southern Vietnamese coast was formed a nearshore strip of low SST and high Chl-a during SW monsoon period.***
- ***Seasonal Chl-a variation in Vietnam waters is different between the north of Vietnam and south of Vietnam. The central of Vietnam waters is the lowest Chl-a concentration in both two seasons.***
- ***This study found that high Chl-a concentration at south of Vietnam waters from July to September during SWM (> 0.65 mg/m³).***

15

Thank you very much !

16

A Multi-Scale Detection Technique for Anomaly on Ocean Surface Using Optical Satellite Images

Chi-Farn Chen and Li-Yu Chang
Center for Space and Remote Sensing Research, National Central University, Chinese Taipei

ABSTRACT

Using satellite images for monitoring oceanic surface has become popular recently. One of the striking feature can be detected from satellite image is the anomalous phenomenon on oceanic surface. In general, it is easy to observe the diversified anomalies, caused by abrupt change of the reflectance on oceanic surface, on the optical satellite images. Among them, the anomaly caused by the pollution of oil spill or discharge of waste water is commonly observed. In this study, a multi-scale detection technique for studying anomaly on oceanic surface from optical satellite image is proposed. The study uses a RX algorithm at first to measure the degree of anomaly for each image pixel. Next, a series of Laplace of Gaussian operators at different scale are applied to extract the possible anomalous patches in different size. Finally, a threshold from the cumulative distribution of the RX algorithm's output is used to extract final anomalous patches. Experiment results show that the proposed method can extract striking anomalous patches at offshore or open water areas in different optical satellite images.

Keywords: Anomaly, Multi-Scale Detection, Satellite Images

1. INTRODUCTION

The radiant intensity at optical sensor is directly related to the reflectance of target. For anomalous targets on ocean surface, their reflectance usually varies a lot with respect the background. Therefore, the anomalous phenomena on ocean surface can be easily distinguished in optical sensors. In general, the causes to form different kinds of anomalies are diverse. The most common example is the anomaly causes by the pollution of oil spill (Brown and Fingas, 2001) or discharge of waste water (Keeler *et al*., 2005). Theoretically, it is not difficult to develop an algorithm to extract those kinds of anomalies from images acquired from optical sensors. In fact, the reflectance responses for ocean surface and its related phenomena generally tend to be very low. This effect makes anomalies on ocean surface be affected by noise very easily. Especially for those anomalies have reflectance much lower than normal sea water. Consequently, it is not possible to set a clear threshold to extract anomalies form background.

2. METHODOLOGY

In this study, a multi-scale detection technique for anomaly on ocean surface from optical satellite image is proposed. The method can be divided into three sections: (1) A RX algorithm (Reed and Yu, 1990) is used at beginning to measure the degree of anomaly for each image pixel from multi-spectral satellite image. (2) For reducing the effect of noise, a series of Laplace of Gaussian operators (Pratt, 1991) at different scale are applied to extract the possible anomalous patches in different size. (3) A threshold from the cumulative distribution of the RX algorithm's output is used to extract final anomalous patches.

2.1 Measuring the degree of anomaly using RX algorithm

The RX algorithm shown in equation (1) actually is no more than a method to retrieve the normalized spectral distance for each pixel from multi-spectral image with respect to image mean.

$$\delta_{RXD}(r) = (r-\mu)^T K_{L*L}^{-1} (r-\mu) \qquad (1)$$

where

K : Covariance matrix of source image.
r: Spectral vector of each pixel.
μ : Image mean.

Originally, RX algorithm is also a method used to extract anomaly from remotely sensed images (Chang and Heinz, 2000). However, the most important assumption for using this algorithm is that the amount of anomalies should much less than the background. In fact, this assumption may not be hold because we actually do not know how much less is the anomalies. In addition, a clear threshold has to be set in this algorithm. This is also not practical for the noisy nature of out data.

2.2 Filtering possible anomalous patches using Laplace of Gaussian operation

Generally speaking, the anomalies are the areas that greater than mean value in normalized distance image. On the other hand, the convex areas of normalized distance image may be potential areas of anomalies. For the purpose to detect convex areas, a second order derivative operator "Laplace of Gaussian" is introduced.

In fact, Laplace of Gaussian is the Laplace of a Gaussian smooth operator. Equation (2) is a 2 dimensional Gaussian smooth operator with standard deviation "s". Equation (3) is the Laplace of Gaussian operator. Fig. 1 illustrates the pattern of Laplace of Gaussian operator.

$$G(x,y) = \frac{1}{\sqrt{2\pi s^2}} \exp\left(-\frac{x^2+y^2}{2s^2}\right) \qquad (2)$$

$$\nabla^2 G(x,y) = \frac{1}{\pi s^4}\left[1 - \frac{x^2+y^2}{2s^2}\right] \cdot e^{-\frac{x^2+y^2}{2s^2}} \qquad (3)$$

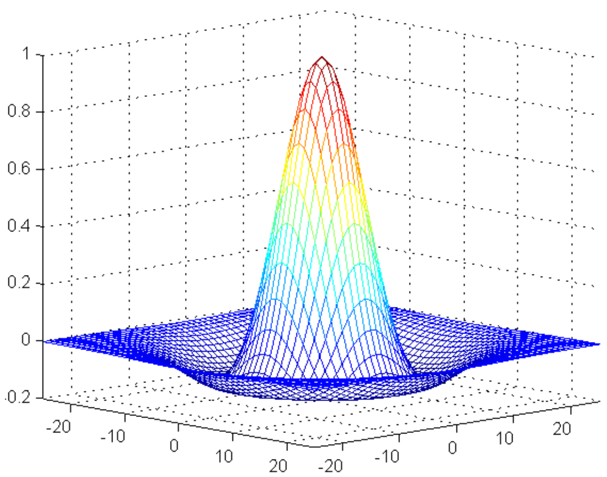

Fig. 1: The pattern of Laplace of Gaussian operator

Different scale of Laplace of Gaussian operator can be acquired by adjusting "s" parameters. The larger of "s" is used, the more smooth effect is achieved. Therefore, convex areas in different scales can be acquired by following procedure:

2.2.1.1 Convolving the normalized distance image with different scale of Laplace of Gaussian operator.

2.2.1.2 Taking positive part of the convolution output.

The following step in this section is to integrate those convex areas in different scales. In this study, we simply use "OR" operation to combine the entire convolution outputs at each scale. The reason that allows us to do this is the convex area in larger scale can always include the convex area in smaller scale. Therefore, after we use "OR" operation to combine all scale's convolution outputs, the convex areas comes from different scales will be merged together.

2.3 Extracting anomalous patches using threshold

The convex areas in different scales acquired in last section are only potential anomalies. To finally conclude a convex area is an anomaly, we need to check the mean of normalized distance for all pixels in this patch. The selection of threshold used for assessing a patch is based on the cumulative distribution function of normalized distance. In this study, the threshold is set to the value that corresponding to 90% of cumulative distribution. A patch will be concluded as an anomaly if the patch mean is greater than threshold.

3 EXPERIMENTAL RESULTS

In this study, two experiments containing different characteristic of anomalies are test.

3.1 Case 1

In this case, the source image is SPOT-5 multi-spectral image. The image acquisition date was on 03/30/2006. The location is in south of Chinese Taipei. Fig. 2 shows the test image for this case. Notice that the anomalies in this dataset are darker than the background. Fig. 3 is the extracted anomalies using proposed scheme.

(a)

(b)

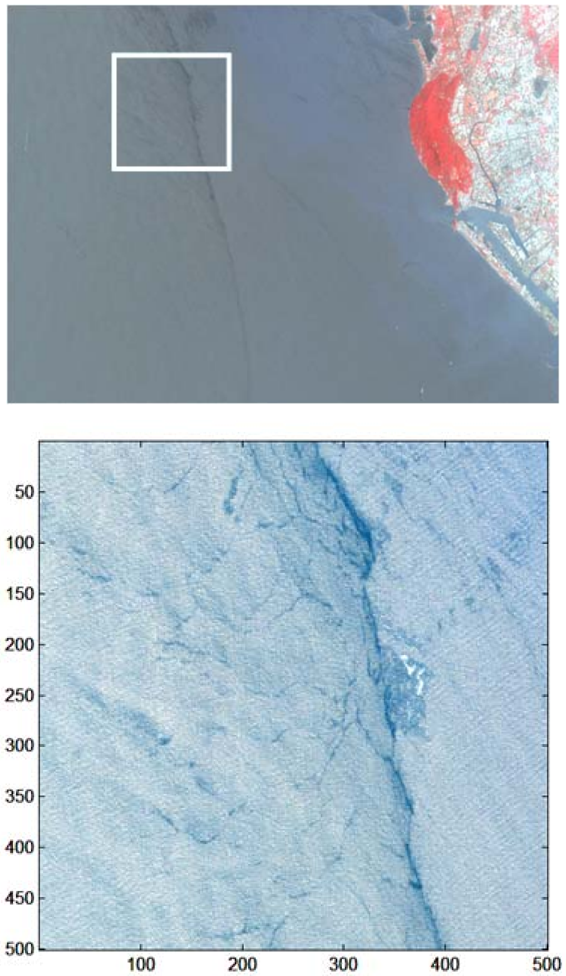

Fig. 2: The test image for case 1, (a) source image and study area for this case, (b) enlarged and enhanced image of study area.

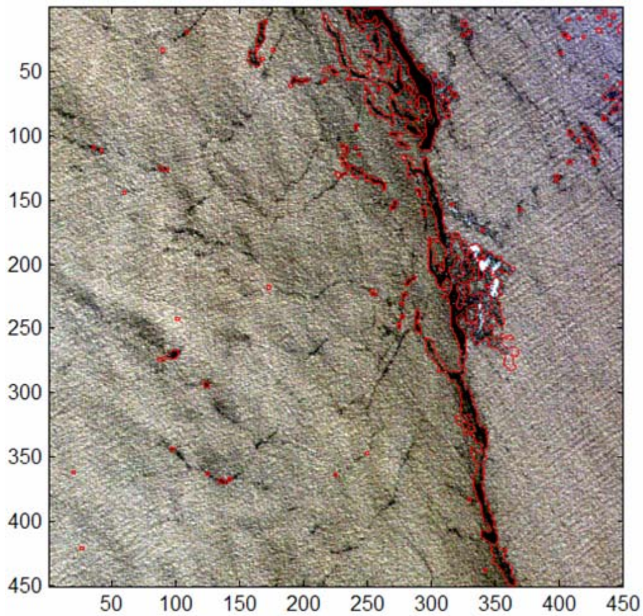

Fig. 3: The extracted anomalies overlay on source image

3.2 Case 2

In this case, the source image is also SPOT-5 multi-spectral image. The image acquisition date was on 07/18/2007. The location is in north of Chinese Taipei. Fig 4 shows the test image for this case. Notice that the anomalies in this dataset are brighter than the background. Fig. 5 is the extracted anomalies using proposed scheme.

(a)

(b)

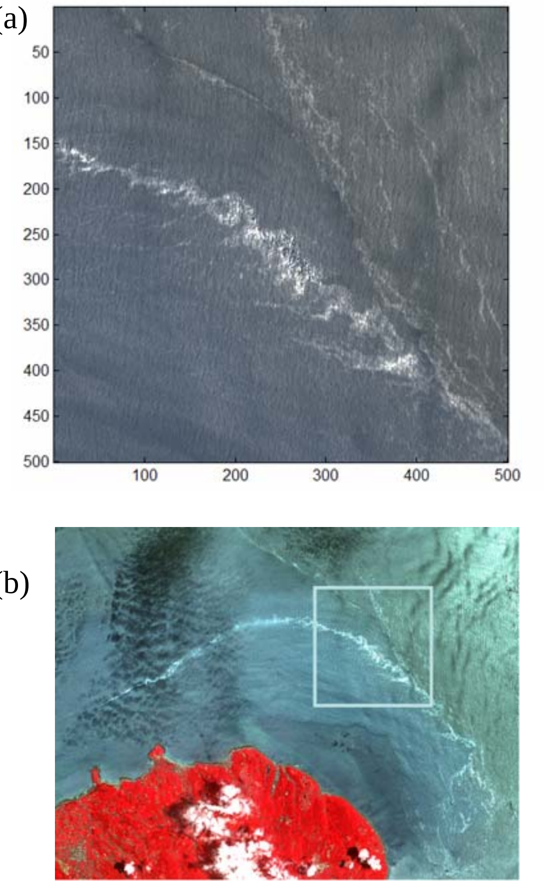

Fig. 4: The test image for case 2, (a) source image and study area for this case, (b) enlarged and enhanced image of study area.

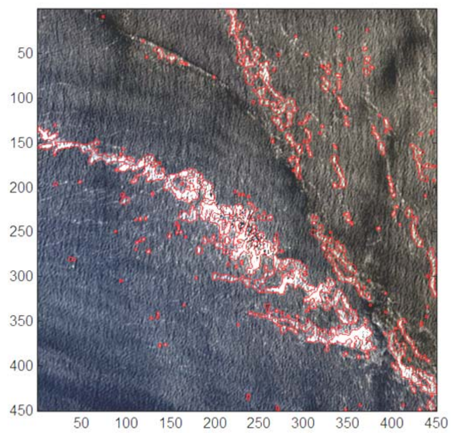

Fig. 5: The extracted anomalies overlay on source image

4. CONCLUSIONS

On ocean surface, the proposed scheme can successfully extract different kinds of anomalies using optical satellite images. Using RXD to retrieve normalized spectral distance enables that various kinds of anomalies can be extracted at the same time. With multi-scale Laplace of Gaussian operator, the noise is effectively reduced and the anomaly in different size can be separated to its corresponding scales for further processing.

The anomalies in larger scale tend to have a smoother boundary because of the stronger smooth effect introduced by large scale Laplace of Gaussian operator. Such problem may be solved by setting up a buffer zone along the boundary and using the anomalies detected in a smaller scale to replace those in this zone. This procedure can be used iteratively until the smallest scale is reached. The only fixed threshold used in proposed scheme is the normalized distance value at 90% of the cumulative distribution. A more adaptive way for estimating this threshold should be carried out to relax this limitation in future researches.

REFERENCES

Brown CE, Fingas MF (2001) New space-borne sensors for oil spill response, Proceedings of International Oil Spill Conference 2001, Tampa, Florida: 911-916

Keeler RN, Bondur VG, Gibson CH (2005) Optical satellite imagery detection of internal wave effects from a submerged turbulent outfall in the stratified ocean, Geophysical Research Letters, 32: L12610

Reed IS, Yu X (1990) Adaptive multiple-band CFAR detection of an optical pattern with unknown spectral distribution, IEEE Transactions on Acoustic, Speech and Signal Processing, 38(10): 1760-1770

Pratt WK (1991) Digital image processing, Wiley, New York

Chang CI, Heinz D (2000) Constrained subpixel detection for remotely sensed images, IEEE Transactions on Geoscience and Remote Sensing, 38(3): 1144-1159

Simulation of Spilled Oil in Seribu Islands Waters

Safwan Hadi1,2, Totok Suprijo1, Haris Sunendar2
1 Resarch Group of Oceanography, ITB
2 Center for Marine and Coastal Development, ITB

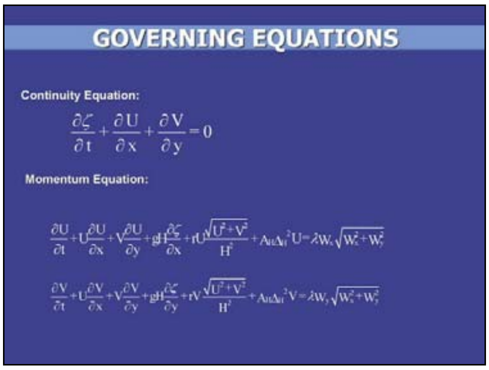

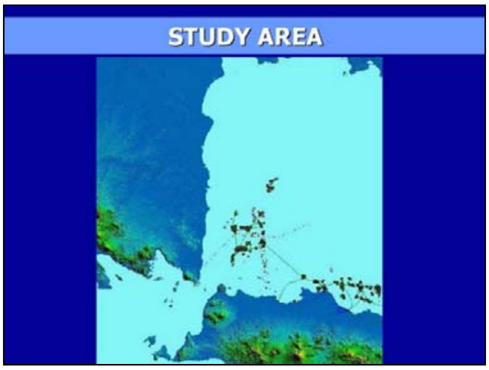

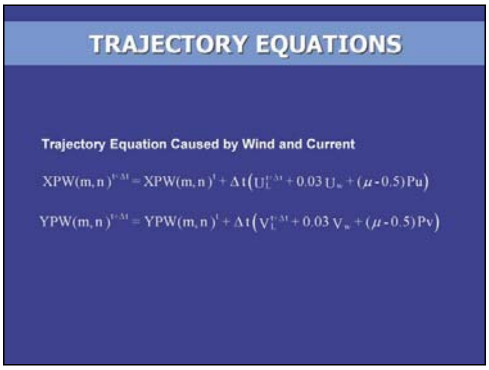

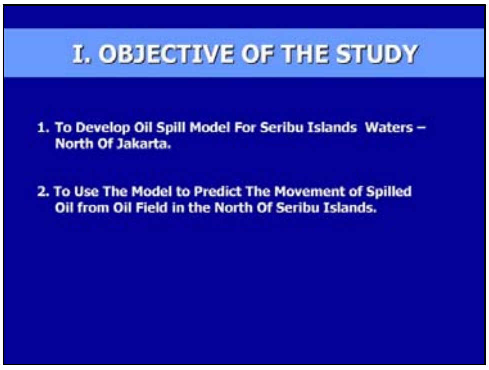

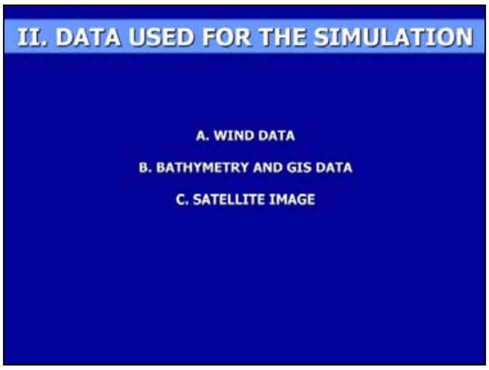

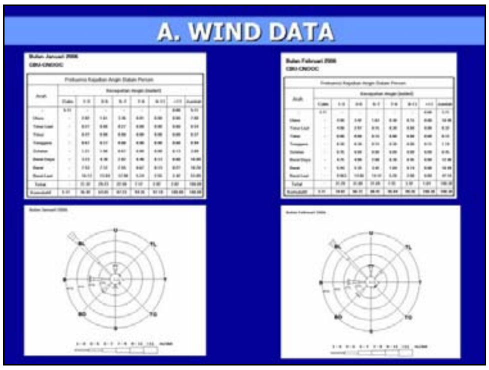
A. WIND DATA

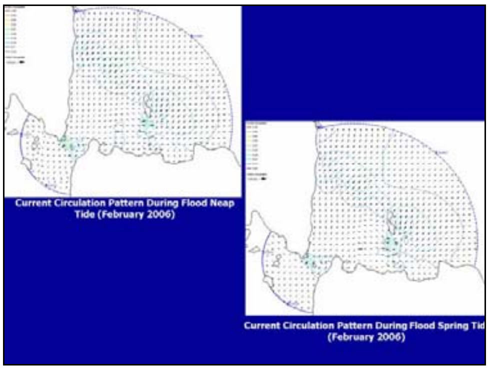
Current Circulation Pattern During Flood Neap Tide (February 2006)
Current Circulation Pattern During Flood Spring Tid (February 2006)

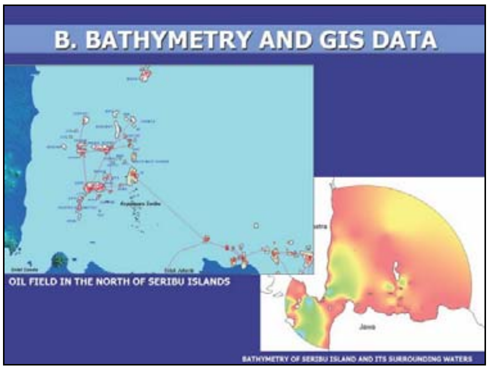
B. BATHYMETRY AND GIS DATA
OIL FIELD IN THE NORTH OF SERIBU ISLANDS
BATHYMETRY OF SERIBU ISLAND AND ITS SURROUNDING WATERS

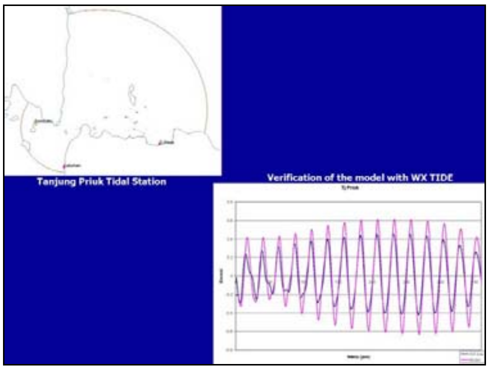
Tanjung Priuk Tidal Station
Verification of the model with WX TIDE

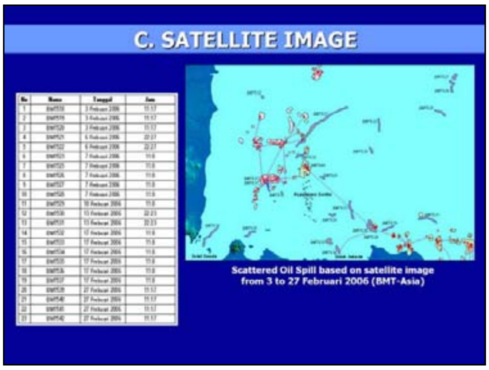
C. SATELLITE IMAGE
Scattered Oil Spill based on satellite image
from 3 to 27 Februari 2006 (BMT-Asia)

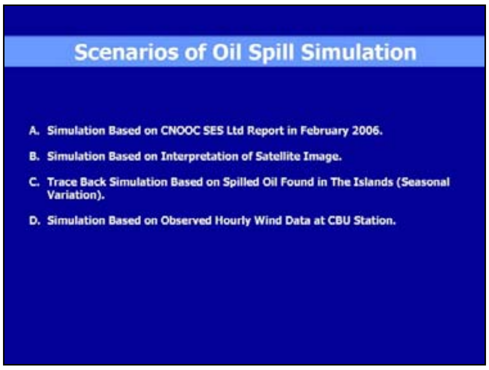
Scenarios of Oil Spill Simulation
A. Simulation Based on CNOOC SES Ltd Report in February 2006.
B. Simulation Based on Interpretation of Satellite Image.
C. Trace Back Simulation Based on Spilled Oil Found in The Islands (Seasonal Variation).
D. Simulation Based on Observed Hourly Wind Data at CBU Station.

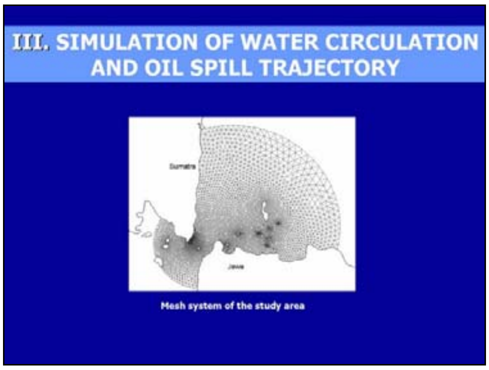
III. SIMULATION OF WATER CIRCULATION AND OIL SPILL TRAJECTORY
Sumatra
Jawa
Mesh system of the study area

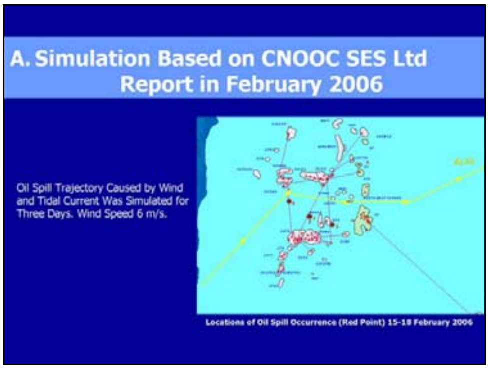
A. Simulation Based on CNOOC SES Ltd Report in February 2006
Oil Spill Trajectory Caused by Wind and Tidal Current Was Simulated for Three Days. Wind Speed 6 m/s.
Locations of Oil Spill Occurrence (Red Point) 15-18 February 2006

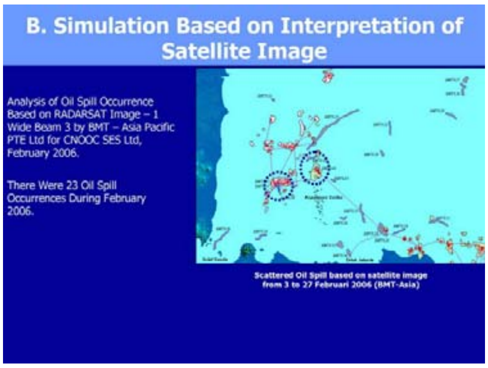
B. Simulation Based on Interpretation of Satellite Image
Analysis of Oil Spill Occurrence Based on RADARSAT Image – 1 Wide Beam 3 by BMT – Asia Pacific PTE Ltd for CNOOC SES Ltd, February 2006.
There Were 23 Oil Spill Occurrences During February 2006.
Scattered Oil Spill based on satellite image from 3 to 27 Februari 2006 (BMT-Asia)

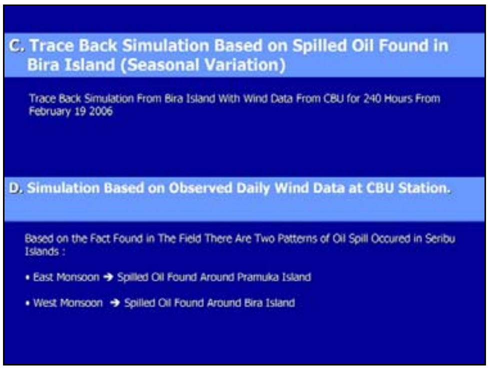
C. Trace Back Simulation Based on Spilled Oil Found in Bira Island (Seasonal Variation)
Trace Back Simulation From Bira Island With Wind Data From CBU for 240 Hours From February 19 2006
D. Simulation Based on Observed Daily Wind Data at CBU Station.
Based on the Fact Found in The Field There Are Two Patterns of Oil Spill Occured in Seribu Islands :
• East Monsoon → Spilled Oil Found Around Pramuka Island
• West Monsoon → Spilled Oil Found Around Bira Island


RESULTS OF OIL SPILL SIMULATION

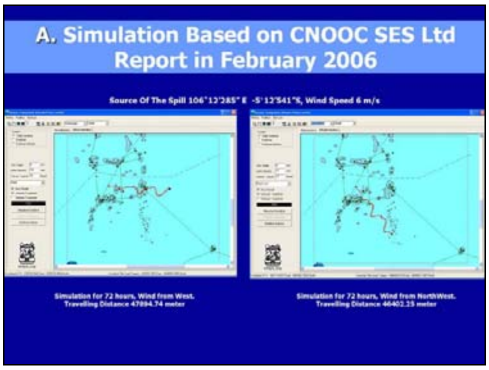
A. Simulation Based on CNOOC SES Ltd Report in February 2006
Source Of The Spill 106˚12'285" E -5˚12'541"S, Wind Speed 6 m/s
Simulation for 72 hours, Wind from West.
Travelling Distance 47894.74 meter
Simulation for 72 hours, Wind from NorthWest.
Travelling Distance 46402.25 meter

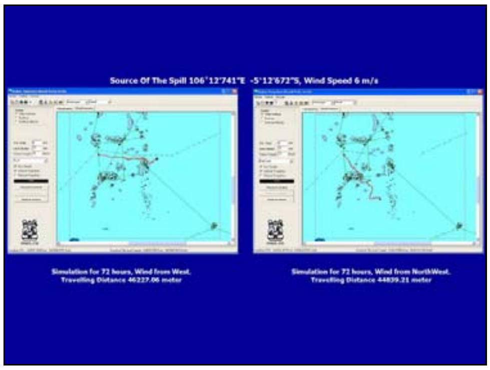
Source Of The Spill 106˚12'741"E -5˚12'672"S, Wind Speed 6 m/s
Simulation for 72 hours, Wind from West.
Travelling Distance 46227.06 meter
Simulation for 72 hours, Wind from NorthWest.
Travelling Distance 44839.21 meter

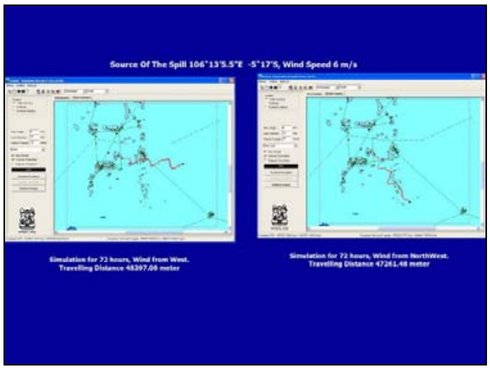
Source Of The Spill 106˚13'5.5"E -5˚17'S, Wind Speed 6 m/s
Simulation for 72 hours, Wind from West.
Travelling Distance 48397.08 meter
Simulation for 72 hours, Wind from NorthWest.
Travelling Distance 47261.48 meter

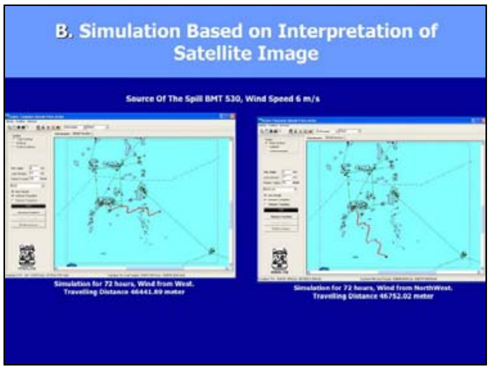
B. Simulation Based on Interpretation of Satellite Image
Source Of The Spill BMT 530, Wind Speed 6 m/s
Simulation for 72 hours, Wind from West.
Travelling Distance 46441.89 meter
Simulation for 72 hours, Wind from NorthWest.
Travelling Distance 46752.02 meter

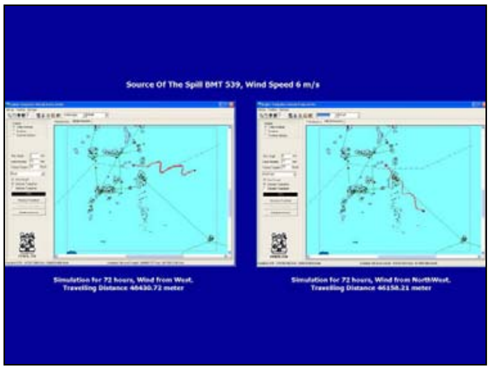
Source Of The Spill BMT 539, Wind Speed 6 m/s
Simulation for 72 hours, Wind from West.
Travelling Distance 46430.72 meter
Simulation for 72 hours, Wind from NorthWest.
Travelling Distance 46158.21 meter

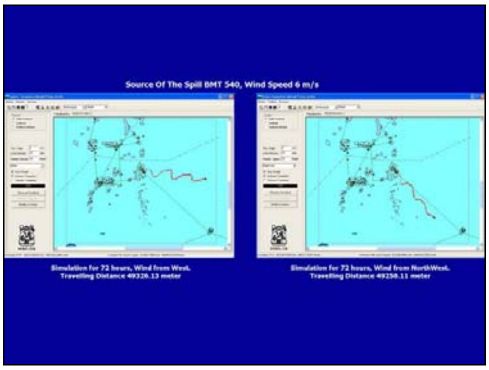
Source Of The Spill BMT 540, Wind Speed 6 m/s
Simulation for 72 hours, Wind from West. Travelling Distance 49326.13 meter
Simulation for 72 hours, Wind from NorthWest. Travelling Distance 49258.11 meter

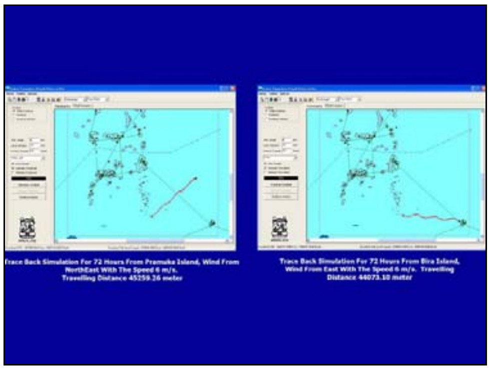
Trace Back Simulation For 72 Hours From Pramuka Island, Wind From NorthEast With The Speed 6 m/s. Travelling Distance 45259.26 meter
Trace Back Simulation For 72 Hours From Bira Island, Wind From East With The Speed 6 m/s. Travelling Distance 44073.10 meter

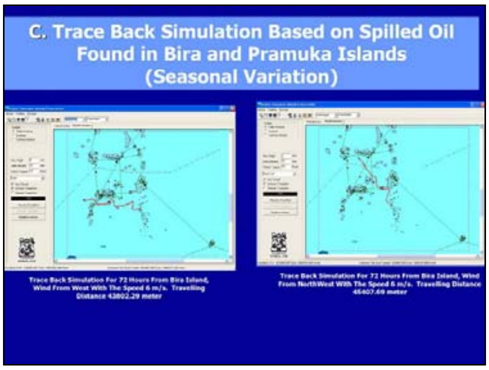
C. Trace Back Simulation Based on Spilled Oil Found in Bira and Pramuka Islands (Seasonal Variation)
Trace Back Simulation For 72 Hours From Bira Island, Wind From West With The Speed 6 m/s. Travelling Distance 43802.29 meter
Trace Back Simulation For 72 Hours From Bira Island, Wind From NorthWest With The Speed 6 m/s. Travelling Distance 45407.69 meter

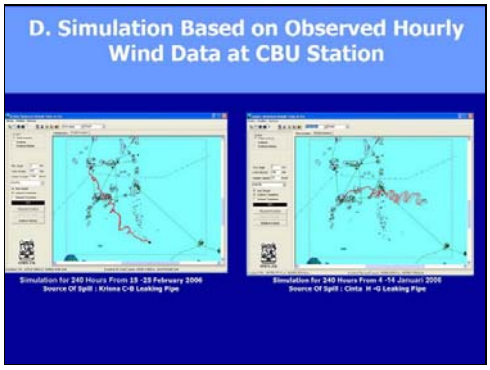
D. Simulation Based on Observed Hourly Wind Data at CBU Station
Simulation for 240 Hours From 15 -25 February 2006
Source Of Spill : Krisna C-B Leaking Pipe
Simulation for 240 Hours From 4 -14 Januari 2006
Source Of Spill : Cinta H -G Leaking Pipe

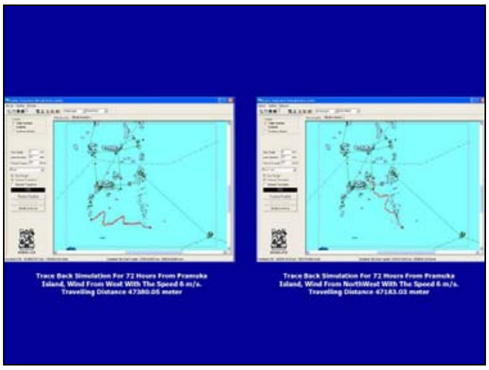
Trace Back Simulation For 72 Hours From Pramuka Island, Wind From West With The Speed 6 m/s. Travelling Distance 47380.05 meter
Trace Back Simulation For 72 Hours From Pramuka Island, Wind From NorthWest With The Speed 6 m/s. Travelling Distance 47183.03 meter

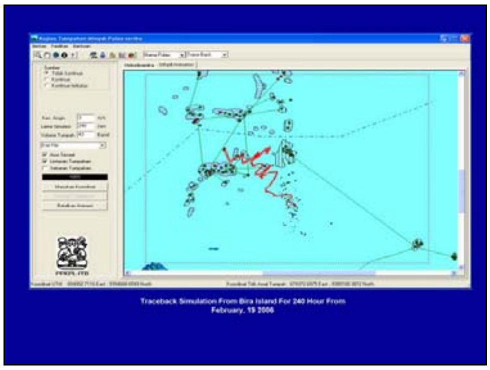
Traceback Simulation From Bira Island For 240 Hour From February, 19 2006

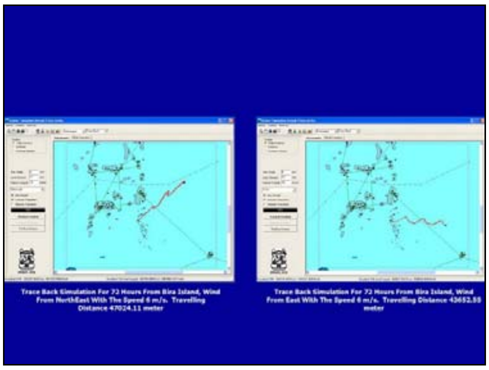
Trace Back Simulation For 72 Hours From Bira Island, Wind From NorthEast With The Speed 6 m/s. Travelling Distance 47024.11 meter
Trace Back Simulation For 72 Hours From Bira Island, Wind From East With The Speed 6 m/s. Travelling Distance 43652.55 meter


IV. CONCLUSION
1. Oil Spill Model Develop in The Study Show Good Capability of Simulating Oil Spill Trajectory in Seribu Islands Water.
2. Oil Platform Situated in the North of Seribu Islands are Potential threat for Oil Pollution in Seribu Islands.
3. Local Government of Seribu Islands Should Develop Mitigation Plan to Reduce the Risk of Oil Pollution in Seribu Islands in The Future.

Identification of Groundtruthing Needs for The Extended Use of Satellite Imagery in Nearshore Habitat Mapping

Karen v. Juterzenka
Department of Marine Science and Technology, Bogor Agricultural University, Indonesia
Email: kvjuterzenka@hazweio.com

Satellite applications have gained more and more significance in marine research as well as for management purposes.

Detailed and sound habitat classification and habitat mapping is one of the pre-requisites for qualified decisions in marine resource planning and conservation. Satellite imagery contributes substantially to the mapping of coastal and nearshore ecosystems, but is still limited by the restriction in dimensions – for waters exceeding the coastal strip - and the spatial resolution. In the past, restrictions of satellite imaging methods had led to some disappointments by ecologists and resource managers regarding its application in research and coastal zone management. New sensors had been developed in the meantime - however, possibly more insights in nearshore habitat details and distribution can be obtained by a closer coupling of satellite imagery and an improved strategy of three-dimensional ecological groundtruthing.

This paper shall contribute to the discussion about groundtruthing needs for coastal and neritic habitat mapping and management purposes by addressing recent examples including Indonesian waters.

To put it short: Some marine ecologists and biological oceanographers are still not very happy about the results they can achieve from satellite imagery – despite promising cover and improved resolution, they may fail in providing „hard“ data in the long run. Ten years ago, Mumby and coworkers proposed the use of airborne digital photography (Mumby et al. 1998) for reef studies, and airborne 3d measurements can reveal terrestrial canopy structure with a spatial resolution of 1-10 m. But even if satellite and airborne sensors and resolution are appropriate, a reliable classification system is needed, e.g. to distinguish corals reefs from seagrass beds and defining habitat boarders for management purposes. The boarders as well as hot spots and weak spots in terms of biodiversity and ecosystem function are most important to detect and monitor environmental changes and habitat loss (Kerr & Ostrovsky 2003). Spatial resolution „as such“ seems not a problem any more, at least concerning the cover of terrestrial and most coastal ecosystems (Turner et al. 2003) as well as man-made (well-defined) structures (Kam et al 2006). As an expression of widespread needs, a minisymposium in the framework of The International Coral Reef Symposium 2008 will cover emerging techniques in remote sensing, also dealing with the question „What types of benthic information can be obtained from remote observation?“ From the perspective of a benthic ecologist and a biological oceanographer there might be another point of view – what can benthic ecology contribute to gain optimal information from remote sensing methods. Earth observation systems already provide the majority of spatial-temporal information on habitat extends, which is needed for coastal management purposes, and new sensor developments always try to bridge actual information gaps (Navalgund & Jayanthi). Probably some gaps can also be filled by approaching the problem from the benthic side, if you cannot see all details from above.

Ecologists as well as managers complain that field and remote sensing data are often collected at divergent spatial scales. The issues might be solved by intensified exchange between remote sensing specialists and field scientists prior to the implementation of field assessment campaigns. Moreover, satellite imaging enables the scientists to identify and set preliminary limits to sensitive areas, which might suffer degradation or damage in the future, and to include this information in the design of ocean-based monitoring and groundtruthing programs before serious changes in habitat extent or habitat structure occur. This might help (1) to extract more valuable information from temporal satellite image series and (2) to improve existing classification systems by identifying the dynamics of marine communities at the ill-defined transition zones between habitats.

Thus, transdisciplinary approaches of remote sensing specialists and marine ecologists might be seen as an integrated tool to extract information about marine community structure down to species level, as well as the functioning of marine systems, from satellite information.

REFERENCES

Kam, S.P., Liew, S.C., Muchlisin, Z.A., Chen. P. (2006) Remote sensing and field assessment of Tsunami effects on coastal pond aquaculture in Northern Sumatra. NAGA Worldfis Center Quaterly, 29: 4-9

Kerr, J.T.,Ostrovsky, M. (2003) from space to species: ecological applications for remote sensing. TREE 18: 299-305

Mumby P.J., Green, E.P., Clark, C.D., Edwards, A.J. (1998) Digital analysis of multispectral airborne imagery of coral reefs. Coral Reefs 17: 59-69

Navalgund, R.R., Jayanthi, S.C. (2002) Role of Earth Observations for Sustainable Development: Emerging Trends. Paper/ICORSE Earth Observation Systems for Sustainable Development

Turner. W., Spector, S., Gardiner, N., Fladeland, M., Sterling. E., Steininger, M. (2003) Remote sensing for biodiversity and conservation. TREE 18: 306-314

Formosat-2 Satellite Imagery Assessment for Coastal Ecosystem Mapping in Western Coast of Banten, Indonesia

Syamsul B. Agus1 and Indra Pratama2
1 Department of Marine Science and Technology, Bogor Agricultural University
2 Agency for Marine and Fishery Research, Ministry of Marine Affairs and Fisheries

ABSTRACT

Coastal ecosystems in West Banten are valuable, providing products and services for the livelihood of its community, and highly threatened. Threats facing coastal ecosystems in West Banten are rapid growth of coastal populations, increasing exploitation of coastal resources, alteration and loss of habitats, also high runoff carrying sediment and other terrestrial-based pollutants from coastal rivers. Mapping of coastal ecosystems will provide significant baseline data for future monitoring and sustainable management of coastal ecosystems in West Banten. Using FORMOSAT-2 data obtained on August 9, 2007, we assess current condition of coastal ecosystems in West Banten area on August 9-11, 2007. Using both data from FORMOSAT-2 satellite imagery and from field assessment, with this paper we exposed map featuring six class of coastal cover-area in West Banten. This study also measured spectral reflectance from 24 objects in West Coast of Banten.

Keywords: FORMOSAT-2, coastal, map, Banten

1. INTRODUCTION

Most of border area in Banten Province, located in 5° 7' 50" - 7° 1' 11" S and 105° 1' 11" - 106° 7' 12" E, represent coastal environment with complex use of its resources (DEPKIMPRASWIL 2003). West Coast of Banten bordering with the Sunda Strait is subject to marine tourism, transportation, industry, fisheries, and conservation. Up to this day a great variety of human activities happen there simultaneously. The main environmental impacts consist of alteration and loss of coastal habitats due to resource exploitation and development, organic and inorganic pollution, volcanic eruption from the Krakatau, and tsunami. Scientific data on coastal ecosystems, land use, landforms, and shoreline and water quality are required periodically to ensure an environmentally effective coastal zone management practices. Maps on various coastal themes form basic input to the coastal zone management models. Conventional maps are quite useful; however, they do not provide up-to-date information. Since coastal zone is very dynamic, periodic mapping is vital for planning effective strategies.

The interpretation of remotely sensed data is the best tool currently available for providing synoptic spatial information on various scales and with reasonable classification and control accuracy. The availability of FORMOSAT-2, which produced hyperspectral data with spatial resolution of 8 m for multispectral and 2 m for panchromatic images, is expected to provide spatially comprehensive coverage at a higher resolution for effective and accurate analyses of different coastal ecosystems exist within one area. There are five spectral bands in FORMOSAT-2, i.e. P: 0,45–0,90µm (panchromatic), B1: 0,45–0,52µm (blue), B2: 0,52–0,60µm (green), B3: 0,63–0,69µm (red), and B4: 0,76–0,90µm (near-infrared). The objective of this research is to test the ability of FORMOSAT-2 data in producing coastal geospatial data, particularly for mapping of coastal ecosystems, i.e. mangrove forests, seagrass beds, and coral reefs, in West Banten area.

2. METHODS

2.1 Study sites

This study was conducted on August 5-7, 2007, in coastal area of West Banten, with geographic reference of 6° 15' 40" - 6° 41' 30" S and 105° 35' 00" - 106° 00' 00" E. West Banten coastal platform extends north-south, bordered with Sunda Strait and is influenced by volcanism activities from Mount Krakatau. Thus, its shorelines and living coral communities were geologically incipient (Tomascik et al 1997). There were two small islands located near the coasts of West Banten, i.e. Popoleh Island and

Karang Gosong Island. There were 22 study sites, particularly to obtain seawater samples, including 3 sites for coral assessment and 1 site for mangroves and seagrass assessment (Figure 1).

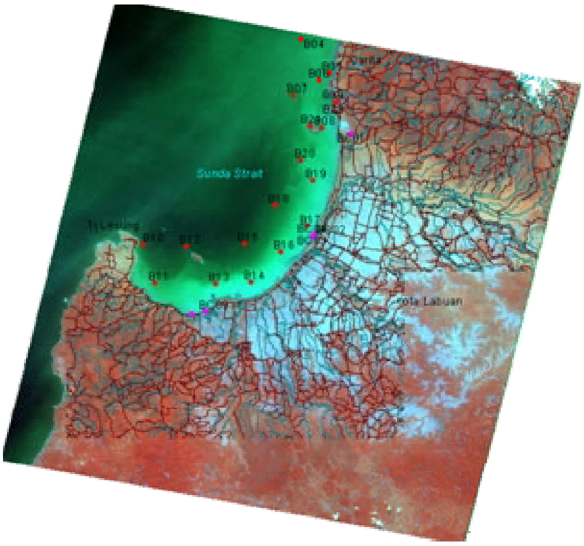

Figure 1. Study sites

2.2 In-situ sampling

In general, *in-situ* sampling conducted comprises of coastal ecosystem assessment and spectroradiometric measurements of sediment types and species. Assessed coastal ecosystems were mangroves, seagrass beds, and coral reefs, which techniques were based on English et al (1997). Reflectance measurements were made to create a spectral library of 24 reflectance spectra encompassing mangroves, other coastal vegetation, fishponds, several types of coastal-substrates and different colors of seawater.

2.3 Satellite image analysis

Morphologies of the beaches, lagoons, mangrove forests, seagrass beds, and coral reefs were classified on the basis of the spectral signatures of their various habitats using images produced from FORMOSAT-2 satellite image obtained on August 9, 2007. Geometric correction was trained with existing ground-truth data and reference map from BAKOSURTANAL were performed using ER Mapper and Arc View (Green et al. 2000).

3. RESULTS AND DISCUSSION

3.1FORMOSAT imagery

The main remote sensing mission for FORMOSAT-2, which was launched in 2004, was to capture satellite images of the Taiwan Island and the surrounding islands and ocean to monitor the environment and its resources. Later on, under international collaborative agreement, FORMOSAT-2 was also used to capture images of other regions in the Asia Pacific. Within the frame of APEC SAKE on Satellite Application on Fishery and Coastal Ecosystem (SAFE), FORMOSAT-2 acquires capture satellite images of Indonesian coastal and archipelagic waters (Figure 2).

Figure 2. Satellite images of West Banten producedby FORMOSAT-2,
= acquisition date July 7, 2006 and
= acquisition date August 9, 2007.

On July 7, 2006, FORMOSAT-2 captured the first satellite image of West Banten. Due to stripping error, the images were incapable for further processing. One year later, FORMOSAT-2 acquires another image of West Banten on August 9, 2007. Panchromatic FORMOSAT-2 images of West Banten are presented in Figure 3, while multispectral FORMOSAT-2 images of West Banten are presented in Figure 4.

(a)

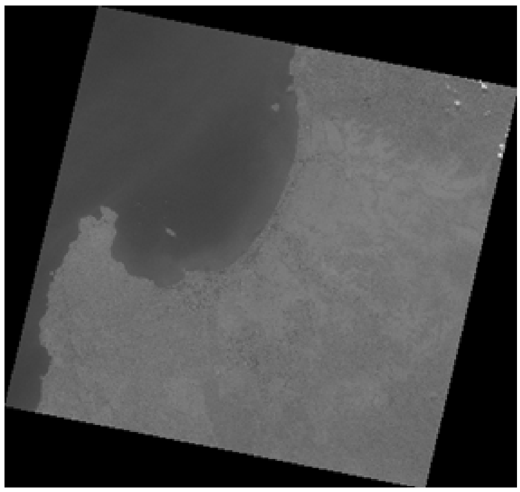

(b) 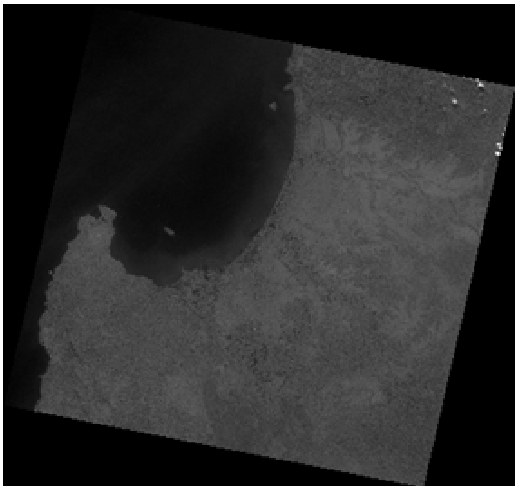

Figure 3. Panchromatic FORMOSAT-2 image of West Banten, (a) prior to geometric correction and (b) after geometric correction.

(a)

(b)

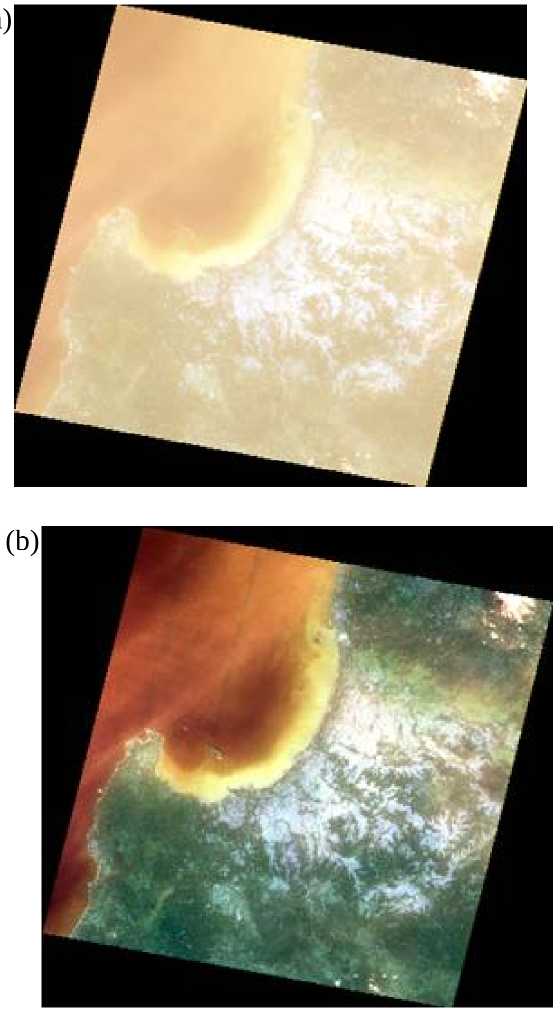

Figure 4. Multispectral FORMOSAT-2 image of West Banten, (a) prior to geometric correction and (b) after geometric correction.

3.2 Coastal ecosystems of West Banten

Coral communities in West Banten are influenced by volcanism and extreme sedimentation due to lots of river discharges, thus resulting in patchy distribution and no significant carbonate accretion to form fringing reefs as if before 1883 Krakatau eruption (Tomascik 1997). From three observed sites, i.e. Popoleh Island, Karang Gundul, and Karang Gosong, the highest cover of hard corals were available in Karang Gundul (43.0%). Benthic communities in Popoleh Island were dominated by soft corals of *Lobophytum*, while calcareous macroalgae of *Halimeda* were common in Karang Gosong (Figure 5). Common Scleractinian corals observed were *Acropora, Pocillopora*, *Stylophora, Porites, Favia*, and *Montipora*.

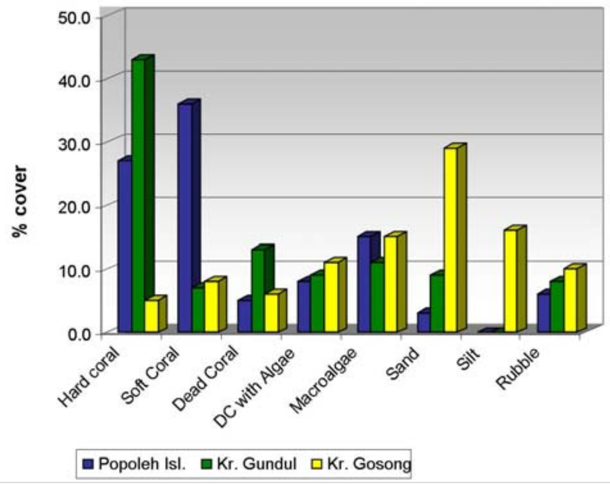

Figure 5. Results of coral reef assessment in West Banten

There was only one species of seagrass observed in the study sites, *Enhalus acoroides*, which is the largest species of seagrass. In relation to general feature of study sites, existing silty to muddy sediments support *Enhalus* to form monospecific meadows. Mangrove vegetation in study sites comprised mainly of *Rhizopora* and *Bruguiera*. Other mangrove species observed in the surroundings were *Avicennia*, *Sonneratia*, *Xylocarpus, Ceriops*, and *Exoecaria*.

High resolution (8 m) classification map was generated for coastal environment of West Banten, Indonesia, from a mosaic of FORMOSAT-2 multispectral images to produce six classes (Figure 6). Contrast-stretched, multi-spectral image maps provided a qualitative method to distinguish different types of seawater (deep, shallow, and high turbid waters), mangrove forests, bushes and other coastal land-vegetation, also rice fields and housings. This map, in a geographic information system (GIS) format, can be used for fieldwork, as base maps for other scientific studies and for management of coral reef ecosystem.

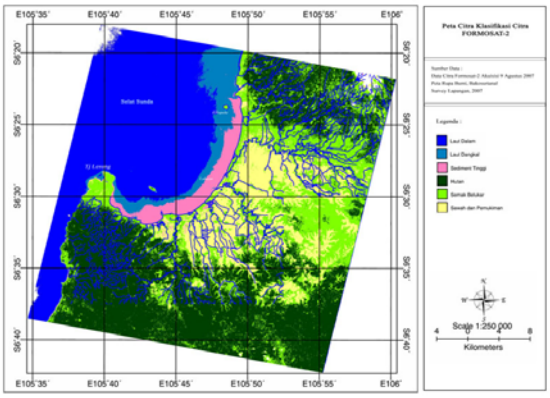

Figure 6. Classified map of coastal environment in West Banten, using multispectral FORMOSAT-2 image with spatial resolution of 8 m.

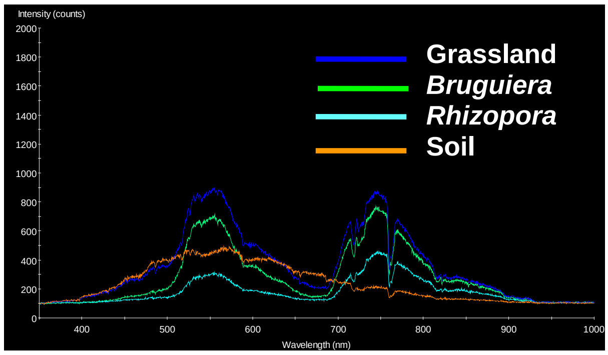

(a)

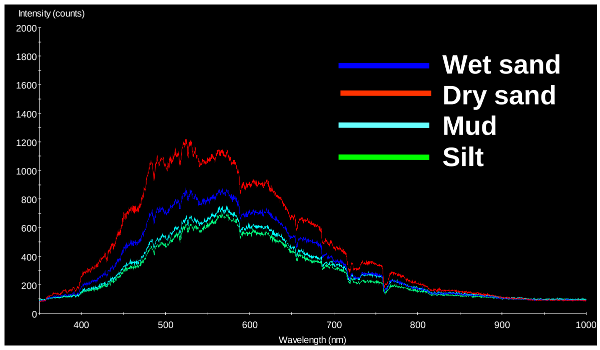

(b)

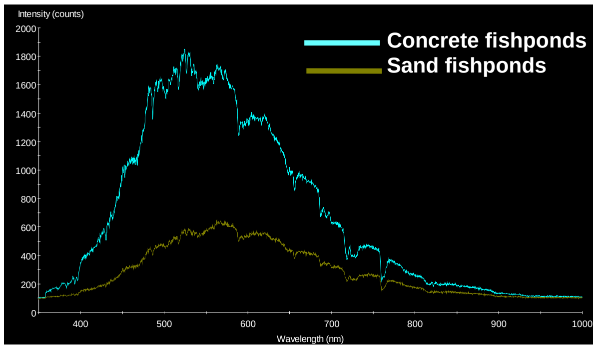

(c)

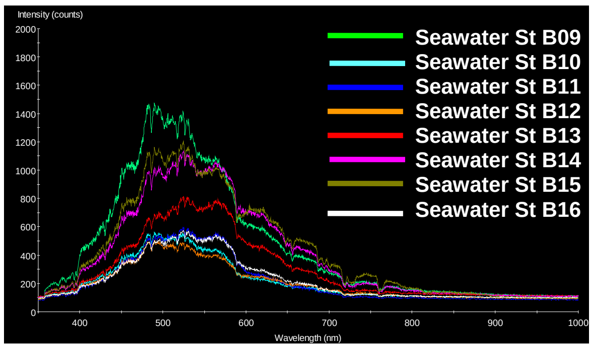

(d)

High resolution (8 m) classification map was generated for coastal environment of West Banten, Indonesia, from a mosaic of FORMOSAT-2 multispectral images to produce six classes (Figure 6). Contrast-stretched, multi-spectral image maps provided a qualitative method to distinguish different types of seawater (deep, shallow, and high turbid waters), mangrove forests, bushes and other coastal land-vegetation, also rice fields and housings. This map, in a geographic information system (GIS) format, can be used for fieldwork, as base maps for other scientific studies and for management of coral reef ecosystem.

3.3 Spectroradiometric measurements

In-situ spectroradiometric measurements play an important role in the development of remote sensing applications, bridging the gap between laboratory optical measurements and measurements from satellite platforms (Dekker et al. 1992). Therefore, this study also measure reflectance properties of various objects. Averaged reflectance spectra for the coastal vegetation, including two species of mangroves, different types of coastal substrates, fishponds, and different types of seawater are shown in Figure 7.

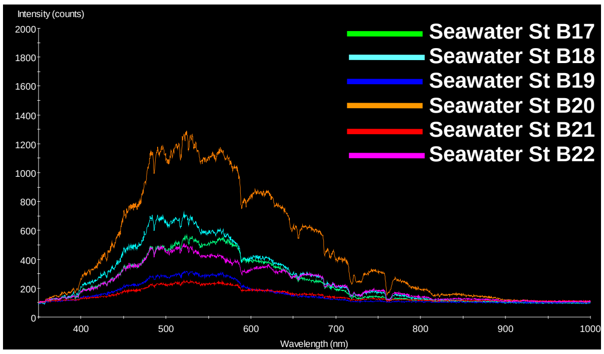

(e)

Figure 7. Observed spectral reflectance of coastal vegetation (a), coastal substrate (b), fishponds (c), and different types of seawater (d, e).

There were two types of fishponds for reflectance measurement, i.e. concrete-based and sand-based. The concrete fishponds spectra had the highest reflectance values (Figure 7c). The coastal vegetation had lower reflectance compared to different coastal land-substrate (Figure 7a and 7b). This indicated that bare sediment around the coasts could be easily separated from other bottom types on the basis of brightness alone.

All coastal vegetation showed a reflectance maximum at around 750 nm, and mangrove reflectance spectra showed the most variation in shape and magnitude within species in comparison with the other groups (Figure 7a). Within them *Rhizopora* had the lowest reflectance values and the least variation in spectral shape (Figure 7a). Figure 7d and 7e illustrate that turbid seawaters have higher reflectance in comparison to clear seawaters. All turbid seawaters exhibit a reflectance maximum at around 500 nm.

4. CONCLUSION

FORMOSAT-2 is able to provide high-quality satellite images for coastal environment mapping. Results from spectroradiometric measurements indicate that:

(1) for the purpose of medium (community) and fine (species) vegetation mapping, it is best to use spectral band B2 and B4 of FORMOSAT-2.

(2) for the purpose of coastal seawater and sediment mapping, it is best to use spectral band B1 and B2 of FORMOSAT-2

(3) for the purpose of fish ponds mapping, it is best to use spectral band B2 and B3 of FORMOSAT-2

ACKNOWLEDGMENTS

This research was supported by the Agency for Marine and Fishery Research of the Indonesian Ministry of Marine Affairs and Fisheries, Department of Marine Science and Technology of Bogor Agricultural University, Agency for the Assessment and Application of Technology, and counterparts in Chinese Taipei especially in providing valuable FORMOSAT-2 data. The assistance of several colleagues during fieldwork is gratefully acknowledged. Special thanks to Adriani whose comments were greatly appreciated in contributing to the final form of this paper.

REFERENCES

Dekker AG, Malthus TJ, Wijnen MM, Seyhan E (1992) The effect of spectral bandwidth and positioning on the spectral signature analysis of inland waters. Remote Sens. Environ. 41: 211–225

DEPKIMPRASWIL. 2003. Buku Profil Penataan Ruang Provinsi Banten. Direktorat Jenderal Penataan Ruang. Departemen Pemukiman dan Prasarana Wilayah.

English, C. Wilkinson and V. Baker (Eds.). 1997. Survey Manual for Tropical Marine Resources 2nd Edition. Australian Institute of Marine Science.

Green EP, Mumby PJ, Edwards AJ, Clark CD (2000) Remote sensing handbook for tropical coastal management. UNESCO, Paris

Tomascik, T, AJ Mah, A Nontji, and MK Moosa. 1997. The ecology of the Indonesian seas, part 2. Periplus editions.

Integration of Satellite Application and Computational Tool for Marine Conservation Area Planning

E. Elvan Ampou, Frida Sidik and Candhika Yusuf
Institute for Marine Research and Observation
Bali, Indonesia

ABSTRACT

The design of a marine conservation area or so called Kawasan Konservasi Laut (KKL) should meet the goals of KKL itself. The objectives for each type of marine conservation area are varies and almost exclusively focused on habitat protection which leads to the conservation of biological diversities and sustainable fisheries. Satellite application has been widely used to support marine designs. This paper describes how we incorporate data on the spatial distribution of key coastal habitats (such as mangrove and coral reef) and water quality with coastal hydrodynamic model for the design of marine conservation area. The study employs field observation, satellite data processing and modeling. Using a computational tool called MARXAN, we combine those biological and physical information as the primary drivers for the selection of sites for marine reserves. The site location is in Pemuteran, Buleleng, Bali.

Keywords: Kawasan Konservasi Laut (KKL), Biological diversity, MARXAN.

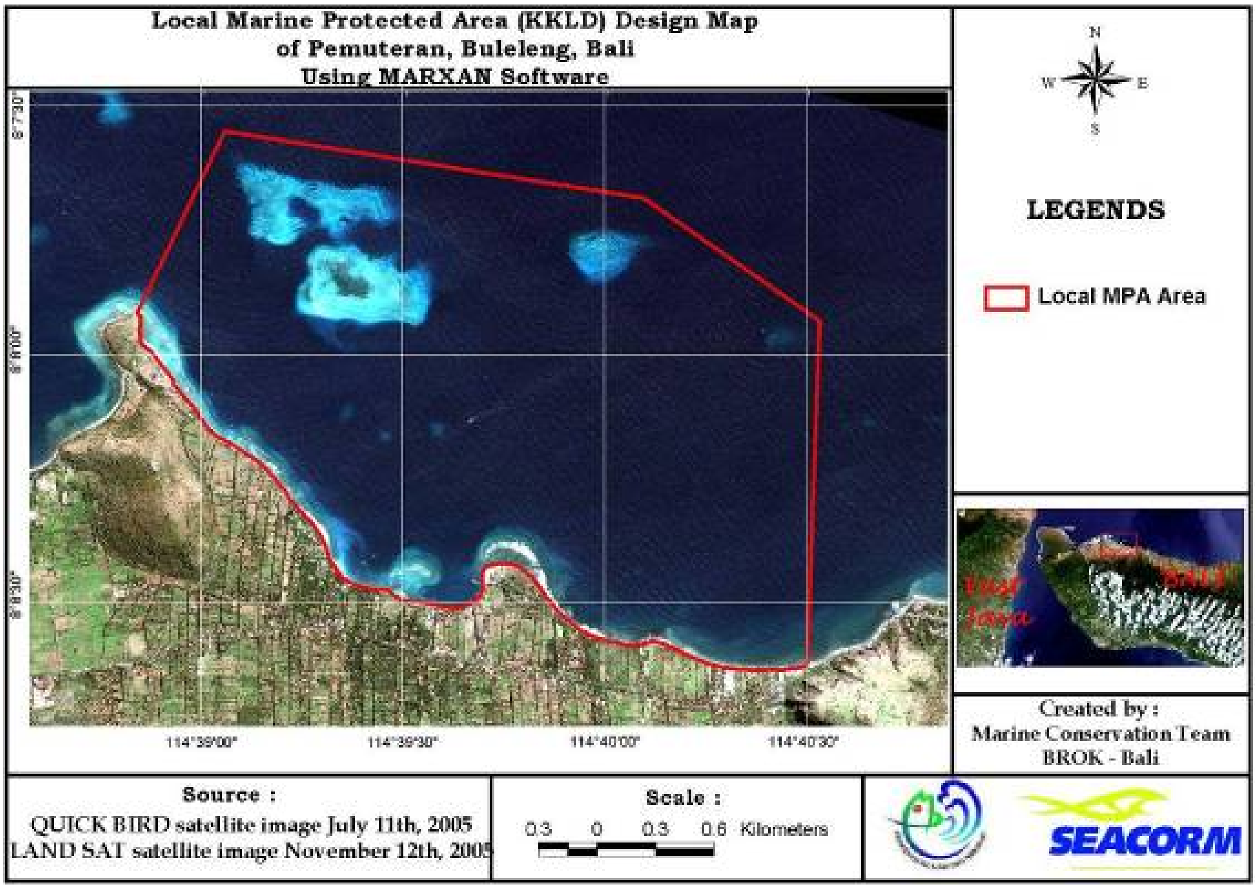

Figure 1. Design Map of MPA in Pemuteran (North Bali) using MARXAN

Biodiversity is defined, and the importance of and threats to marine biological diversity are assessed. A review of current scientific knowledge with respect to marine biological diversities are presented, along with commentary on the particular threats to diversity in the various types of marine ecosystem. This is followed by a general discussion of the ways in which government and the public can protect marine biological diversity to support Marine Conservation Area Planning with integrated to satellite application and computational tool.

1. METHODS

1.1 Time and Place

The Surveys of Coral Reef were carried out in September 9th 2007 until September 10th 2007 at the Pemuteran, Buleleng. (North of Bali).

1.2 Equipments

***Table 1**. Equipments*

Equipments	Function
Jukung boat and speed boat	Transportation
Rope18 meters	To draw manta tow surveyor
Manta board	Data board
Pencil	Write data
Masker, Snorkel, Fins	Skin Dive
SCUBA Gear	Diving
String Liners (50 meters)	Line Transect
GPS (Global Positioning System)	To acquires point of coordinate
Stopwatch / jam	To acquires point of time
Underwater camera	Documentation

1.3 . Manta Tow

The purposes of Manta Tow method are for assessing broad-scale changes in reef cover due to cyclone damage, coral bleaching and outbreaks of the Crown-of-thorns starfish, *Acanthaster plancii*. A good synopsis of the method is given in English *et al.* (1997) which forms the basis of the following description.

The category or percent cover refers to Rogers, C., Garrison, G., Grober, R., Hillis, Z-M., dan Franke, M.A. (1994) figure 2.

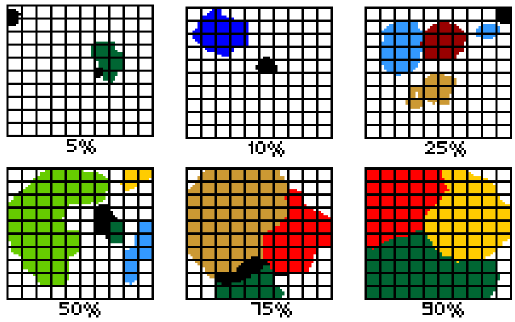

Figure 2. Percentage of Life Form

1.4 Coral Reef Survey

The Line Intercept Transects (LIT) is fairly rapid to deploy in field. A fiber glass tape measure is laid close to the reef contour and the length (cover) of each reef category is recorded. A faster variant is the point intercept transect in which only the type of reef category is noted at equidistant points along the line (e.g. every 20 cm). The cover of each category is calculated by the ratio of number of points per category to the total number of points. The main limitation with line and point intercept transects is that they tend to under-sample heterogeneous areas with low cover of reef categories (e.g. areas of scattered corals) (English *et al.*, 1997). Transect throughout 50 meters in depth 5 and 10 meters cross the coast line.

The function of this method is to descript the percent cover of life form.

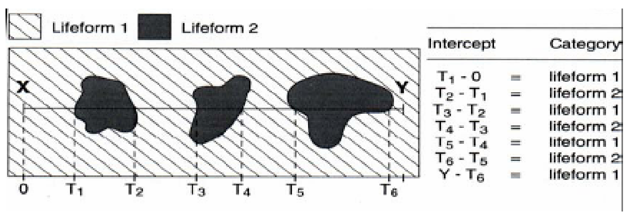

Figure 3. Line Intercept Transect method (English et al, 1997).

Table 2. Remarks of *benthic life form*

***benthic life form* code**	**Description**
ACB	Acropora branching
AEN	Acropora encrusting
ASM	Acropora sub massive
CA	Coraline Algae
CE	Coral Encrusting
CF	Coral Foliosa
CM	Coral Massive
CSM	Coral Sub Massive
DC	Dead Coral
DCA	Dead Coral Alge
Diploastrea heliopora	*Diploastrea heliopora*
EUP	Euphyllia
FAV	Faviidae
FNG	Fungia
GAL	Galaxea
GON	Goniopora
Millepora	Millepora
MNT	Montipora
PAC	Pachyseris
PBR	Porites Branching
PEC	Pectinia
PLA	Platygyra
POC	Pocilopora
POR	Porites
RB	Rubble
RCK	Rock
SC	Soft Coral
SD	Sand
SER	Seriatopora
SPG	Sponge
T.squamosa	*Tridacna squamosa*
Tunicate	Tunicate

(English *et al.*, 1997)

1.5 Reef Fish Survey

The basic principle of plot-less Belt Transects is similar to the manta tow, the main difference being that observers are not towed behind a boat. This affords a useful means of independence allowing the use of scuba and permitting very shallow areas to be surveyed safely. Since the observer can get much closer to the sea bed, it is possible to record more detailed data on bottom features. In the species-rich Indo-Pacific, this may include coral and algal life forms include Reef Fish (for examples, see English *et al*. 1997)

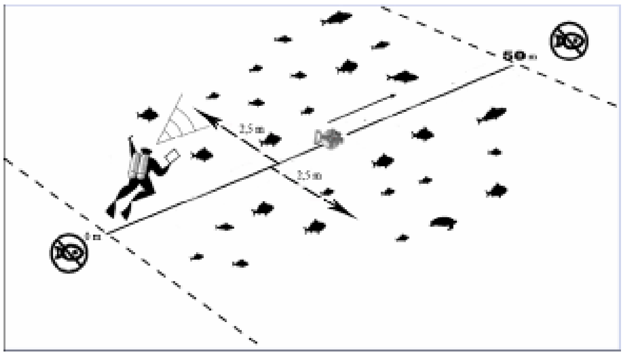

Figure 4. Visual Census use Belt Transect Method (English *et al.*,1997)

2 RESULT AND DISCUSSION

2.1 Manta Tow

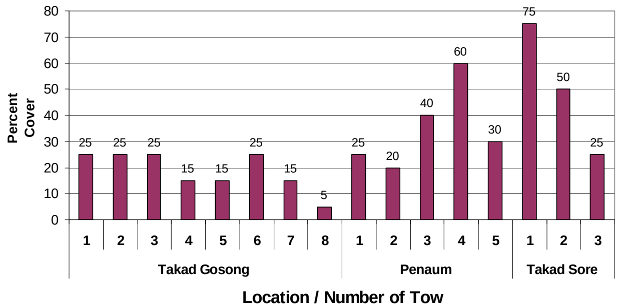

Graphic 1. Percent Cover of Life Form

Based from the manta tow surveys on *Pemuteran* area, “Takad Sore” and “Penaum” were included in the category of “Damaged to Recovery” Life Form. Whereas in “Takad Gosong” the percent cover of life form were included in the category of “Damaged to Critical” Life Form.

3. CORAL REEF

3.1. Percent Cover

Based from the LIT surveys on coral reef, indicates that in “Penaum” have a higher percentage of life form than “Takad Sore”. Penaum = 72.74 % in the deepness 3 m and 52.20 % in the deepness 10 meters (Healthy Lifeform). Mean while in Takad Sore = 15.48 %; 6 m and 3.40 %; 10 m which included in the category of damaged/critically.

Table 3. *Benthic Life Form* distribution in two side (Penaum and Takad Sore)

No	Life Form	Penaum	Takad Sore
1	ACB	+	+
2	AEN	+	-
3	ASM	+	-
4	CA	+	+
5	CE	+	-
6	CF	+	-
7	CM	+	+
8	CSM	+	+
9	DC	-	+
10	DCA	+	+
11	*Diploastrea heliopora*	-	+
12	EUP	-	+
13	FAV	+	+
14	FNG	+	+
15	GAL	+	+
16	GON	-	+
17	MILLEPORA	-	+
18	MNT	-	+
19	PAC	-	+
20	PBR	+	-
21	PEC	+	+
22	PLA	-	+
23	POC	+	+
24	POR	+	+
25	RB	+	+
26	RCK	-	+
27	SC	+	+
28	SD	+	+
29	SER	-	+
30	SPG	+	+
31	T. squamosa	-	+
32	TUNICATE	-	+

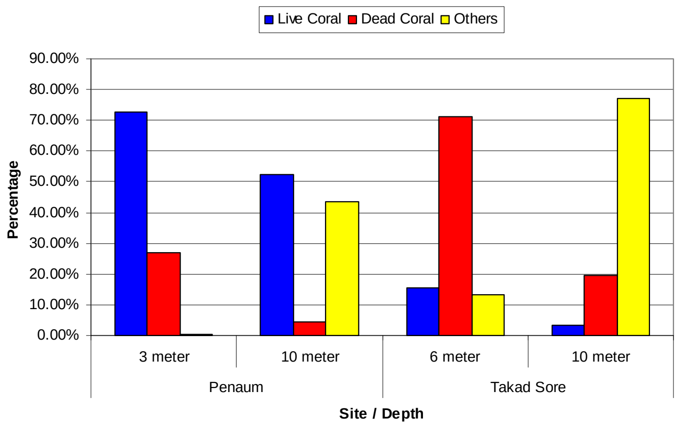

Graphic 2. The Ratio of Death Coral, Life Coral and *others* in two sites

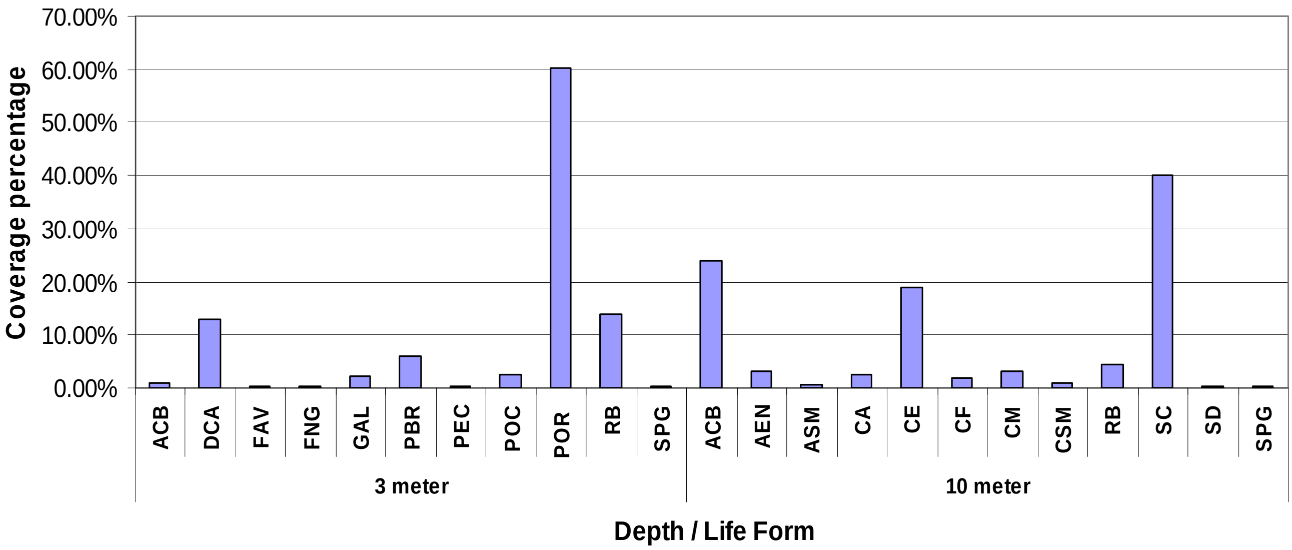

Graphic 3. Percent Cover of Benthic Life Form in Penaum

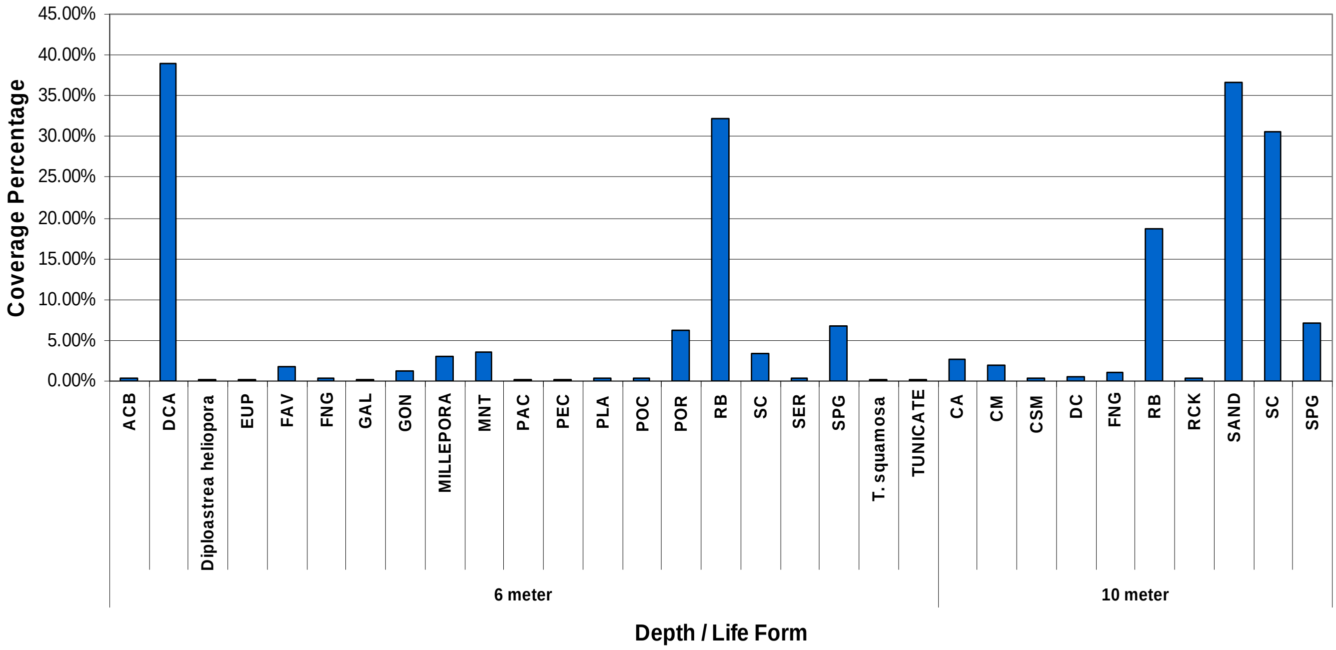

Graphic 4. Percent Cover of Benthic Life Form in Takad Sore

3.2 Coral Reef's Ecology Index

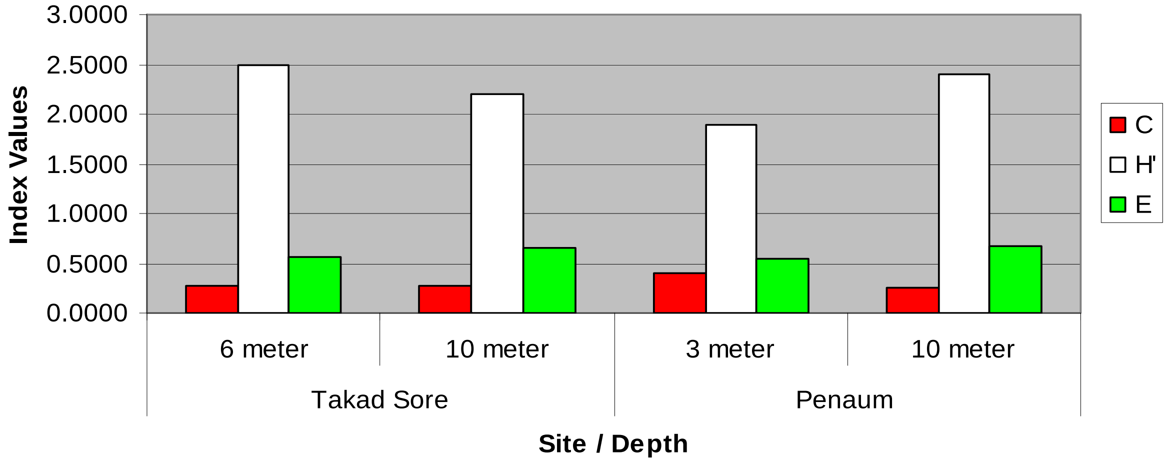

Graphic 5. Index Ecology ratio of Coral Reef at two sites

Based on the ecological index values, "Takad Sore" have a low domination level (C = 0.2674; 6m and 0.2686; 10m) with a small diversity level (H = 2.4917; 6 m and 2.2024; 10 m) and the uniformity level medium to high (E = 0.5673; 6 m and 0.6671; 10 m).

Such as well in "Penaum" have a low domination level (C = 0.4039; 3 m and 0.2579; 10 m) with a small diversity level (H = 1.8825; 3 m and 2.3915;10 m) and the uniformity level medium to high (E = 0.5442; 3 m and 0.6671; 10 meter).

4. REEF FISH

4.1. Reef Fish Abundant r

Based from *visual census* on the belt transect method, there were a total of 446 individuals from 15 families of reef fish. In "Takad Sore" = 256 individuals from 15 families of reef fish.

The reef fish families encountered during the surveys such as Acanthuridae (*Surgeonfishes*) and Chaetodontidae (*Butterflyfishes*), where as the most encountered reef fish families were Caesionidae (*Fusiliers*) and Pomacentridae (*Damselfishes*).

Table 4. Reef Fish Family Presence.

No.	Reef Fish Family	Family Presence			
		Takad Sore		Penaum	
		6 m	10 m	3 m	10 m
1	Acanthuridae	+	+	+	+
2	Aulostomidae	+	-	-	-
3	Balistidae	+	-	-	-
4	Blenniidae	+	-	-	-
5	Caesionidae	-	+	+	+
6	Chaetodontidae	+	+	+	+
7	Holocentridae	+	-	-	-
8	Labridae	+	-	-	-
9	Muraenidae	-	-	+	-
10	Pomacanthidae	+	+	-	+
11	Pomacentridae	+	-	+	-
12	Scaridae	+	+	-	+
13	Serranidae	-	+	+	-
14	Siganidae	+	-	-	-
15	Zanclidae	+	-	+	+

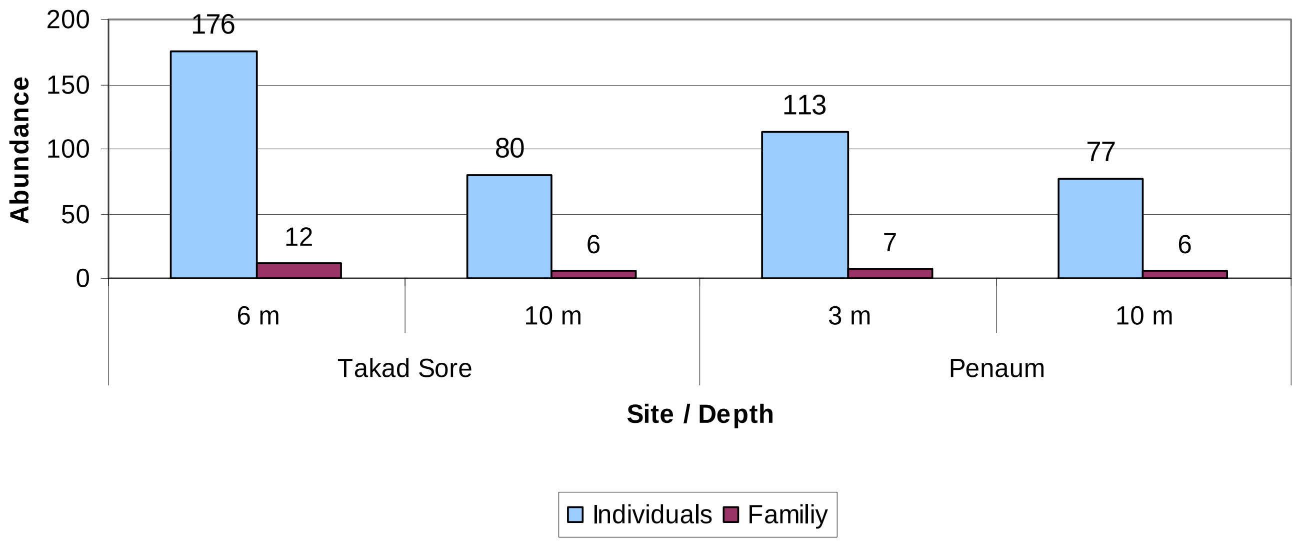

Graphic 6. Reef Fish Abundant

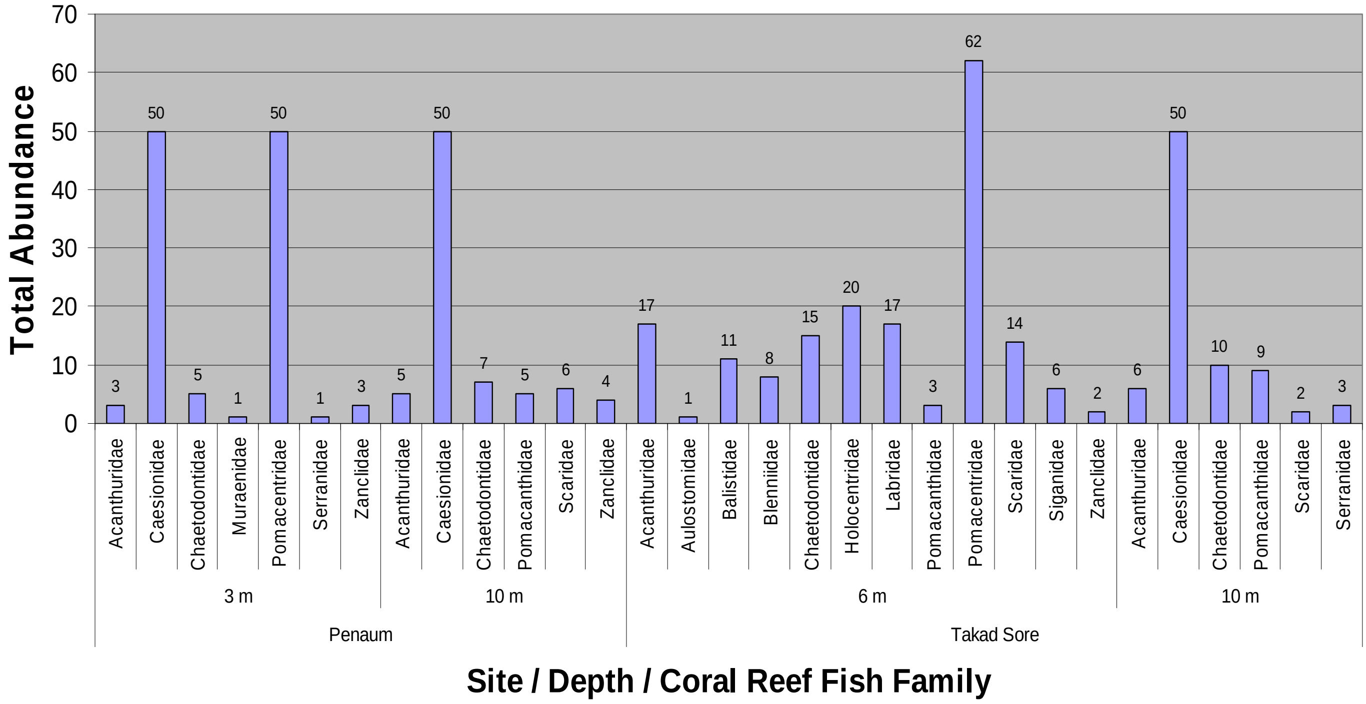

Graphic 7. Reef Fish Abundant and Total Individual per Family

4.2. Coral Reef Fish's Ecology Index

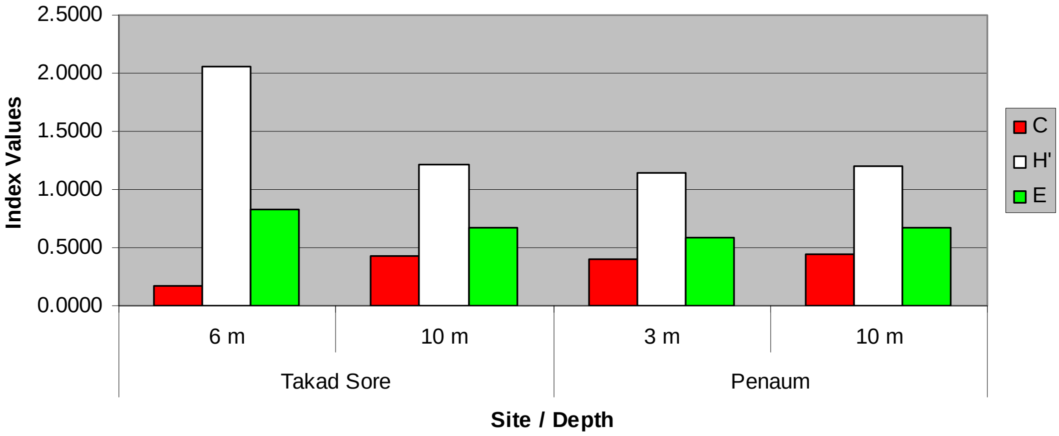

Graphic 7. Index Ecology ratio of Coral Reef Fish at two sites

Based on the ecological indexes calculation result, "Takad Sore" have low domination index values (C = 0.1768 at the depth of 6 meter and C = 0.4266 at 10 meter depth), average values of diversity index (H = 2.0561 at the depth of 6 meter and H = 1.2091 at 10 meter depth) and average to high evenness index values (E = 0.8274 at the depth of 6 meter and E = 0.6748 at 10 meter depth).

The similar results were also occurred at "Penaum" where it have low domination index values (C = 0.3951 at the depth of 3 meter and C = 0.4471 at 10 meter depth), average values of diversity index (H = 1.1359 at the depth of 3 meter and H = 1.2060 at 10 meter depth) and average to high evenness index values (E = 0.5837 at the depth of 3 meter and E = 0.6731 at 10 meter depth).

5. APPLIED TO MARXAN

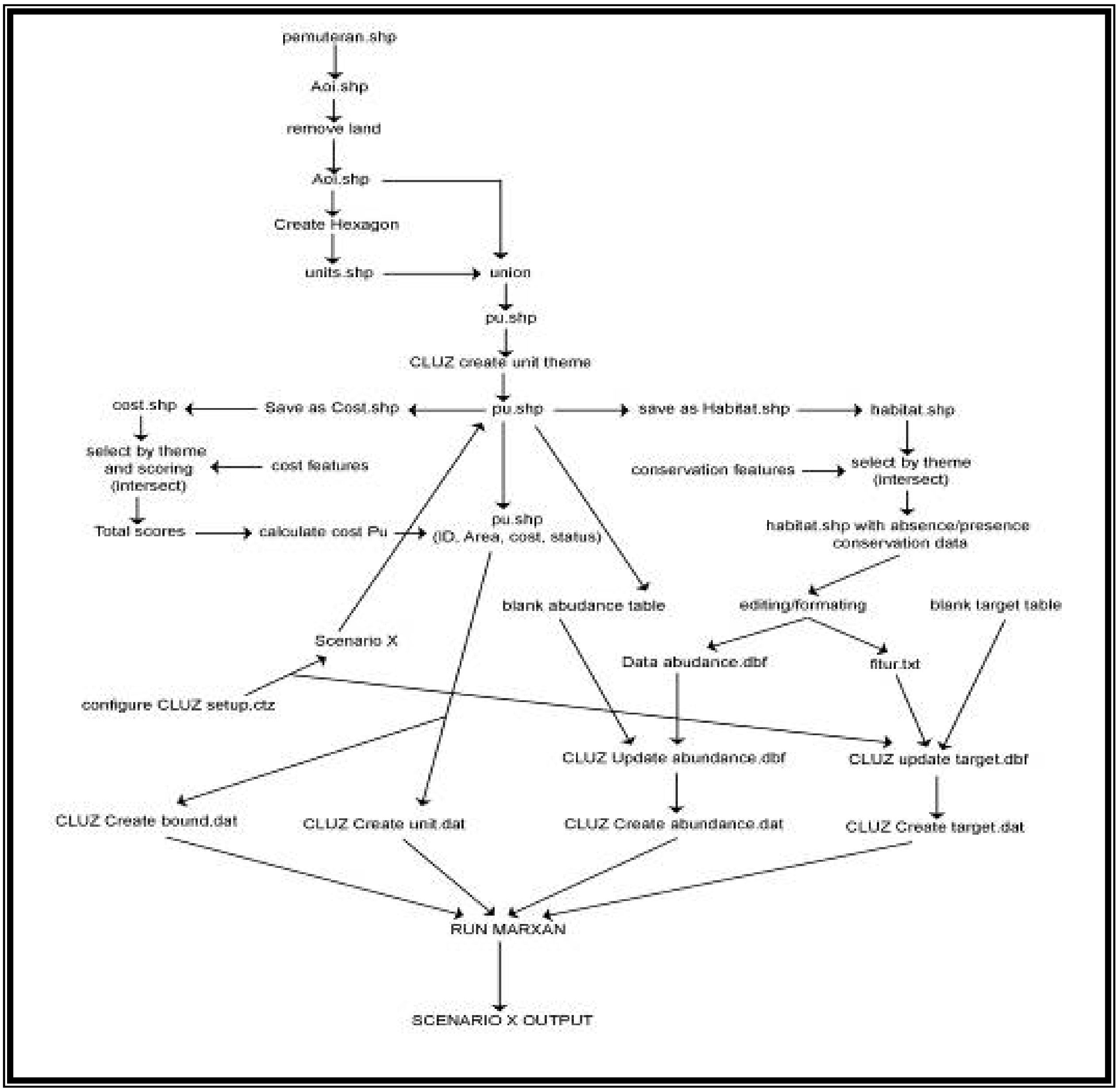

Figure 5. Flowchart of Running Marxan

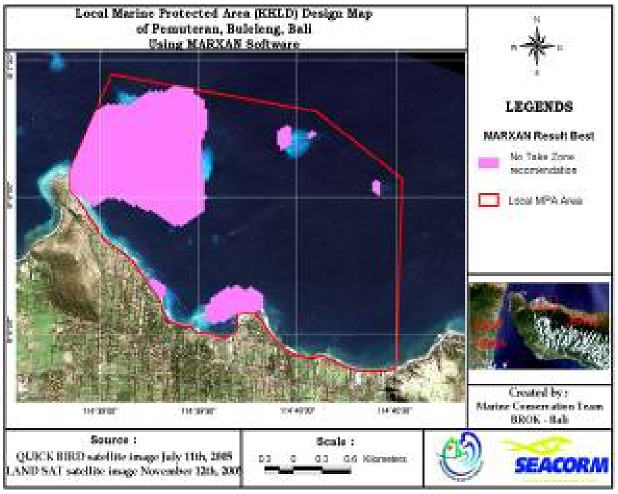

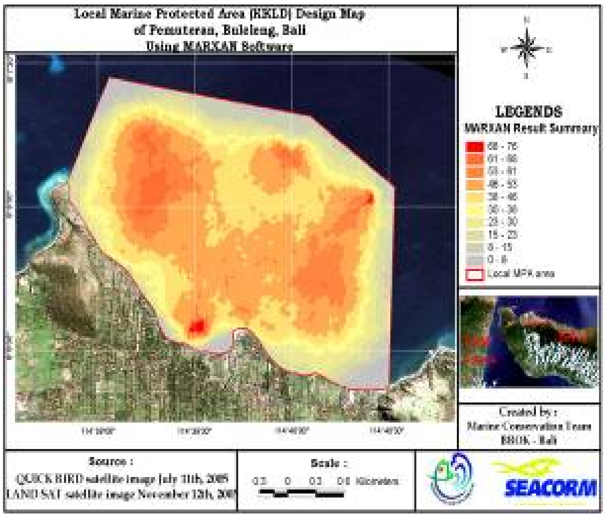

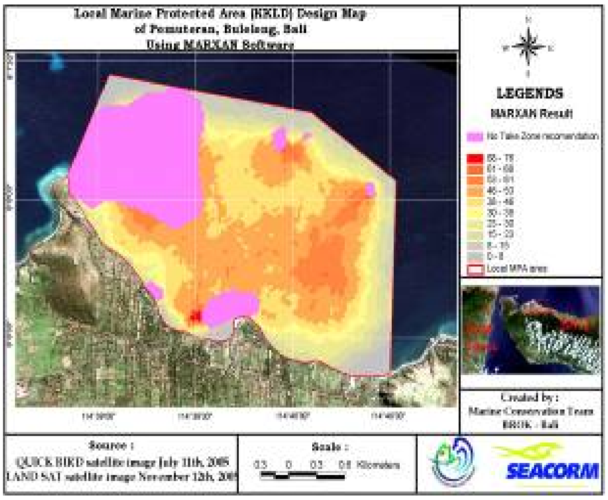

Figure 6. Local Marine Protected Area Using Marxan Software at Pemuteran – Buleleng, Bali.

6. SURVEY DOCUMENTATIONS

(Photo by : Elvan Ampou and Candhika Yusuf)

Manta Tow survey

Diversities of soft coral founded at Takad Sore

Coral of Genus Platygyra at Takad Sore

Line Intercept Transect (LIT) survey

Diversities of coral reef fishes at Takad Sore

Tridacna squamosa at Takad Sore

REFERENCES

Allen, G. Steene, R. Humann, P dan Deloach, N. 2003. Reef Fish Identification : Tropical Pacific. Star Standard Industries. Pte Ltd. Singapore. 457 pp.

Azhar, I. dan E.N. Edinger. 1996. Ekotipologi Terumbu Karang pada Perairan P. Cemara Kecil, P. Menyawakan dan Gosong Cemara, Taman Nasional Laut Karimunjawa. Sub BKSDA Jawa Tengah dan Universitas Diponegoro – McMaster University Project. Semarang

English S, C.Wilkinson, V. Baker (eds).1997. Survey Manual for Tropical Marine Resources (2nd Edition). Australian Institute of Marine Science. ASEAN-Australia Marine Project

Krebs, C.J. 1985. The Experimental Analysis of Distribution and Abundance Third edition. Harper and Row Publishers. New York.

Legendre, L. dan P. Legendre. 1983. Numerical Ecology. Elsevier Science Publication. New York

Ludwig JA, Reynolds JF, 1988, Statistical ecology: a primer on methods and computing. Wiley-Interscience Publications. New York

Odum, E. P. 1971. Fundamental of Ecology. Third Edition. W. B. Sunders Company. Toronto. 574 pp.

Pielou C. 1966. The measurement of diversity on different types of biological collections. Amer. Nat. 94:25-36.

Rogers, C., Garrison, G., Grober, R., Hillis, Z-M., and Franke, M.A., 1994, Coral Reef Monitoring Manual for the Caribbean and Western Atlantic. (St. John: National Park Service, Virgin Islands National Park).

Sukarno. 1994. Ekosistem Terumbu Karang dan Masalah Pengelolaannya. Materi Kursus Pelatihan Metodologi Penelitian Penentuan Kondisi Terumbu Karang. P3O LIPI. Jakarta

Sukmara A., A.J. Siahainenia., C. Rotinsulu, C. 2001. Panduan Pemantauan Terumbu Karang Berbasis – Masyarakat Dengan Metoda Manta Tow. Proyek Pesisir. Publikasi Khusus. University of Rhode Island, Coastal Resources Center, Narragansett, Rhode Island, USA.

Satellite Monitoring of Fishing Vessels as A Tool to Localize and Estimate The Fishing Activity

E. Walker[1,2], N. Bez[1,2] and P. Gaspar[1,2]

[1]Marine Ecosystem Modelling and Monitoring by Satellites, Satellite Oceanography Division, CLS, Ramonville, France

[2]Centre de Recherche Halieutique Méditerranéenne et Tropicale, IRD, Sète, France

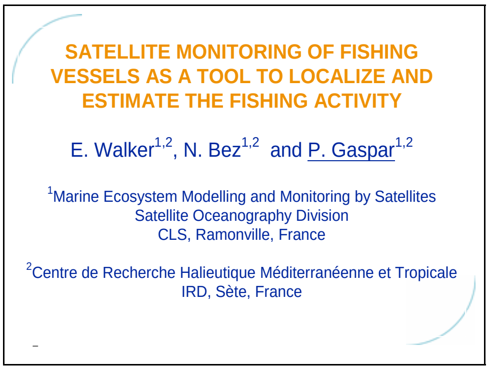

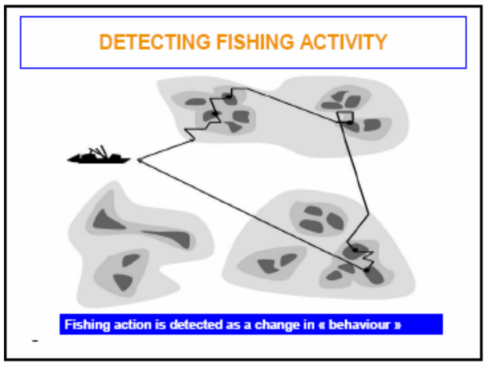

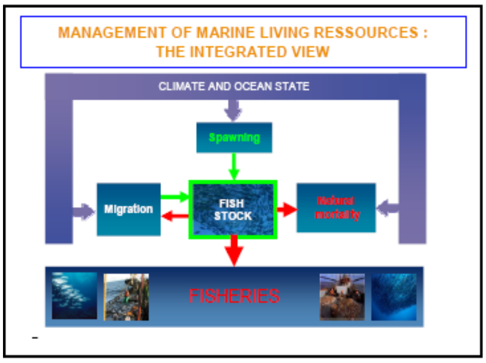

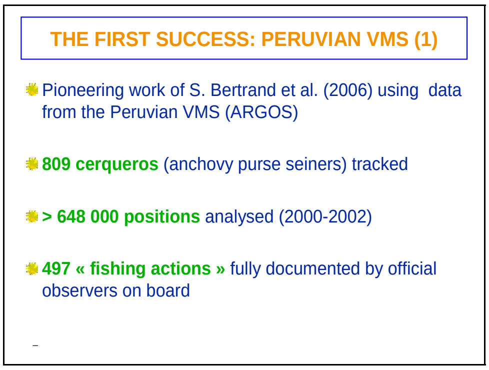

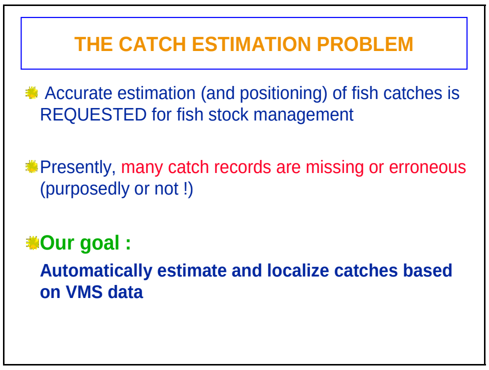

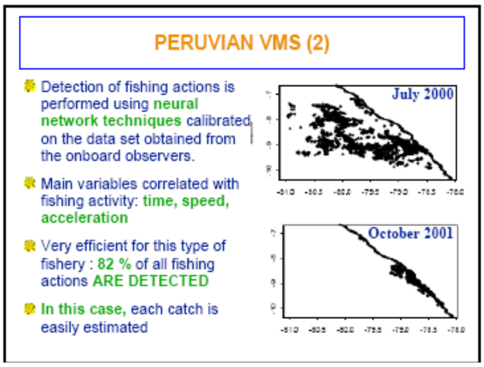

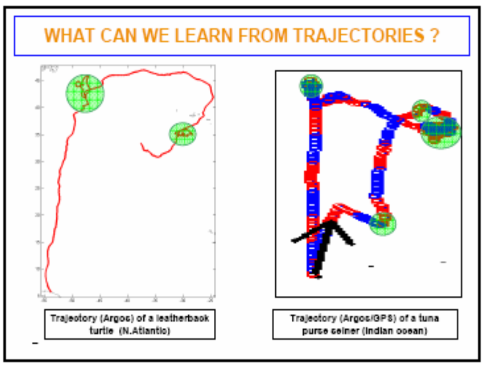

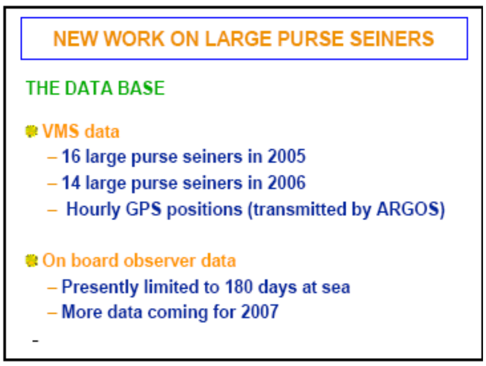

DATA BASE ORGANISATION

- BY FISHING TRIP
  - Begins when the vessel is > 15 miles from harbour and stops at 15 miles from the next harbour stop
- DAY/NIGHT
  - Day positions = one hour before sunrise to sunset

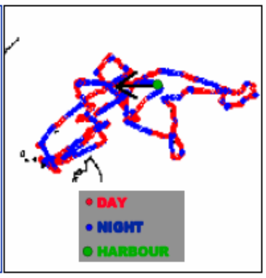

NEXT STEPS

ON GOING EFFORTS TO

- Identify « unusual » weather conditions by adding weather forecasts to the list of explanatory variables
- Precisely analyze the effects of missing VMS data on the detection rate
- Obtain better detection rates with more elaborate algorithms (neural network)

ANALYSIS OF SPEEDS

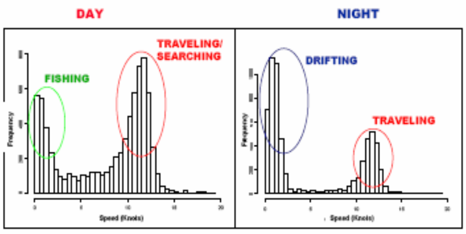

FUTURE WORK

- Develop algorithms to estimate catches based on VMS tracking data
- Work on other fishing gears (trawlers, long line)

OPERATIONAL SUCCESS CRITICALLY DEPENDS ON

- ✓ Availability of high-quality observer data set
- ✓ Continuous day to day monitoring of the state of the fleet and the VMS

A SIMPLISTIC ALGORITHM FOR DETECTING FISHING

V_i V_{i+1} (t_i, X_i)

If [(vessel not in harbour)

and (t_i during DAY)

and (V_i and V_{i+1} > 1.3 knots)]

Then (t_i, X_i) = time/position of fishing action

Results for 7 fishing trips on 4 vessels

TRIP N°	VESSEL N°	% of detection
1	1	63 %
2	1	80 %
3	2	74 %
4	3	83 %
5	3	30 %
6	4	0 %
7	4	7 %

PRELIMINARY CONCLUSIONS

FOR LARGE PURSE SEINERS

- In « usual » conditions, high detections rates (~ 75 %) can be obtained with very simple algorithms.
- Detection rate drops rapidly in « unusual » weather conditions as the vessel movements become atypical.
- Detection rate is even worse (close to 0) when VMS data are missing (vessel 4 with >30 % of missing hourly positions).

A Conceptual Design of Operational Oceanography in The Eastern Indian Ocean

Dr. Fadli Syamsudin
Agency for the assessment and application of technology (BPPT)
and Indian ocean panel(10P) member

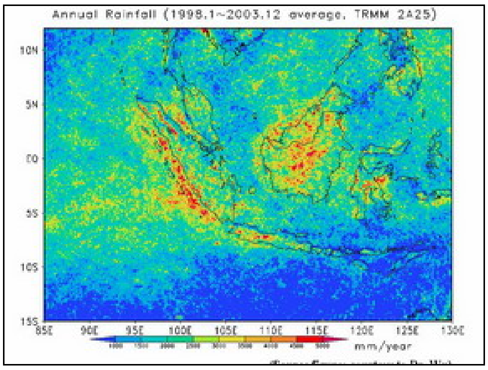

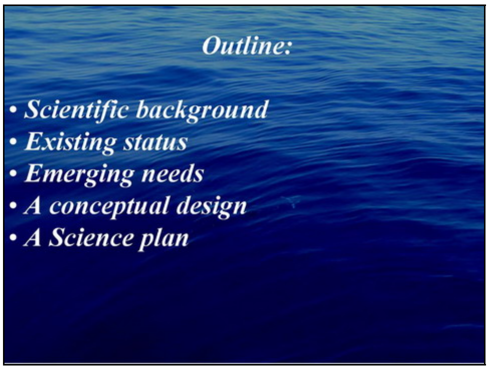

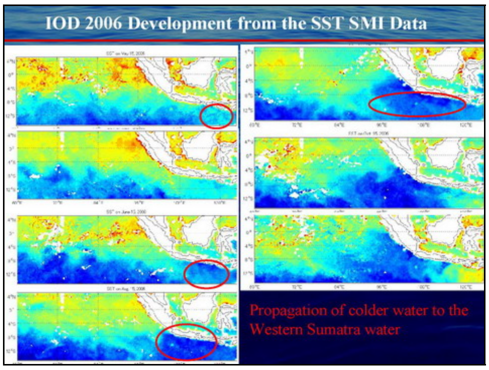

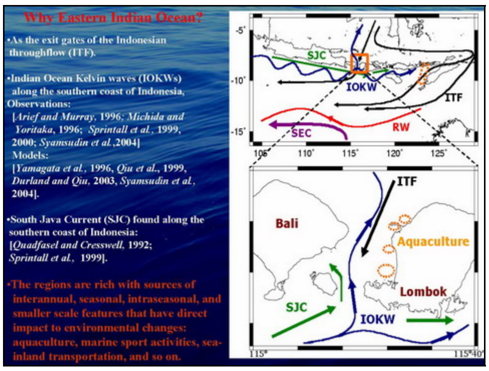

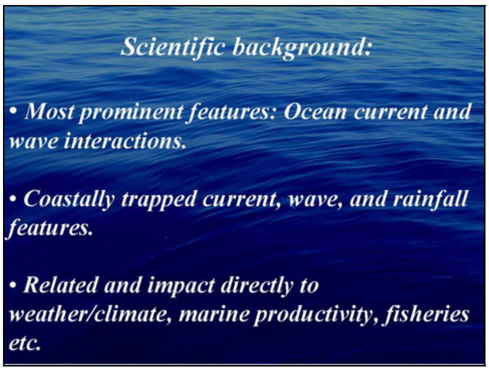


Existing Status

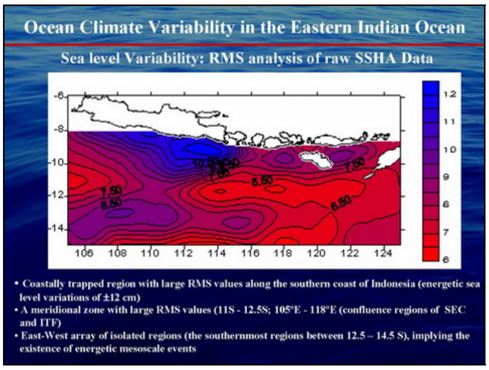
Ocean Climate Variability in the Eastern Indian Ocean
Sea level Variability: RMS analysis of raw SSHA Data
• Coastally trapped region with large RMS values along the southern coast of Indonesia (energetic sea level variations of ±12 cm)
• A meridional zone with large RMS values (11S - 12.5S; 105°E - 118°E (confluence regions of SEC and ITF)
• East-West array of isolated regions (the southernmost regions between 12.5 – 14.5 S), implying the existence of energetic mesoscale events

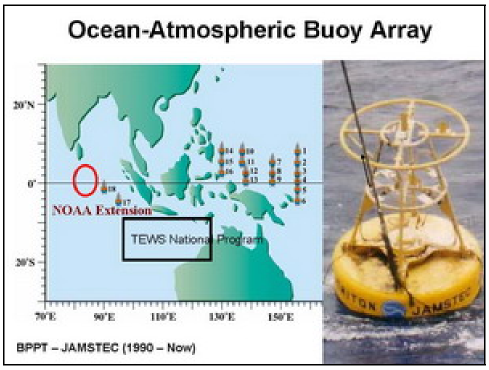
Ocean-Atmospheric Buoy Array
NOAA Extension
TEWS National Program
BPPT – JAMSTEC (1990 – Now)

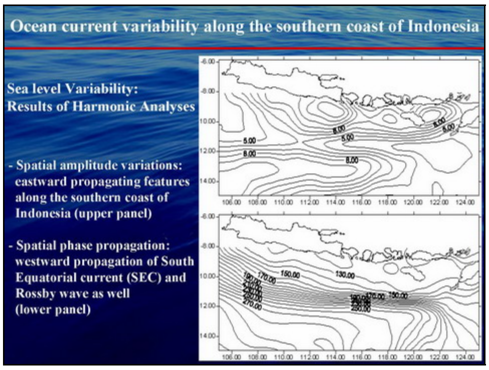
Ocean current variability along the southern coast of Indonesia
Sea level Variability:
Results of Harmonic Analyses
- Spatial amplitude variations: eastward propagating features along the southern coast of Indonesia (upper panel)
- Spatial phase propagation: westward propagation of South Equatorial current (SEC) and Rossby wave as well (lower panel)

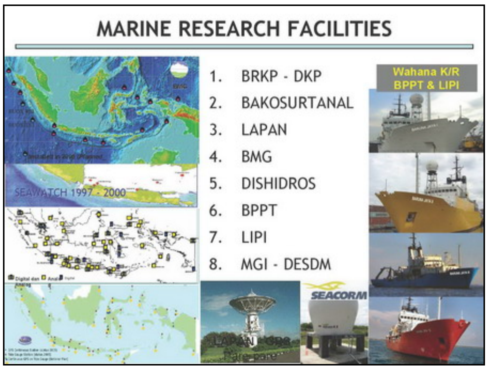
MARINE RESEARCH FACILITIES
1. BRKP - DKP
2. BAKOSURTANAL
3. LAPAN
4. BMG
5. DISHIDROS
6. BPPT
7. LIPI
8. MGI - DESDM
Wahana K/R
BPPT & LIPI
SEAWATCH 1997 - 2000
SEACORM

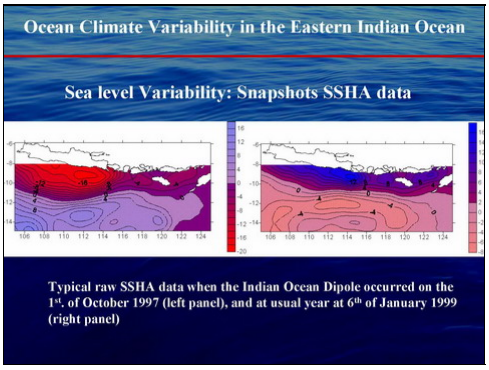
Ocean Climate Variability in the Eastern Indian Ocean
Sea level Variability: Snapshots SSHA data
Typical raw SSHA data when the Indian Ocean Dipole occurred on the 1st. of October 1997 (left panel), and at usual year at 6th of January 1999 (right panel)


Emerging Needs

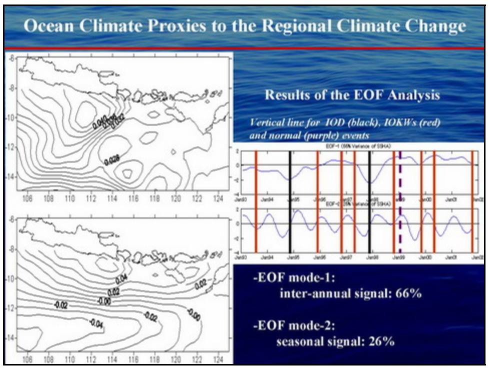
Ocean Climate Proxies to the Regional Climate Change
Results of the EOF Analysis
Vertical line for IOD (black), IOKWs (red) and normal (purple) events
-EOF mode-1:
inter-annual signal: 66%
-EOF mode-2:
seasonal signal: 26%

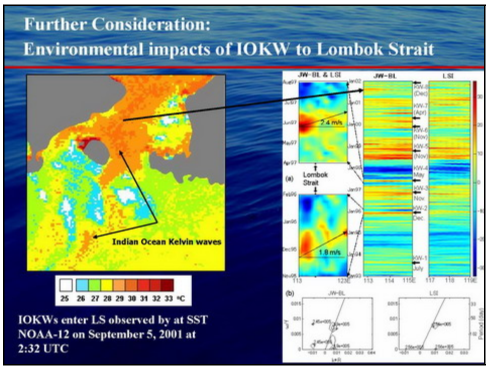
Further Consideration:
Environmental impacts of IOKW to Lombok Strait
Indian Ocean Kelvin waves
25 26 27 28 29 30 31 32 33 °C
IOKWs enter LS observed by at SST NOAA-12 on September 5, 2001 at 2:32 UTC
JW-BL
LSI
Lombok Strait
2.4 m/s
1.8 m/s

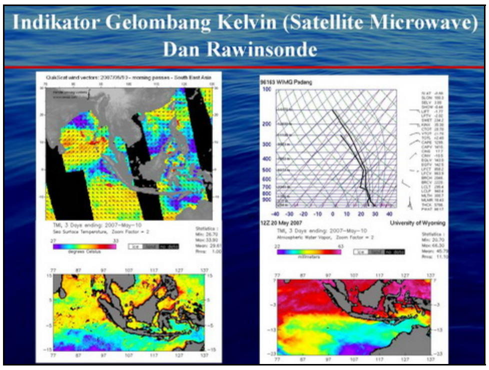
Indikator Gelombang Kelvin (Satellite Microwave)
Dan Rawinsonde
University of Wyoming

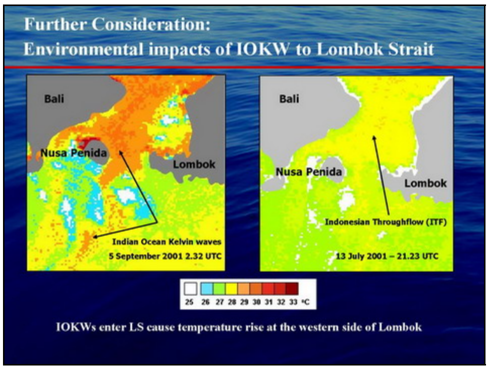
Further Consideration:
Environmental impacts of IOKW to Lombok Strait
Bali
Nusa Penida
Lombok
Indian Ocean Kelvin waves
5 September 2001 2.32 UTC
Bali
Nusa Penida
Lombok
Indonesian Throughflow (ITF)
13 July 2001 – 21.23 UTC
25 26 27 28 29 30 31 32 33 °C
IOKWs enter LS cause temperature rise at the western side of Lombok

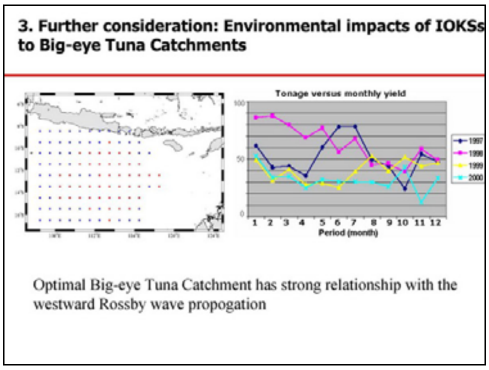
3. Further consideration: Environmental impacts of IOKSs to Big-eye Tuna Catchments
Tonage versus monthly yield
1997
1998
1999
2000
Period (month)
Optimal Big-eye Tuna Catchment has strong relationship with the westward Rossby wave propogation

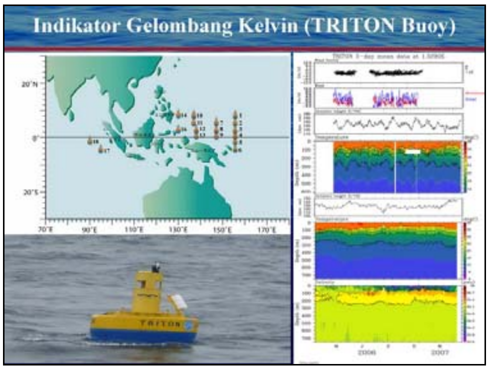
Indikator Gelombang Kelvin (TRITON Buoy)
20°N
0°
20°S
70°E
90°E
110°E
130°E
150°E
170°E
TRITON
2006
2007


A Conceptual Design

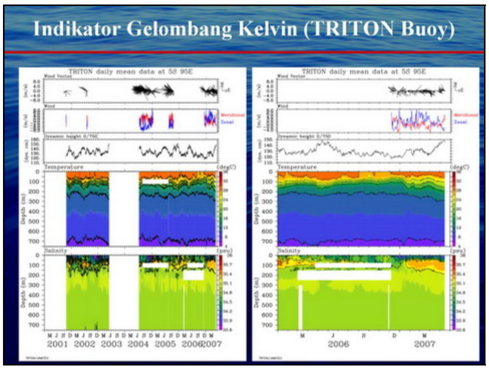
Indikator Gelombang Kelvin (TRITON Buoy)
TRITON daily mean data at 5S 95E
TRITON daily mean data at 5S 95E
Wind Vector
Temperature
Salinity
2001 2002 2003 2004 2005 2006 2007
2006
2007

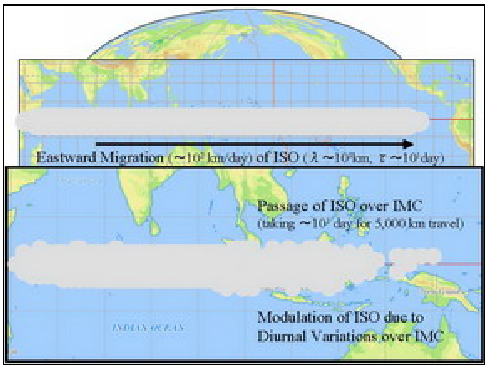
Eastward Migration (~10² km/day) of ISO (λ ~10⁴km, τ ~10² day)
Passage of ISO over IMC
(taking ~10¹ day for 5,000 km travel)
Modulation of ISO due to
Diurnal Variations over IMC
INDIAN OCEAN

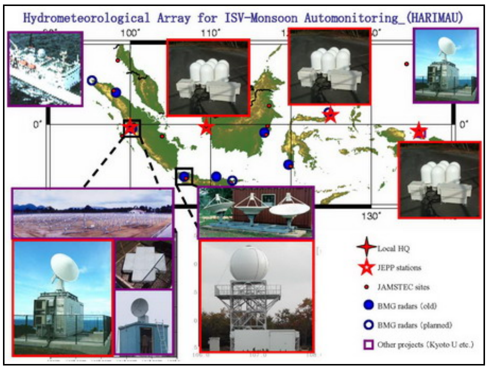
Hydrometeorological Array for ISV-Monsoon Automonitoring (HARIMAU)
Local HQ
JEPP stations
JAMSTEC sites
BMG radars (old)
BMG radars (planned)
Other projects (Kyoto U etc.)

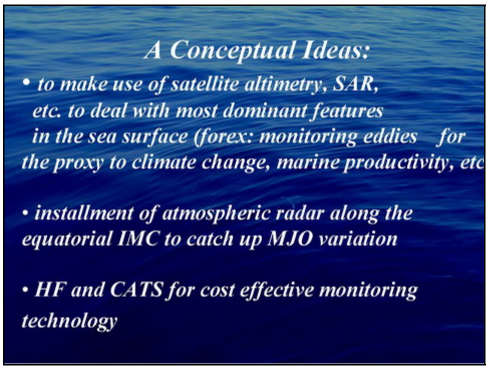
A Conceptual Ideas:
• to make use of satellite altimetry, SAR, etc. to deal with most dominant features in the sea surface (forex: monitoring eddies for the proxy to climate change, marine productivity, etc
• installment of atmospheric radar along the equatorial IMC to catch up MJO variation
• HF and CATS for cost effective monitoring technology

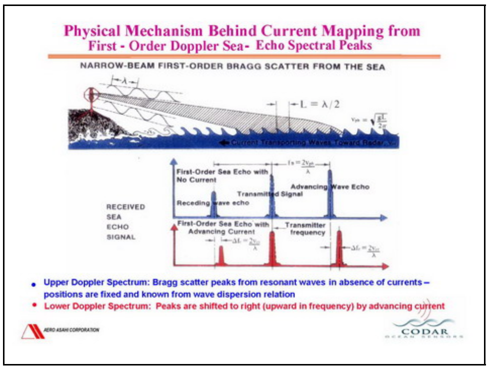
Physical Mechanism Behind Current Mapping from First - Order Doppler Sea- Echo Spectral Peaks
NARROW-BEAM FIRST-ORDER BRAGG SCATTER FROM THE SEA
RECEIVED SEA ECHO SIGNAL
• Upper Doppler Spectrum: Bragg scatter peaks from resonant waves in absence of currents – positions are fixed and known from wave dispersion relation
• Lower Doppler Spectrum: Peaks are shifted to right (upward in frequency) by advancing current
CODAR

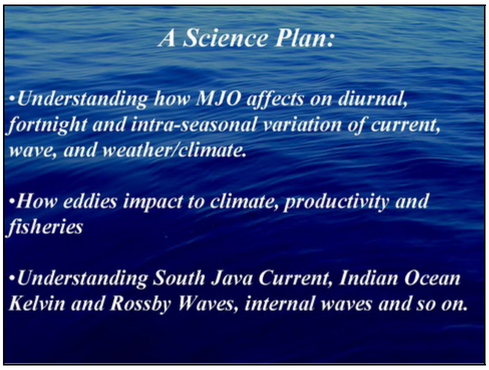
A Science Plan:
•Understanding how MJO affects on diurnal, fortnight and intra-seasonal variation of current, wave, and weather/climate.
•How eddies impact to climate, productivity and fisheries
•Understanding South Java Current, Indian Ocean Kelvin and Rossby Waves, internal waves and so on.

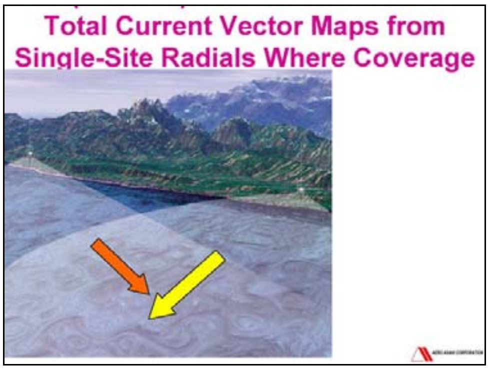
Total Current Vector Maps from Single-Site Radials Where Coverage

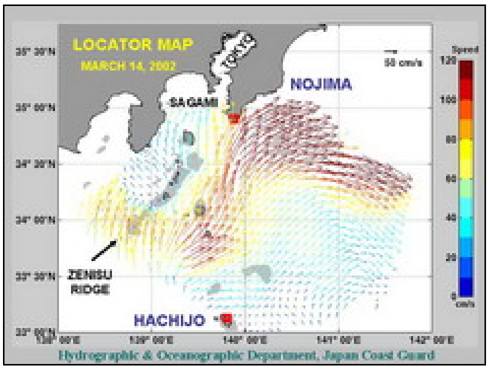
LOCATOR MAP
MARCH 14, 2002
SAGAMI
NOJIMA
ZENISU RIDGE
HACHIJO
Hydrographic & Oceanographic Department, Japan Coast Guard

The Operational Oceanographic Observation

Prof. Dr.-Ing. Chia Chuen Kao
National Cheng Kung University
Tainan, Taiwan, Republic of China

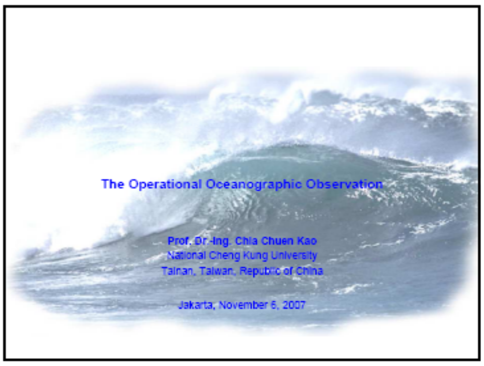

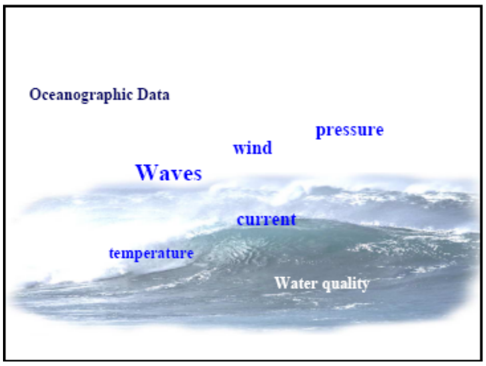

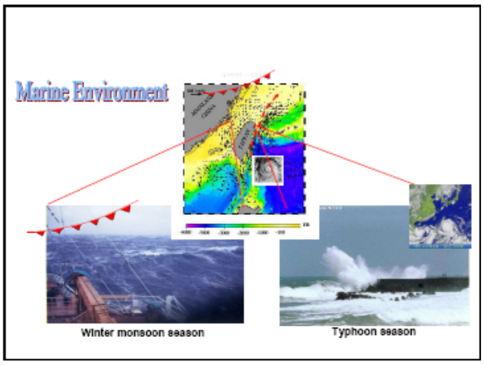

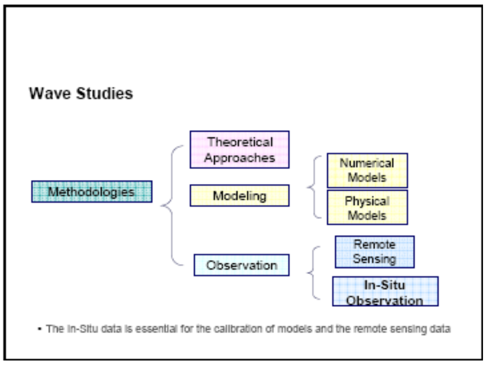

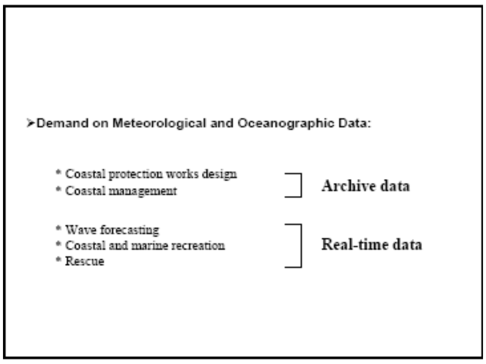

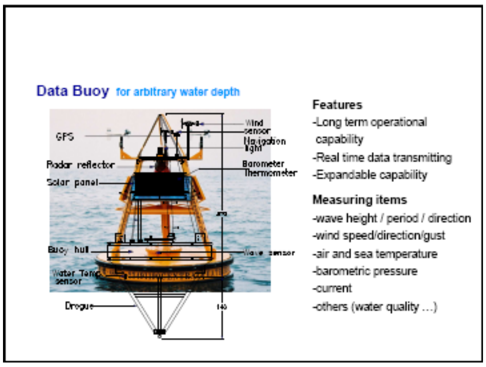
Data Buoy for arbitrary water depth
GPS
Radar reflector
Solar panel
Buoy hull
Water Temp sensor
Drogue
Barometer
Thermometer
Features
-Long term operational capability
-Real time data transmitting
-Expandable capability
Measuring items
-wave height / period / direction
-wind speed/direction/gust
-air and sea temperature
-barometric pressure
-current
-others (water quality ...)

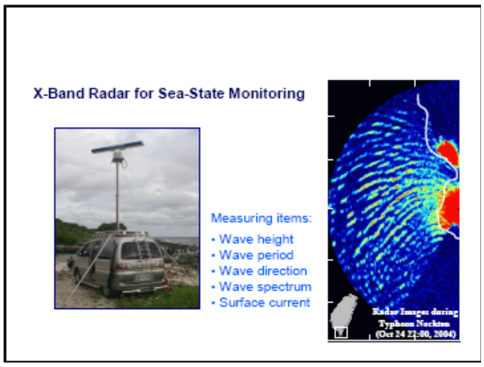
X-Band Radar for Sea-State Monitoring
Measuring items:
• Wave height
• Wave period
• Wave direction
• Wave spectrum
• Surface current
Radar Images during Typhoon Nockten (Oct 24 22:00, 2004)

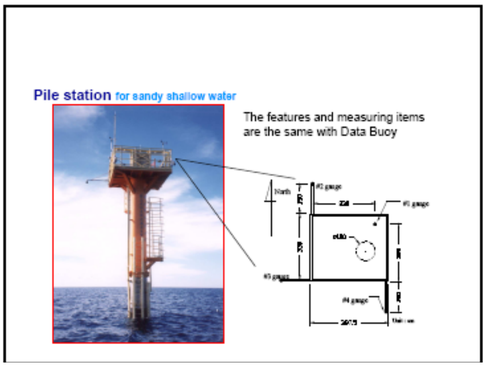
Pile station for sandy shallow water
The features and measuring items are the same with Data Buoy

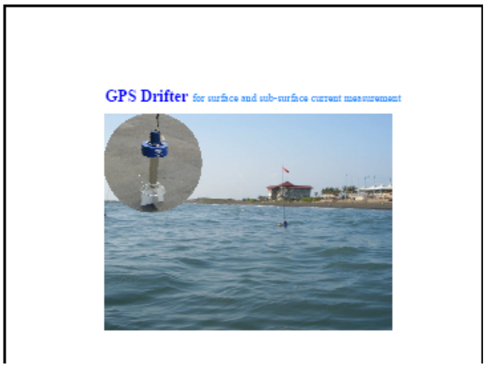
GPS Drifter for surface and sub-surface current measurement

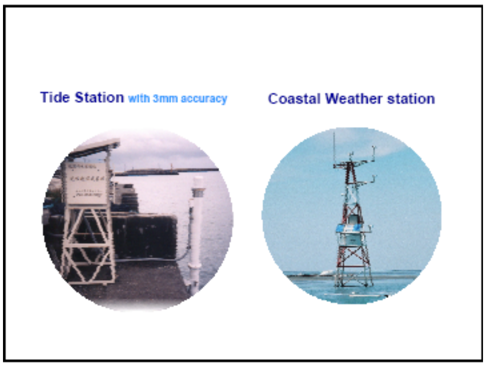
Tide Station with 3mm accuracy
Coastal Weather station

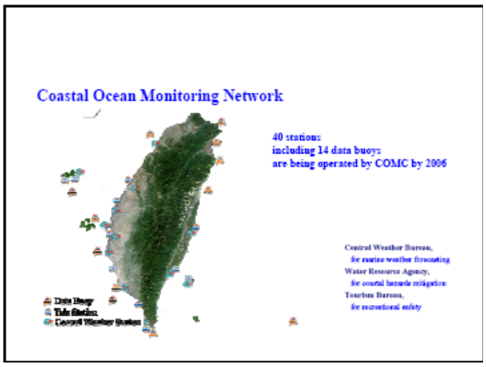
Coastal Ocean Monitoring Network
40 stations
including 14 data buoys
are being operated by COMC by 2006
Central Weather Bureau,
for marine weather forecasting
Water Resource Agency,
for coastal hazards mitigation
Tourism Bureau,
for recreational safety
Data Buoy
Tide Station
Coastal Weather Station

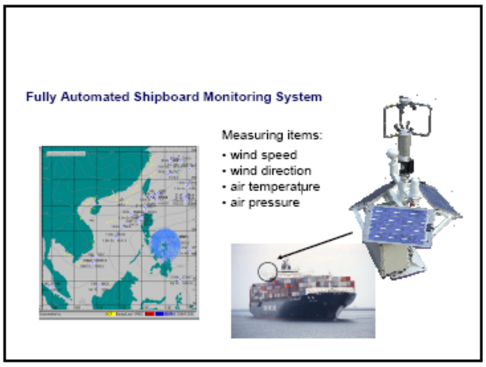
Fully Automated Shipboard Monitoring System
Measuring items:
• wind speed
• wind direction
• air temperature
• air pressure

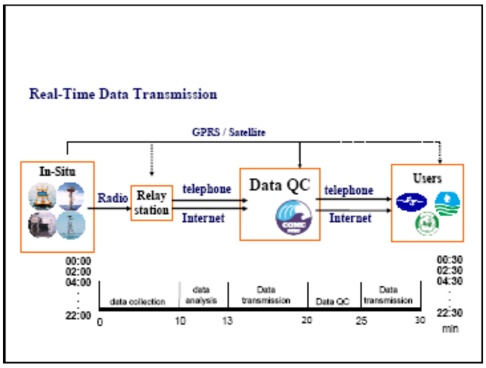
Real-Time Data Transmission
GPRS / Satellite
In-Situ
Radio
Relay station
telephone
Internet
Data QC
telephone
Internet
Users
00:00
02:00
04:00
22:00
data collection
data analysis
Data transmission
Data QC
Data transmission
0
10
13
20
25
30
00:30
02:30
04:30
22:30
min

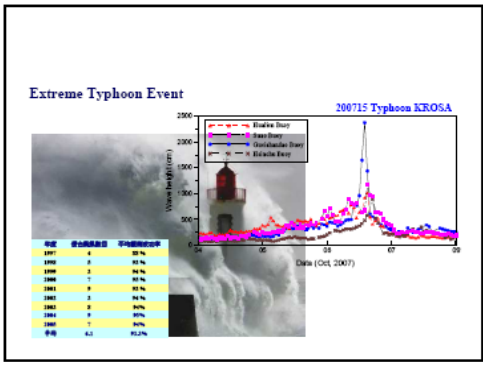
Extreme Typhoon Event
200715 Typhoon KROSA
Wave height (cm)
Date (Oct, 2007)

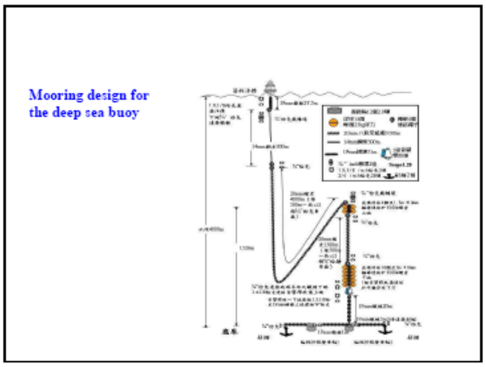
Mooring design for
the deep sea buoy

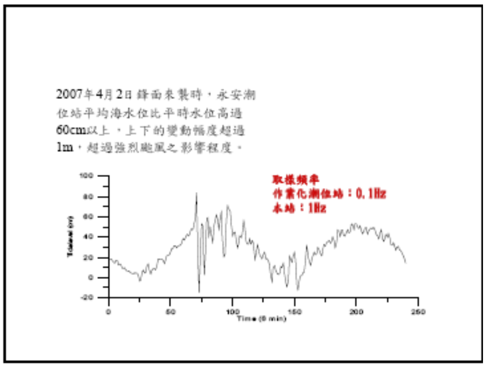
2007年4月2日鋒面來襲時，永安潮
位站平均海水位比平時水位高過
60cm以上，上下的變動幅度超過
1m，超過強烈颱風之影響程度。
取樣頻率
作業化潮位站：0.1Hz
本站：1Hz
Time (6 min)

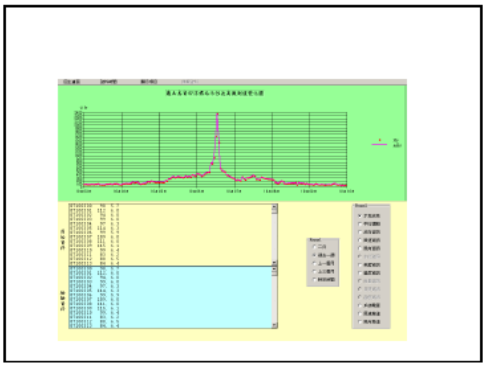

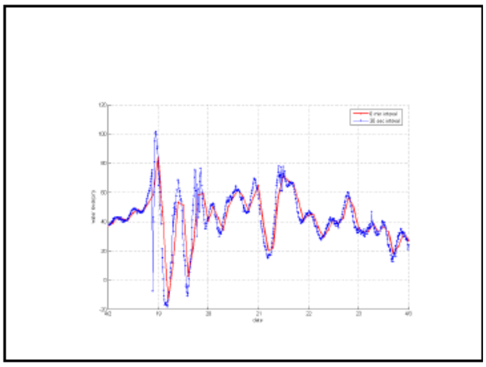

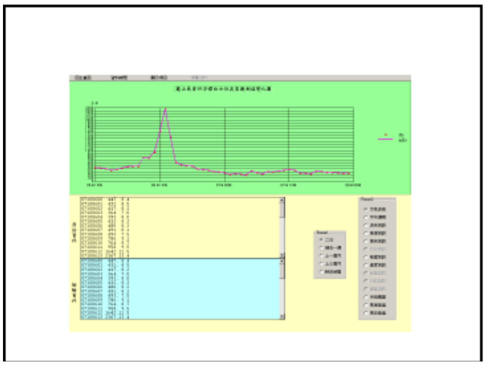

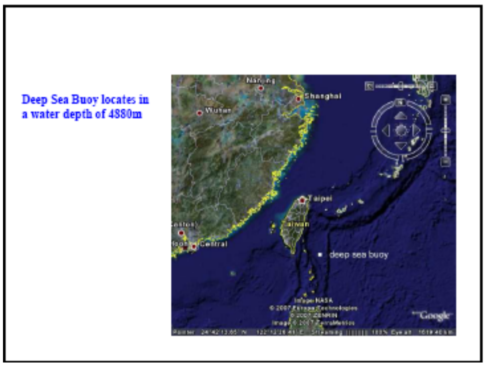
Deep Sea Buoy locates in
a water depth of 4880m
Shanghai
Taipei
deep sea buoy

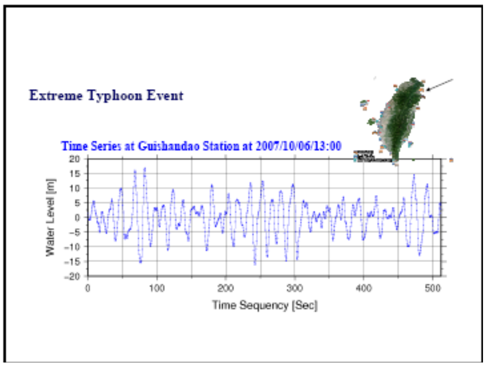
Extreme Typhoon Event
Time Series at Guishandao Station at 2007/10/06/13:00
Water Level [m]
Time Sequency [Sec]

2007年4月2日鋒面來襲時，永安潮位站平均海水位比平時水位高過60cm以上，上下的變動幅度超過1m，超過強烈颱風之影響程度。

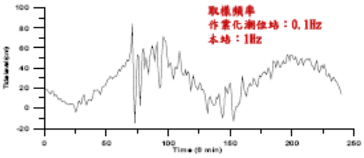

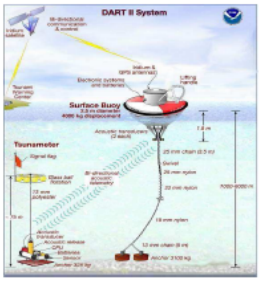

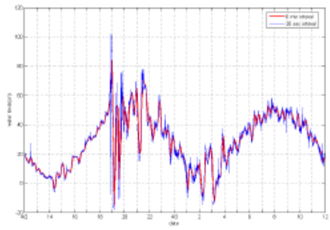

Deep-ocean Assessment and Reporting of Tsunamis (DART™)

DART II PERFORMANCE CHARACTERISTIC / SPECIFICATION SUMMARY

Mandatory Characteristic	Specification
Measurement sensitivity	Less than 1 millimeter in 6000 meters; 2 * 10-7
Sampling interval, internal record	15 seconds
Sampling interval, event reports	15 and 60 seconds
Sampling interval, tidal reports	15 minutes
Tsunami data report trigger	Automatically by tsunami detection algorithm
Data flow, BPR to TWC	Less than 3 minutes after triggered event

Desired Characteristic	Specification
Reliability and data return ratio	Greater than 80%
Maximum deployment depth	6000 meters
Minimum deployment duration	1 year
Operating Conditions	Beaufort 9

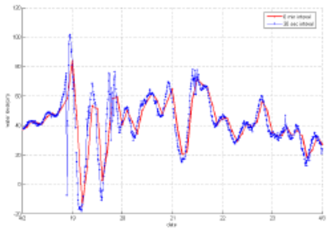

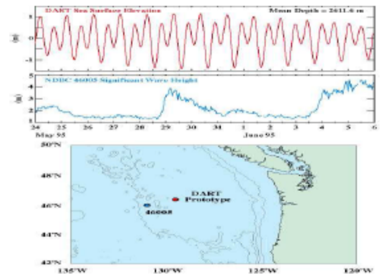

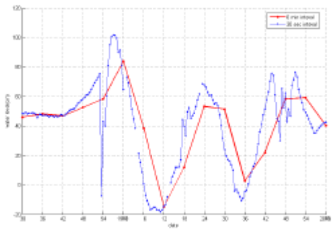

http://nctr.pmel.noaa.gov/Mov/DART_04.swf

for an impressive movie

http://www.ndbc.noaa.gov/dart.shtml

for real time data

A Typhoon Swell Freak Wave Hindcast Example

Nai Kuang Liang
Institute of Oceanography
National Taiwan University
Chinese Taipei

A Typhoon Swell Freak Wave Hindcast Example

Nai Kuang Liang
Institute of Oceanography
National Taiwan University
Chinese Taipei

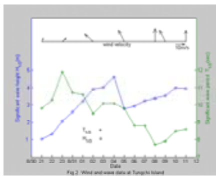

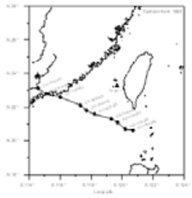

Introduction

- The typhoon or hurricane may generate huge waves within its domain. However, swells usually propagate faster than the typhoon itself and appear outside the typhoon.
- As a typhoon/hurricane approaches a location in the ocean quickly, the enhanced swell may be higher than those in the storm.

Introduction

- The typhoon can be regarded as a wave generator.
- As the typhoon is stationary, the situation is different from that approaching a station.
- As the typhoon approaches the observer, the travel time for the wave energy becomes shorter. This results in an increase in the wave energy flux.

Introduction

- If the typhoon approaching speed is close to the swell energy speed, i.e. the group velocity, a medium scale typhoon/hurricane may generate an extraordinary high swell.
- I named this wave height accumulation phenomenon as the typhoon swell Doppler effect.

Introduction

- If a typhoon is stationary, the swells appear within duration T_D. If the same typhoon is moving, the swell appearance time becomes T_D'.
- The total amount of energy passing through the cross section of a unit wave crest length is the same for the two cases.

$$\int_0^{T_D} (1/8)\rho g H^2 C_g dt = \int_0^{T_D'} (1/8)\rho g H'^2 C_g' dt$$

Introduction

- For $C_g = C_g'$
- Then $\int_0^{T_D} H^2 dt = \int_0^{T_D'} H'^2 dt$
- Assume that $H'/H = \lambda$, called the wave height modification factor and H is not a function of time t. Then

$$\lambda = (T_D / T_D')^{1/2}$$


中國時報
罕見巨浪狂飆 南方澳四漁船遭擊沈
造成一死二失踪 五人輕重傷
瘋狗浪突襲
這麼大的海浪 四十年沒見過

Freak Wave

- Freak waves, so-called rogue waves or monster waves are known as a maritime myth, because they are nearly impossible according to traditional ocean wave theory.
- The freak wave has been explained by the focused current and nonlinear effects. According to some research, an unusual, unstable wave type may form a single wave that ‘sucks’ energy from other waves.
- However, the moving wind system is another reason.

Case Study 1

- Two days ago, a medium scale typhoon Janis had been in the area around 19°N, 136°E and moved fast toward Taiwan.
- The data of typhoon Janis are shown in Table I. There was unfortunately no wave measurement.

Freak Wave

- On January 1st 1995 an extreme single wave of 26 meters was measured under the Draupner oil-platform in the North Sea.
- On December 12, 1978 the cargo ship Muenchen, a state-of-the art cargo ship, disappeared in the mid-Atlantic.
- In March, 2001, two reputable ships were crippled to the point of sinking. The Bremen and Caledonian Star were carrying hundreds of tourists across the South Atlantic. At 5am on 2 March the Caledonian Star’s First Officer saw a 30m wave bearing down on them.

Case Study 1

Table I Data of typhoon Janis

Month	Day	Time (local)	Latitude	Longitude	Central Pressure (hPa)	Radius of Beaufort Scale No.7 (km)	Note
8	4	20	16.5	139.6	990	150	
	5	2	17.3	138.5	990	150	
		8	18.6	137.5	980	200	
		14	19.1	136.3	970	200	
		17	19.5	135.75	962.5	250	interpolated
		19	19.77	135.38	957.5	283	interpolated
		20	19.9	135.2	955	300	
		21	20.05	134.98	954.2	300	interpolated
		23	20.35	134.55	952.5	300	interpolated
	6	2	20.8	133.9	950	300	
		8	21.7	133.2	950	350	
		14	22.7	132.2	950	350	
		20	24.1	131.2	945	350	

Case Study 1

- At about 4 a.m. on August 7, 1992, four fishing ships were totally destroyed by sudden huge waves in the vicinity of Suao Harbor(24.63°N, 121.93°E) at the east coast of Taiwan.
- One man died, two persons were missing and five fishermen were wounded. As the accident was close to the harbor, some wrecks were drifted to shore.
- One fisherman reminded that he has never confronted such big waves in his 40 years’ fishing career.

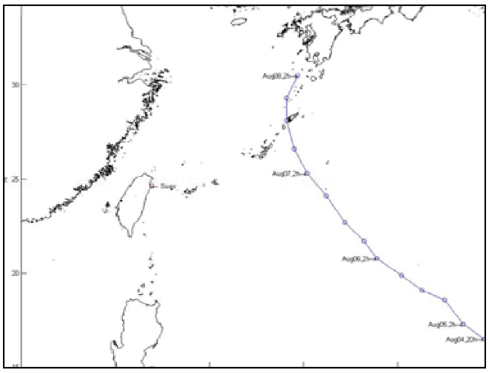

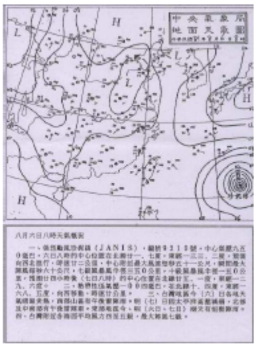

Case Study 1

- Using my “typhoon swell prediction scheme” and assuming Kuroshio current being 2.5 knot, the hindcasted wave are shown in Table II.
- Ts is assumed to be 1.2Tp, where Tp is the peak wave period.

Case Study 1

Table II Hindcasted typhoon Janis swell

No.	Day	Time	H1/3 (Meter	TS (Sec.)	λ	DD (N.M.)	TD' (Hour)	Approaching Speed (knot)	Note
1	7	20.6	0.96	8.28	2.29	1026.8	1.15		
2		9.88	1.17	10.49	1.414	940.6	-10.7	14.36	overrun
3		7.85	1.53	11.66	1.414	886.1	-2.03	12.4	overrun
4		5.58	2.14	12.9	1.414	827.8	-2.26	12.77	overrun
5		4.73	2.59	13.64	1.414	802.1	-0.85	12.85	overrun
6		4.46	2.8	14.0	1.414	789.6	-0.27	12.5	overrun
7		4.73	40.5	14.05	19.85	774.7	0.0025	14.9	

Case Study 1

- Due to the swiftly approaching speed around 14 knots and the quickly enhancing typhoon strength increasing from 970 hPa to 955 hPa in 6 hours, the data from No. 2 through No. 6 in Table II are always overrun.

Case Study 1

- No. 7 is the first datum which is not overrun and the wave height modification factor amounts to 19,85.
- The wave height 40.5m must be over-estimated. But the wave height must be huge. Because the wave height modification factor is sensitive to the typhoon data. The number ought not be emphasized.

Case Study 2

- At about 2 p.m., October 23, 1987, regardless of the invasion of Typhoon Lynn, 304 teachers and pupils of Hydraulic Elementary School of Pingtung County came to Mau-Bi-Tou coast for a tour(near southern tip of Taiwan,21.91°N, 120.725°E).
- As the pupils walked one by one along aisle to the coral reef, suddenly huge waves attacked the coast and 9 pupils were drowned in the sea. The whole nation dropped in a great grief.
- At the meantime, the typhoon scale has transferred from “strong” to “medium” and its center was about 500 km away but has moved fast previously toward Mau-Bi-Tou. On the next day, the headline of United Daily News wrote: “Typhoon Far Away, Hazard Close to Eyes”.

颱風遠在天邊？災難近在眼前！

國小師生郊遊 變生貓鼻頭

滔天巨浪拍岸 吞噬九學童

風狂浪急 未封閉步道 墾丁公園 任遊客涉險

怪師長疏忽 喊打聲起 望海的母親 哀慟昏厥

邱主席極表痛心 促查明校方責任

傷心過度 老師癲癇

Case Study 2

Table III Data of typhoon Lynn

Month	Day	Time (local)	Latitude	Longitude	Central Pressure (hPa)	Radius of Beaufort Scale No.7 (km)
10	20	20	17.9	139.3	920	300
	21	2	17.9	138.3	915	300
		8	18.0	137.3	910	300
		14	18.0	135.9	925	300
		20	18.3	134.2	925	300
	22	2	18.6	132.8	930	300
		8	18.3	130.9	945	350
		14	18.0	129.2	945	400
		20	18.0	128.0	945	400

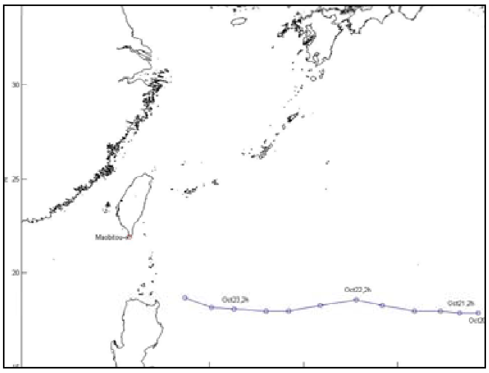

Case Study 2

No.	Day	Time	H1/3	TS	λ	DD
1	23	12.3	5.03	15.7	1.41	522.5
2		12.9	5.06	15.7	1.40	512.5
3		13.5	5.1	15.7	1.40	502.5
4		14.1	5.14	15.7	1.40	492.5
5		14.7	5.18	15.7	1.39	482.7

∗ Assuming zero current speed

Case Study 2

Table IV Hindcasted typhoon Lynn swell

No.	Day	Time	H1/3 (Meter	TS (Sec.)	λ	DD (N.M.)	TD' (Hour)	Approaching Speed (knot)	Note
1	22	17.2	3.8	16.7	1.49	1020.3	2.7	10.0	
2		20.6	4.0	16.9	1.47	963.8	2.8	10.0	
3	23	1.3	3.0	16.1	1.16	887.5	4.44	14.0	
4		3.4	5.7	16.1	2.09	789.7	1.38	17.3	
5		6.7	4.1	15.8	1.47	708.3	2.76	14.3	
6		9.7	4.7	15.3	1.60	613.1	2.36	19.2	
7		11.7	7.6	15.7	2.15	532.6	1.29	17.3	
8		15.3	5.3	15.7	1.40	472.8	3.07	12.0	

Case Study 2

- If the longitude at 17h is perturbed from 128.6 to 128.7, the hindcasted swell at 14.1h, wave height is 7.1 meter.
- This is similar to that on the news paper!

Conclusion

- This hindcast can answer the reason of the accident. And It can be predicted.
- As a typhoon is approaching quickly
  or its strength increasing fast, somewhere hundreds nautical miles away from typhoon, freak wave may take place at sometime.

∗A little typhoon parameter perturbation may result to a freak wave.

Case Study 2

- The accident took place after 2 p.m..
- Interpolating typhoon data between14h～20h, Oct. 22 each hour linearly, only longitudes are changed:

Time	longitude
15	129
16	128.8
17	128.6
18	128.4
19	128.2

Thank You
for your Attention

Monitoring of Marine Resources in Indonesia’s Small Outer Islands (Case: Manterawu Island, North Sulawesi)

Dendy Mahabror, Nicco P, Dedy Aan

ABSTRACT

In Indonesia archipelago, small outer islands are an important territorial base point. Monitoring for marine resources in these islands is important to know global warming phenomenon. Manterawu Island located in North Sulawesi is one of small outer island in Indonesia. This island have ± 750,66 Ha of land and surrounding by mangrove ± 1356,83 Ha and coral reef ± 494,77 Ha. Topography elevation of this island is about 3 meters. The interesting thing from this island is it has a potential sub surface sink. This study will assess an operational oceanography method to be implemented to the island. The goals of the method are to monitor sea level rise and coral bleaching affected by global warming. Some instruments will be installed in Manterawu Island such as tide gauge, meteorology and oceanography measurement station.

Keyword: small outer islands, global warming, manterawu islands, operational oceanography

1. INTRODUCTION

In Indonesia archipelago, outer islands has strategic value as base point from base islands of Indonesia on arrangement Indonesia territorial areas, Exclusive Economical Indonesian Zone, and Indonesia base continental, For exploit and resources management on outer islands, Indonesia issue to presidential degree in 2005 no 78 about small outer islands management.

The one of outer islands is Manterawu island or usually community called Mantehage. It’s located in north Sulawesi in north Minahasa regency was bounded by Philippine. Manterawu island has big potential such as tour area, Conservation, and fisheries potential.

. Marine potential in Manterawu island not used yet optimally because it’s geography position in outer Indonesia. The way of resources small outer islands on fisheries and marine are develop observation stations on marine and fisheries

Development of marine observation station have two benefit such the fist as to development marine observation station and nature laboratory for research and growing marine resources especially in potential areas. Second as medium to increasing control and safety small islands through to observation station for justification NKRI area.

2. PURPOSE

Marine resources potentials monitoring for small outer islands Indonesia.

3. BENEFIT

As one of monitoring system global warming effect to existence small outer islands.

4. METHODOLOGY

Method In this activity is accumulate primer data with survey mangrove plotting, coral reef and bathymetry will be compilation with ASTER Image data.

5. SURVEY RESULT

In 2007 have been doing Marine resources potential monitoring in Manterawu which one of small outer islands in north Sulawesi.

This island occupied by ± 2000 people which they are as farmer especially coconut farmer and rice farmer unirrigated agricultural field. Fisherman is the second profession in this island and they are use fishing gear traditional.

This island surrounded by mangrove woods especially rhizophora species and Bruguera, etc. It’s function for wave detention and spawning ground, crustacea and other biotic.

This is result data spatial and data survey:

Result ASTER data process indicate to Manterawu Island have several dominant part as land, mangrove and coral reef. Beside that Manterawu island have characteristic oceanography such as drop off bathymetry as far as shoreline. Coverage of Coral reef is large and many variety. Mangrove forest is biggest part in Manterawu island, its founded as far as shoreline.

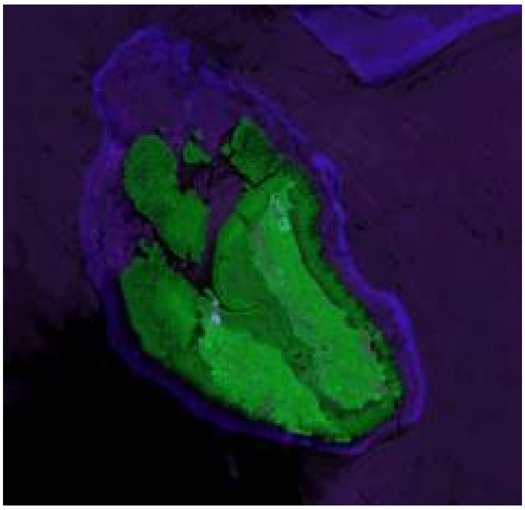

Figure 1: ASTER Citra Data Manterawu Island.

6. LANDS

Result ASTER data process indicate to Manterawu island have ± ***750,66 Ha***. Manterawu land is have 2 part, east land and west land. This island of consist Buhias, Tangkasi, Bango and Tinongko village.

Figure 2: Land Of Manterawu Island.

About 1/3 Main land of Manterawu island is critical land many of growing by shrubs. It's having an area of ± 220 Ha have potential to growing so that can increase economy local community. Jarak plant is long time to know by local community, but a little knowledge they have, now that plant not exploit anymore.

Exploit critical area give additional value for community area live. In this case *jarak* plant for ± 220 Ha area, its possible to produce 880 ton every harvest if assumed for 1 ha has plants 2500 trees with produced ± 2 kg per tree. Long time ago *jarak* produced torch fuel for lightning by local community.

Beside potential critical areas Manterawu land experience to treat for sink because of topography elevation oscillate 3 meters susceptible to increase surface sea. Local community called this island is sink of island because this island have a different with another island on there. Beside that land of island can not see from outside because other than only have topography elevation about 3 meter, its have land surrounding by mangrove forest.

Figure 3: Jarak Plant in Manterawu.

7. MANGROVE

Mangrove woods frequently called as bakau woods, bod woods or tidal woods, formed are devolution ecosystem between land and sea. Mangrove ecosystem have big gradient environment quality, so only kind have tolerant that environment condition such can survive and grow.

Manterawu island from processing ASTER data indicate have an area of mangrove forest about

± ***1356,83 Ha.*** Manterawu island domination by mangrove woods with Rhizopora type where that widely bigger than land coral reef. This woods consign 2 land in Manterau island. In around linecoast Manterawu island there are mangrove woods heavy enough so can categorical so it can help to protect coast and spawning ground.

Figure 4: Coverage of Mangrove in Manterawu.

Covered mangrove woods in this island extent enough, even though exceed that land. Mangrove growing in this island there are 18 type such as Acanthus ilicifolius, Bruguiera cylindrica, Ceriops decandra, Excoecaria agallocha, Heritiera littoralis, Nypa fruticans, Rhizophora apiculata, Sonneratia alba, Terminalia cattapa and Xylocarpus granatum.

8. CORAL REEFS

Coral Reefs is organism that alive at tropic sea bottom and formed to be sea biotic lime produce especially reef type and lime produce algae ($CaCO_3$) and formed of ecosystem strong enough to hold up to wave. Coral reef is ecosystem marine the most productive and highest biodiversity.

Figure 5: Coverage of Coral in Manterawu.

Result ASTER data process coral reef indicate to Manterawu island have an area of ± ***494,77 Ha***. Coral reef about ± 500m from shoreline and surrounding manterawu island. Mangrove and coral reef made ecosystem manterawu island will be guard and environment carrying capacity adequate enough. It can forming of the ocean park and this area is a part of Bunaken marine park.

Result Data survey by line transect method at north, south, east and west Manterawu island so can founded coral reef such as :

1. North Manterawu
   Domination coral reef Non-Acropora encrusting type, dead coral reef (16%). It indicate that hydrodynamic effect is big. This fact because of type and form coral reef alive in area have influence from wave and flow.
2. South Manterawu
   Domination coral reef Non-Acropora encrusting type, Non-Acropora Sub-Massive and dead coral reef (2%). It indicate that characteristic of environment in south manterawu waters influences by effluence intensity and big hydrodynamic compulsion (wave and flow) also at location exposure sub area.
3. East Manterawu
   Domination Acropora Branching type, Non acropora sub-massive and dead coral reef 5%. Emergent domination acropora branching equal with another type decide that characteristic of hydrodynamic in waters wave and flow and also have enough effluence intensity. Differences domination coral reef type in east manterawu between acropora branching and non acropora sub-massive decide that bathymetry in waters steep enough. And have difference location alive characteristic which Non Acropora Sub massive for shallow waters while Acropora Branching live in more deep waters.
4. West Manterawu
   Dominating coral reef are Acropora Branching and Non acropora sub-massive while dead coral 7%. Emergent domination acropora branching equal with another type decide that hydrodynamic characteristic in waters wave and flow and also have effluence intensity enough. Differences domination coral reef type in west manterawu between acropora branching and non acropora sub-massive decide that bathymetry in waters steep enough. And have difference location alive characteristic which

Non Acropora Sub massive for shallow waters while Acropora Branching live in more deep waters.

9. OCEANOGRAPHY

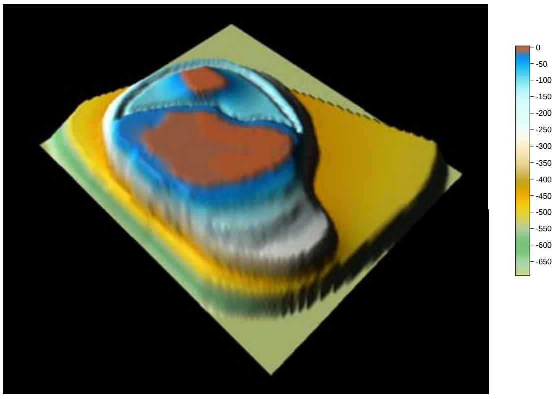

Figure 6: Bathymetry Simulation with Surfer Process.

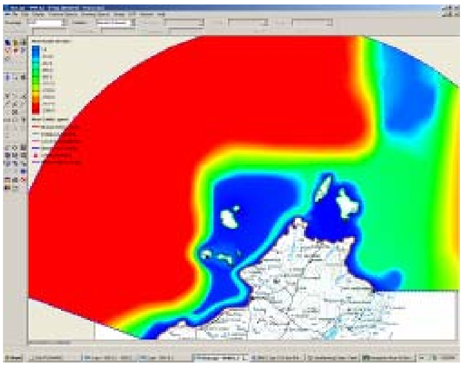

Figure 7: Bathymetry Simulation with SMS Process.

Characteristic bathymetry of Mantehage island there are many drop off. High extreme is more than 500m. Manterawu island surrounding there are reef wall which as coast protection from wave.

On deep sea waters, wave movement be happen on upper ocean. Automatically not effect to underside close to sea bottom (because on deep sea, vertical distance from sea bottom to upper, so far). But depth bathymetry in this island is extreme enough which 5m until hundreds meters the distance only 100-200 m.

With this characteristic of bathymetry therefore wave movement from deep sea big enough but will be happen diffraction effect from large coral barrier in around this island. Beside that ocean flow in depth more than 25m is danger. Point flow strong enough is at mantehage side west this fact motivate characteristic of reef growing more domination reef branching exact is close by reef wall.

Under flow dashing reason forming of gua ceruk. At much gua ceruk there are potential fall if upper coral was brittle.

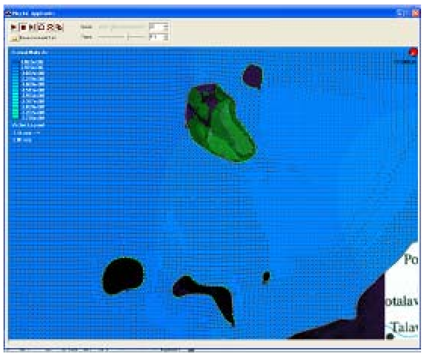

Figure 8: Current in Manterawu Island.

Characteristic this island are many kind, these island have most marine resources and low topography, but there are threat from global warming.

Global warming is the global average air temperature near the Earth's surface rise 0.74 ± 0.18 °C (1.33 ± 0.32 °F) during the last 100. This event could become more severe in the coming decades. The expected global warming from the greenhouse effect is likely to raise sea level a few feet in the next one hundred years and may increase the frequency of severe storms as well.

There are loss potential will be happened if nothing marine potential management resources and monitoring in small outer Indonesia island, such as:

a. Have been bleaching coral reef. Coral reef sometimes live at temperature oscillate 28^o-31^oC. If water sea temperature to go above 31^oC coral reef damage not be avoided anymore. This condition will be happen within less than 25 meter.

b. Coastal zone and small island has altitude under 2 meters lossing chance. If assumed increasing water sea level 1 meter at sloping 2% during 100 year is significant coastal zone, Including Indonesia small islands have sub surface sink about 4.050 Ha per year. Small island have potential sub surface sink ± 2000 islands.

Emergent global warming phenomenon like anomaly monsoon, water sea increasing and often breaker in this area which never happened before. Marine observation station in small outer island have potential suffer damage to global warming phenomenon effect. It is give input policy to management small island Indonesia.

The one of reason, why small outer island is need marine resources monitoring because of several years have been global warming phenomenon. It have effect especially for state formed by islands like Indonesia and whole small island in Indonesia have high land not more than 3m to sea surface and abundant marine resources.

The water that makes these islands desirable, however, also places them at risk. The beautiful homes with their oceanfront views are vulnerable both to storms, which can cause sub surface sink potential and erosion on shoreline.

Figure 7 provides a cross section of a barrier island washing over: the island erodes from the ocean side until it reaches a critical width, generally about 400-700 feet (Leatherman 1979), after which the erosive forces of storms tend more to push sand landward onto the bay side of the island. The net effect of the wash over process is similar to rolling up a rug; as the island rolls landward, it builds upward and remains above sea level.

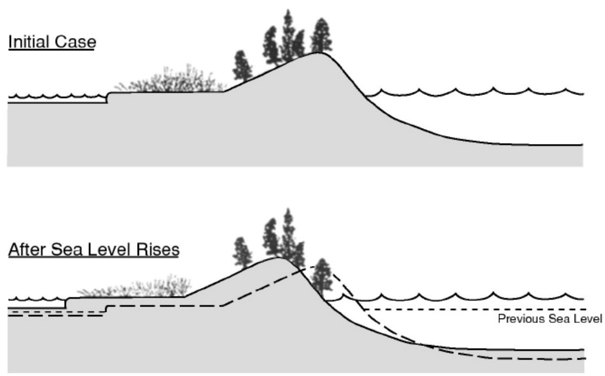

Figure 9: Natural Response Undeveloped Barrier Island to Sea Level Rise.

Base on IPCC (Intergovernmental Panel Climate Change) research between 1970-2004, In Indonesia have been increasing temperature average 0,2-1^{o}C. Global temperature increase on last 100 years, earth temperature increase about 0,7^{o}C, next since 1900 sea level increase 1-3 mm/years. If assumed every year have been increasing se level 3-5mm so next 100 years increasing 500mm.

Manterawu island have topography about 3m to mean sea water level (MSL). With that assume therefore in 500 possible these island will be sink.

Other effects of global warming may exacerbate these impacts. Warmer temperatures could increase the frequency and severity of hurricanes 50 percent (Emmanuel 1988), increasing both erosion and the salinity of estuaries and aquifers would increase, threatening water supplies and aquatic life.

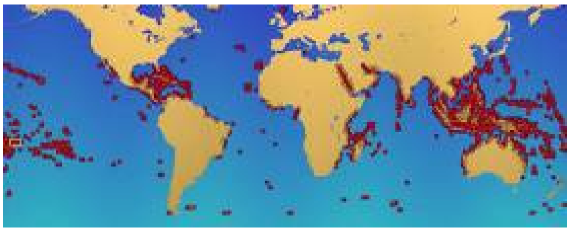

Figure 10: Distribution of Coral in The World.

Coral reef bleaching, the whitening of diverse invertebrate taxa. Of the causing stressors of coral reef bleaching, many are related to local environmental degradation and reef overexploitation. Of the stressors mentioned above, only sea water temperature and solar irradiance have possible global factors driving changes and extremes. Global warming, along with ENSO events, change sea water temperatures. Ozone depletion increases the amount of UVR reaching the Earth’s surface, and possibly causing coral bleaching events.

Increased sea temperatures and solar radiation (especially UV radiation), either separately or in combination, have received consideration as plausible large-scale stressors. In most instances, wherever coral reef bleaching was reported, it occurred during the summer season or near the end of a protracted warming period.

Coral bleaching was reported to have occurred during periods of low wind velocity, clear skies, calm seas and low turbidity, when conditions favor localized heating and high penetration of short wave length (UV) radiation. Also less oxygen is held by water at higher temperatures. Potentially stressful high sea temperatures and UV radiation flux could conceivably cause coral reef bleaching on a global scale with suspected greenhouse warming and the thinning of the ozone layer.

As reef building corals live near their upper thermal tolerance limits, small increases in sea temperature (.5 –1.5 degrees C) over several weeks or large increases (3-4 degrees C) over a few days will lead to coral dysfunction and death.

In 1990, 1995, and 1998 is the hot years in 20 century. Increasing earth temperatures according Nature Journal happened:

1. Low: 0.8 - 1.7 °C as much as 9-13% species would be extinct with various level.
2. Middle: 1.8-2.0°C,. 15-20% would be extinct.
3. High: over 2.0 °C, 21-32% would be extinct.

Beside that increasing sea water temperatures about 2-3°C coral reef will be die because coral bleaching impact. This happening in Australia, Thailand, Filipina, Indonesia, Jamaica, Bahama, etc in 1997/1998 El Nino effect.

Marine and fisheries Department enounce, in two periods (2005-2007) Indonesia have been loss 24 small islands be sinking.

Much as 24 small islands include 3 islands in Nanggroe Aceh Darussalam, 3 islands in north Sumatera, 3 islands in Papua, 5 Islands in Riau, 2 islands in west Sumatra, 1 island in south Sulawesi, and 7 in Seribu island (NAW).

Figure 11: Marine Observation System.

This phenomenon so BROK (Balai Riset dan Observasi Kelautan) will be doing marine observation for small islands there have potential will be sink and marine resources damage. That monitoring is remote sensing method and in situ measurement. There are monitoring concept done for several next years such as:

10. CONCLUSION

This study “Monitoring of Marine Resources in Indonesia’s Small Outer Islands” have conclusion such as :

1. Topography elevation of this island is about 3 meters. The interesting thing from this island is it have a potential sub surface sink
2. This island have ± 750,66 Ha of land and surrounding by mangrove ± 1356,83 Ha and coral reef ± 494,77 Ha.
3. Characteristic bathymetry of Mantehage island there are many drop off. High extreme is more than 500m. Manterawu island surrounding there are reef wall which as coast protection from wave.
4. Some instruments will be installed in Manterawu Island such as tide gauge, meteorology and oceanography measurement station. This station have most Important to monitoring marine resources and existence small outer island.
5. Marine station observation most important for some forecast hydrodynamic in Indonesian sea such as :
   a. Weather Forecasting
   b. Reduce Loss of Life and Property from Disasters
   c. Protect and Monitor Our Ocean Resource
   d. Understand, Assess, Predict, Mitigate and Adapt to Climate Variability and Change
   e. Sustainable Agriculture and Land Degradation
   f. Protect and Monitor Water Resources
   g. Monitor and Manage Energy Resources

Renewable Ocean Energy for The APEC Region

Nai Kuang Liang
Institute of Oceanography. National Taiwan University, Chinese Taipei

Renewable Ocean Energy for the APEC Region

Nai Kuang Liang
Institute of Oceanography
National Taiwan University
Chinese Taipei

Wave Power

- There are many wave power patents in the world.
- The most feasible concept is using the air as a medium. The navigation light buoy is an example.

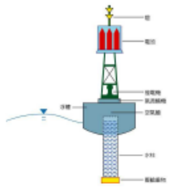

Energy Density

- Kinetic < Potential < Thermal
- 1 m/s current=0.05 meter head
- 1 gram water exits one cal. heat as it decreases 1 degree Celsius. This heat can raise itself 420 meters height!

Closed Cycle OTEC

- OTEC is the abbreviation for Ocean Thermal Energy Conversion. The closed cycle is using ammonia as the heat transfer medium within a closed loop.

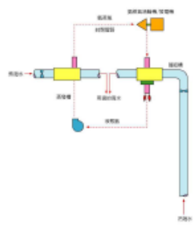

Ocean Current

- The energy density of ocean current is very low. It is similar to wind energy.
- The issue is how to install and maintain the big sea water turbine at deep ocean.

Open Cycle OTEC

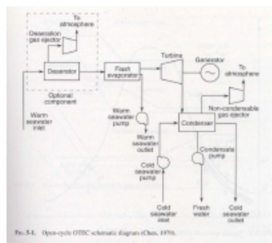

Tidal Power

- The tidal power plant is like the dam power plant.
- The technology is already commercialized.

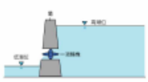

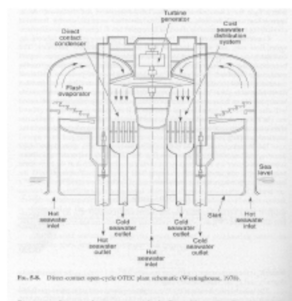

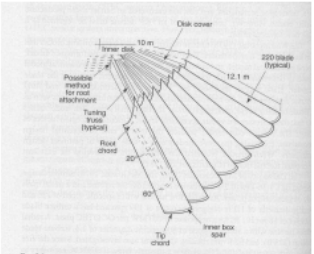

FIG. 5-9. Partial assembly of composite turbine rotor (Penney, 1986).

OTEC

- Because the cold water flow rate is very large, the cold water pipe diameter should be very large, say 10 meters.

OTEC

- Avery $ Wu(1994) estimated that about 3 CMS cold and warm sea water can generate 1 MW net power.
- The sea surface temperature in the tropical and sub-tropical region is quite stable day and night, year round. In fact, the sea surface is a large, perfect solar board.
- Avery $ Wu(1994) estimated that the global useful sea area can generate power exceeding 10 million MW without changing the sea surface temperature.

Shelf-mounted OTEC

- For shelf-mounted OTEC the only problem is the bottom cold water pipe. Because of the sediment slumping, the bottom cold water pipe safety becomes unpredictable.

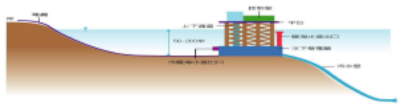

OTEC

Copy from the book "Renewable ocean energy from the ocean – A guide to OTEC"

useful tropical ocean area, the total power generated on board would exceed 10 million MWe; if each plant generated 200 MWe of net power, the plants would be spaced 32 km (20 miles) apart. For comparison, the total U.S. electricity-generating capacity in 1987 was 165 thousand MWe.

Floating OTEC

- The moored floating OTEC plant is a good concept. The CWP is much easier than that of shelf-mounted OTEC. If the electric power is to be transmitted to shore, there is a distance limit.
- Another option is to electrolyze water to become hydrogen and oxygen then synthesize them with coal to produce the methanol and ammonia as fuel, which can be transported everywhere.
- A drifting grazing OTEC plantship is another choice.

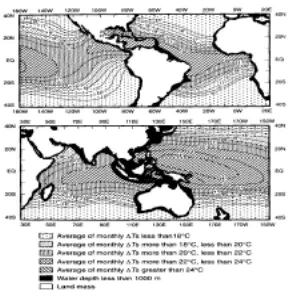

FIG. 1-1. Ocean temperature resource for OTEC (U.S. Department of Energy, Assistant Secretary Energy Technology, Division of Solar Technology).

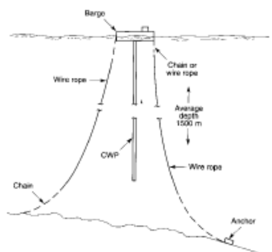

FIG. 1-9. Diagram of mooring options for an OTEC barge (Ross and Wood, 1981).

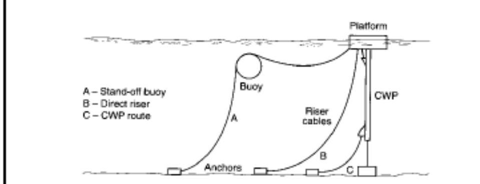

FIG. 1-10. Diagram of power cable deployment options for moored OTEC power plant (Schultz et al., 1981).

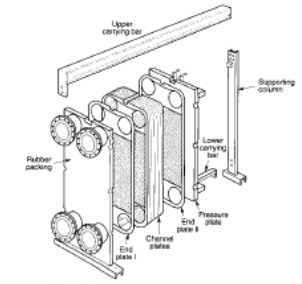

FIG. 4-17. Schematic view of Alfa-Laval plate heat exchanger (Berndt and Connell, 1978).

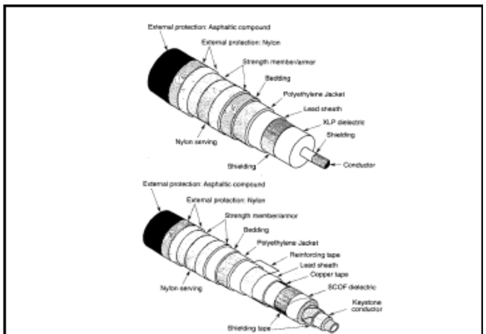

FIG. 4-62. Cable construction for underwater power transmission (Kurt, 1981).

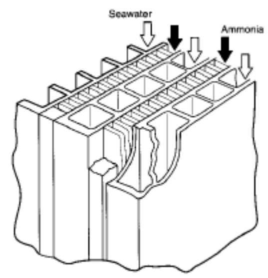

FIG. 1-8. Fluid flow paths in plate heat exchanger.

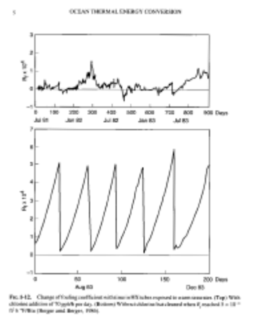

FIG. 4-42.

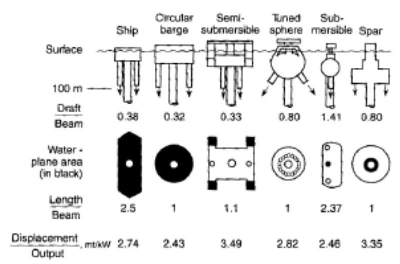

FIG. 1-11. Alternative platform configurations for moored OTEC power plants (Waid, 1978).

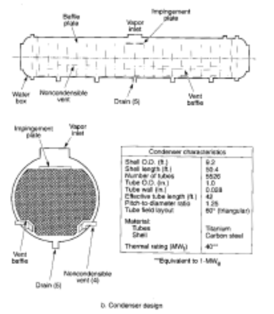

FIG. 4-13b. (continued).

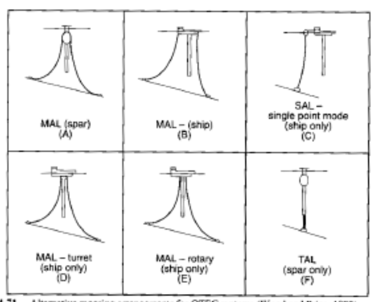

FIG. 4-71. Alternative mooring arrangements for OTEC systems (Wood and Price, 1980).

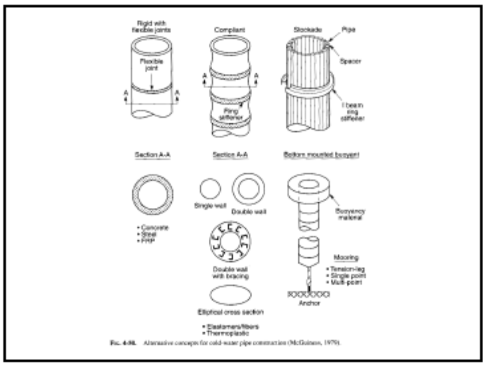

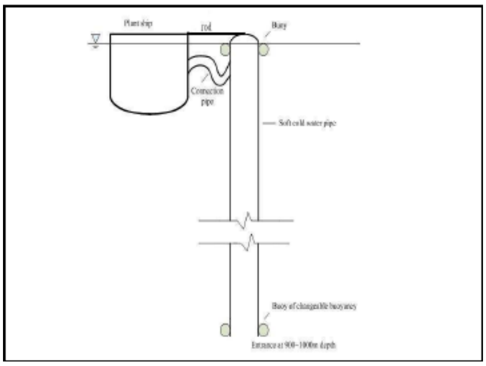

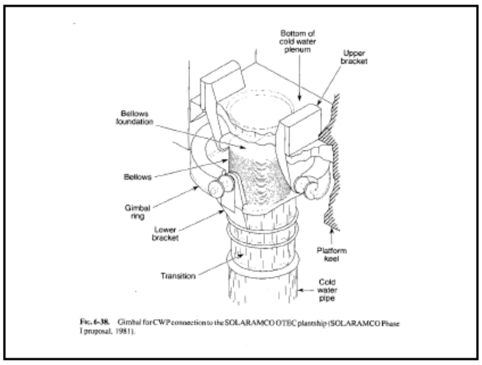

Fig. 6-38. Gimbal for CWP connection to the SOLARAMCO OTEC plantship (SOLARAMCO Phase I proposal, 1981).

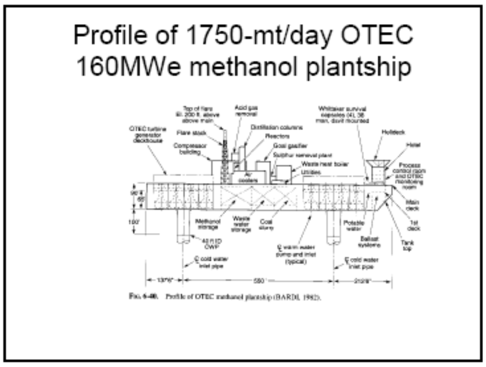

Fig. 6-40. Profile of OTEC methanol plantship (BARDI, 1982).

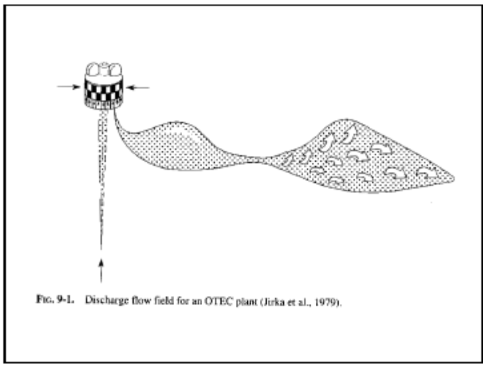
FIG. 9-1. Discharge flow field for an OTEC plant (Jirka et al., 1979).

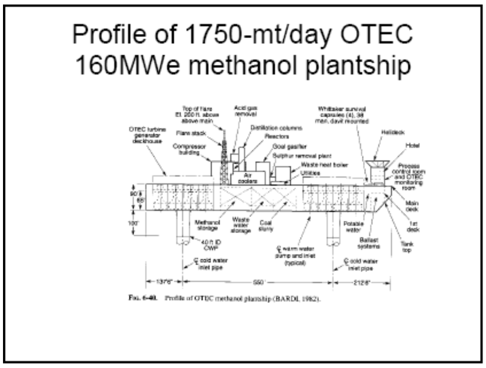

Fig. 6-40. Profile of OTEC methanol plantship (BARDI, 1982).

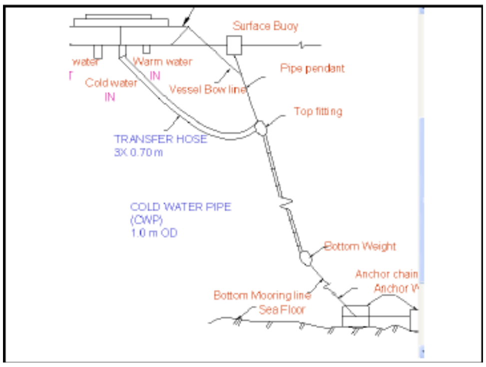

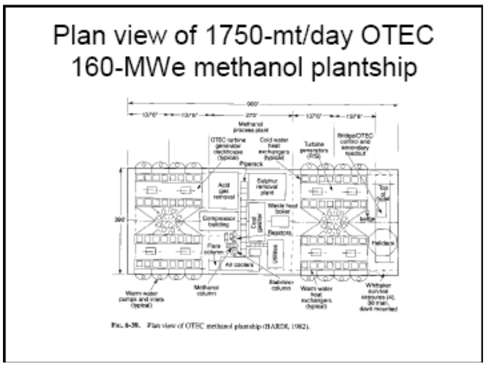

Fig. 6-39. Plan view of OTEC methanol plantship (BARDI, 1982).

Cost Estimate for Grazing OTEC First 200-MWe Methanol Plantship

Subsystem	Cost ($M1990)	Uncertainty
Platform	190.7	-14.0 -- +16.9%
Power system	180.4	-23.4 -- +17.6%
Water ducts	30.8	-24.9 -- +69.0%
CH_3OH production	311.2	-16.5 -- +16.5%
CH_3OH synthesis	68.0	-15.0 -- +15.0%
Service & maintenance	39.2	-15.0 -- +15.0%
Electrolysis	58.4	-30 -- +35.0%
Deployment	39.0	-30.6 -- +81.4%
Acceptance, incl. fac., E&A	45.1	-20 -- +20%
Weighted cost uncertainty		-13 -- +24%
Direct cost	855.6	
Interest during construction (15% of direct cost)	131	
Tot. investment		
Nominal	986	
Minimum	789	
Maximum	1292	

Note: 1990\$=1980\$x1.369=1983\$x1.128

Open Cycle OTEC

- The open cycle OTEC has the shortcoming that the water vapor pressure is low. Therefore, the turbine should be very large. Hence it is not suitable for a plantship.
- If instead of plantship an artificial island, which can be built by the light reinforced concrete, is used, the open cycle OTEC may be feasible because the heat exchanger and ammonia are not necessary. The plant capacity can be several GW.

OTEC Methanol Financing

- Mossman (1989) proposed a financial evaluation for a 200MWe OTEC methanol plantship. Two years of financed construction followed by an operating life of 25 years are assumed. The analysis calculates a quantity termed "the adjusted present value" (APV), which measures the profitability of a potential venture.
- Some assumptions are the following:

1. Permanent financing interest rate is 13%.
2. An interest rate of construction financing is 12%.
3. The debt is 80%.
4. The design methanol production rate per OTEC plantship is 199 million gallons per year. The annual coal cost is 23,5 million dollars (470,000 tons/year at \$50/ton). Coal and methanol shipping costs are \$20/ton each.
5. Operating and maintenance costs are assumed to be \$50.9M/year.
6. The cost of the second vessel is 0.8 times that of the first and an experience factor of 0.93 for each doubling of he number produced.
7. The government provides an incentive commitment for the production of low-polluting vehicle fuels.
8. An investment tax credit (ITC) of 10% has been used.

Note: The crude oil price in 1990 was \$20/bbl.

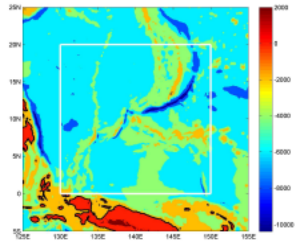

OTEC CLOSED-CYCLE COST EVALUATION 373

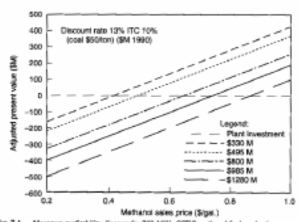

FIG. 7-1. Mossman profitability diagram for 200-MWe OTEC methanol fuel production.

1945-2005颱風

- zonal_0_5and125_130
- TD TS Hu1 Hu2 Hu3 Hu4 Hu5
- number 1.0 0.0 0.0 0.0 0.0 1.0 0.0
- zonal_0_5and130_135
- TD TS Hu1 Hu2 Hu3 Hu4 Hu5
- number 1.0 0.0 0.0 0.0 0.0 1.0 0.0
- zonal_0_5and135_140
- TD TS Hu1 Hu2 Hu3 Hu4 Hu5
- number 8.0 0.0 1.0 0.0 0.0 0.0 0.0
- zonal_0_5and140_145
- TD TS Hu1 Hu2 Hu3 Hu4 Hu5
- number 12.0 0.0 0.0 0.0 0.0 1.0 0.0
- zonal_0_5and145_150
- TD TS Hu1 Hu2 Hu3 Hu4 Hu5
- number 11.0 1.0 1.0 0.0 0.0 0.0 0.0

Profit to investor with OTEC methanol (discount rate=13%;construction interest=12%; ITC=10%;APV=0)

Plant No.	n^{th} plant Inves.($M)	Total prod. (Bgal/y)	Sales Price ($/gal)	Gasoline price incl. import and carbon tax ($/gal)	CH_3OH price incl. auto cost and carbon tax ($/gal)	Net profit to investor replacing gasoline by CH_3OH ($B/y)
1	960	0.20	0.75	1.53	1.56	-0.003
2	768	0.40	0.70	1.53	1.47	0.013
3	768	0.60	0.68	1.53	1.44	0.029
4	714	0.80	0.67	1.53	1.42	0.051
8	664	1.6	0.64	1.53	1.37	0.143
16	618	3.2	0.62	1.53	1.33	0.35
32	575	6.4	0.60	1.53	1.29	0.85
64	534	13	0.58	1.53	1.25	1.97
128	497	25	0.55	1.53	1.21	4.50
256	462	51	0.53	1.53	1.18	10.0
427	438	85	0.52	1.53	1.15	18.0
512	430	102	0.51	1.53	1.14	22.0

Note: In automobile miles/gal, 1.8 gallons CH_3OH=1.0 gallon gasoline.

1945-2005颱風

- zonal_5_10and125_130
- TD TS Hu1 Hu2 Hu3 Hu4 Hu5
- number 51.0 27.0 7.0 3.0 2.0 3.0 2.0
- zonal_5_10and130_135
- TD TS Hu1 Hu2 Hu3 Hu4 Hu5
- number 75.0 41.0 8.0 6.0 4.0 3.0 3.0
- zonal_5_10and135_140
- TD TS Hu1 Hu2 Hu3 Hu4 Hu5
- number 107.0 42.0 13.0 10.0 4.0 4.0 1.0
- zonal_5_10and140_145
- TD TS Hu1 Hu2 Hu3 Hu4 Hu5
- number 105.0 39.0 19.0 5.0 5.0 2.0 2.0
- zonal_5_10and145_150
- TD TS Hu1 Hu2 Hu3 Hu4 Hu5
- number 114.0 39.0 14.0 5.0 1.0 2.0 3.0

1945-2005颱風

- zonal_10_15and125_130
- TD TS Hu1 Hu2 Hu3 Hu4 Hu5
- number 106.0 114.0 45.0 23.0 12.0 28.0 26.0
- zonal_10_15and130_135
- TD TS Hu1 Hu2 Hu3 Hu4 Hu5
- number 120.0 115.0 41.0 24.0 15.0 27.0 22.0
- zonal_10_15and135_140
- TD TS Hu1 Hu2 Hu3 Hu4 Hu5
- number 125.0 87.0 55.0 24.0 16.0 24.0 17.0
- zonal_10_15and140_145
- TD TS Hu1 Hu2 Hu3 Hu4 Hu5
- number 103.0 88.0 46.0 14.0 9.0 22.0 11.0
- zonal_10_15and145_150
- TD TS Hu1 Hu2 Hu3 Hu4 Hu5
- number 102.0 88.0 17.0 16.0 8.0 12.0 11.0

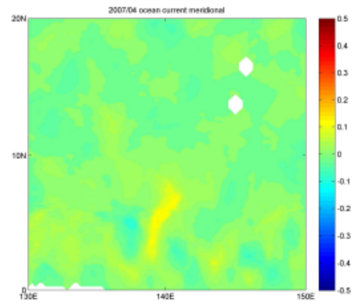

1945-2005颱風

- zonal_15_20and125_130
- TD TS Hu1 Hu2 Hu3 Hu4 Hu5
- number 73.0 88.0 69.0 32.0 32.0 47.0 33.0
- zonal_15_20and130_135
- TD TS Hu1 Hu2 Hu3 Hu4 Hu5
- number 65.0 104.0 53.0 25.0 31.0 43.0 30.0
- zonal_15_20and135_140
- TD TS Hu1 Hu2 Hu3 Hu4 Hu5
- number 62.0 88.0 36.0 27.0 28.0 28.0 32.0
- zonal_15_20and140_145
- TD TS Hu1 Hu2 Hu3 Hu4 Hu5
- number 74.0 67.0 40.0 19.0 18.0 21.0 17.0
- zonal_15_20and145_150
- TD TS Hu1 Hu2 Hu3 Hu4 Hu5
- number 49.0 62.0 27.0 14.0 15.0 13.0 7.0

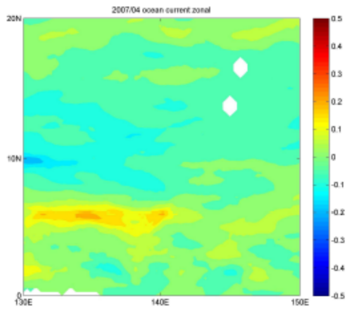

Saffir-Simpson Scale

- TD-----< 34 (海浬knots)
- **Tropical Storm**TS-----34-63
- **Hurricane**1------64-82
- **Hurricane**2------83-95
- **Hurricane**3------96-112
- **Hurricane**4------113-134
- **Hurricane**5------>134
- **(1 knot = 1.15mph = 1.852 km/h)**
- （美國一級颶風等於我們中度颱風）

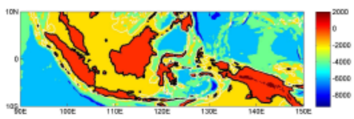

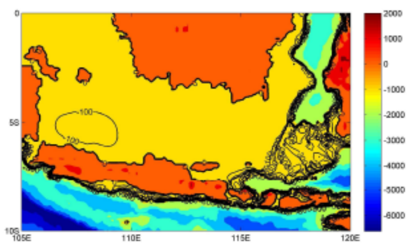

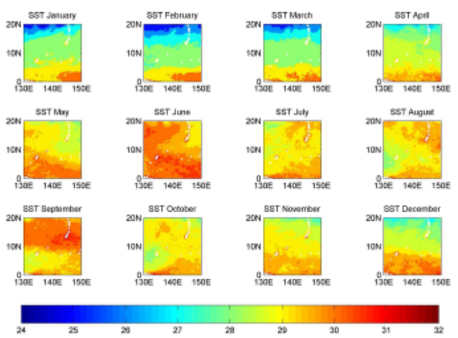

Conclusion

- The key technologies can be studied and assessed separately.
- Once all technologies are accomplished, a small scale pilot plant, say 5 MW, may be built.
- An international cooperation is encouraged. Due to the favorable marine environment, Indonesian may be the best site to test the pilot plant.

The Energy from Taiwan Current

Cho-Teng Liu
Institute of Oceanography
National Taiwan University

The Energy From Taiwan Current

Cho-Teng Liu
Institute of Oceanography
National Taiwan University
ctliu@ntu.edu.tw

- Potential power generation (PPG)
  = (available ocean energy)
  *(extractable fraction)
  *(power generation efficiency)
- Profits = PPG * (Benefits/kW - cost/kW)
  benefits = selling price, enhanced fishing, …
  cost in the sense of dollar value, environmental impact, …

Comparison of ocean energy

Ocean energy	Total amount	Amount at a point	availability	technology
Ocean wave	medium	low	coastal	Low
OTEC	high	high	open ocean	High
Tidal height	small	high	Bay, estuary	Low
Ocean current	Medium	High	Along current	medium
Salinity				

Why it is not commercialized yet? No guaranteed profits!

- **Technological barrier**
  (scale of the system is beyond any existing ocean engineering system)
- **Uncertainty on the investment**
  (no experience on system of similar principle, nor scale)
- **Initial investment is too large**
  (US$9B for a commercial OTEC)

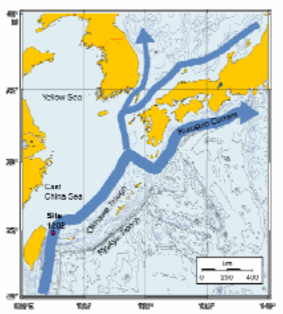

Taiwan Current and Kuroshio

What can we do now?

- Collect and analyze data to find the best site for testing
- Develop prototype systems
- Integration of international efforts

Efforts made in Chinese Taipei

- Find potential sites
- Survey the available KE for power generation
- Collect available technology: designs and field tests
- Long term plan

Find a place that has high current speed and is close to Taiwan, and shallow.

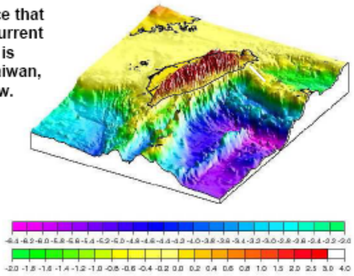

3-D bathymetry (NTUIO)

Power transport in a current

- Power transported by ocean current (J/s/m/m)：
- P = 0.5 ∫ ρv^3 dz dx
- ρ is water density, about 1024 kg/m^3
- v is current speed, m/s
- dz dx is a small cross section of current

- Finding location of high speed current is the most important task

One section of current speed NE of Taiwan

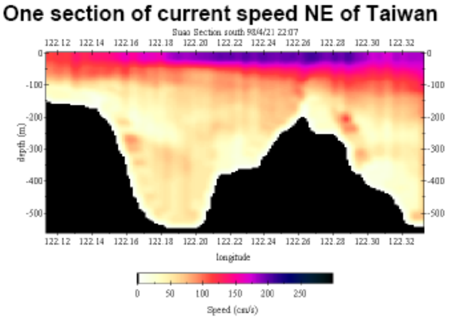

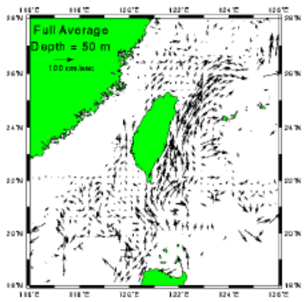

Mean Current Speed at 50 m depth (from NTUIO)

One section of power flux NE of Taiwan

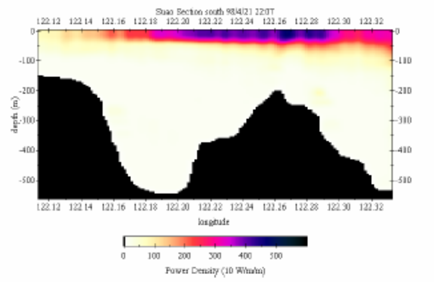

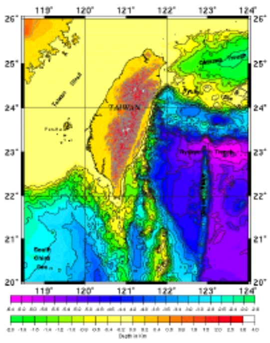

Power generating system is simpler at shallower depth, and closer to shore

Bathymetry (from NTU)

Total power from 1-section across the Taiwan Current

- 1.35 GW off Suao (at NE of Taiwan Island)
- It is a conservative estimate because most of the ocean current energy is contained in the form of potential energy; once the K.E. is extracted from Taiwan Current, some PE will be converted to K.E.
- Total available PE for the subtropical North Pacific is 40 peta Joule

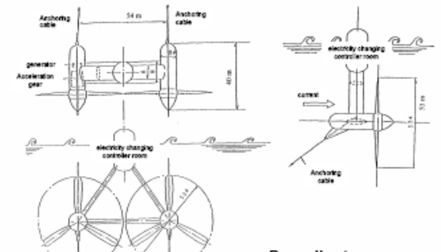

Propeller type
similar to wind power turbine

Helical Turbine (stable rotation and power generation)

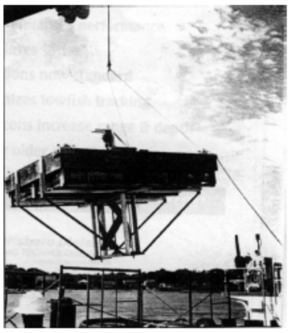

Axial turbine proposed in the Coriolis Project

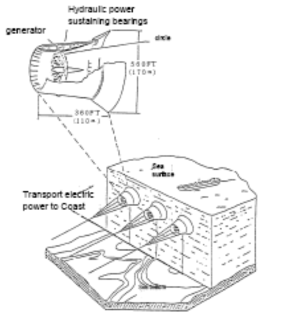

Tidal Current Energy

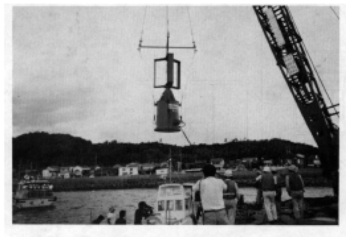

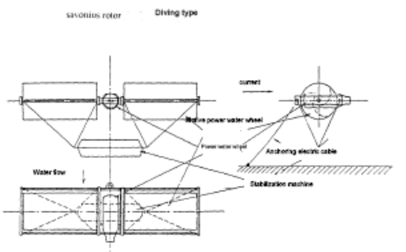

Underwater Savonius Wheeler type

What happened to the earlier studies

- in **Japan**:
  the result is discouraging
  – too little power was generated by tidal current with axial turbine
  => no participation by oceanographers, nor ocean engineers
  => the design may be wrong
- in **USA**:
  huge turbine was built to extract KE from Gulf Stream.
  no report on the result of the field study
  => it is likely that there was loss of equipment
  => real ocean current is really powerful,
  safety measures should be scaled up with the system
- in other places:
  no known field experiment of a large system was successful

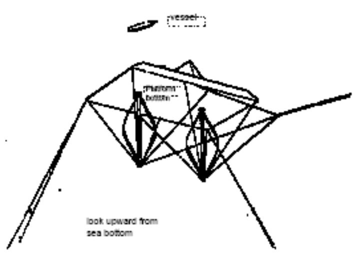

Darrieus turbine and platform

Coupling 3-D Models of Ocean Physics and Biogeochemistry to Fish Population Dynamics Models to Monitor Marine Living Resources in a Context of Global Change

Patrick Lehodey, Inna Senina and Philippe Gaspar

Satellite Oceanography Division Marine Ecosystem Modelling and Monitoring by Satellites

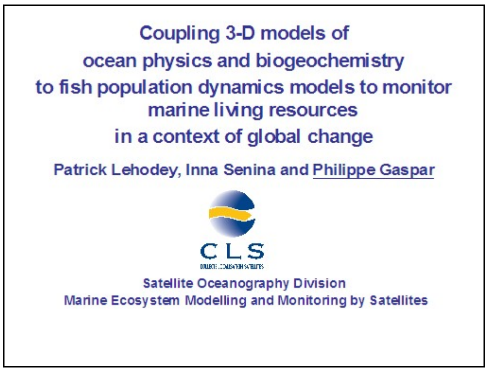

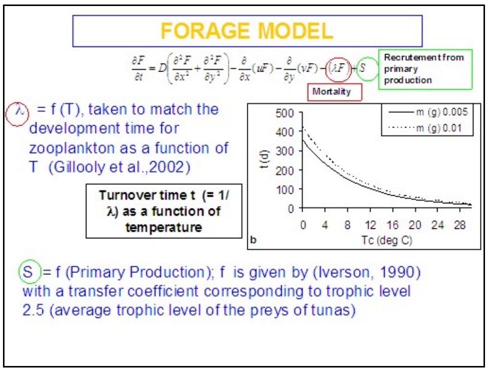

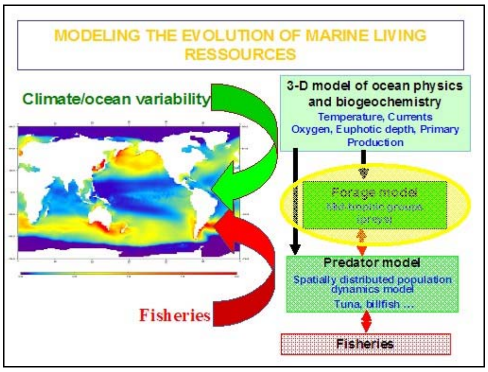

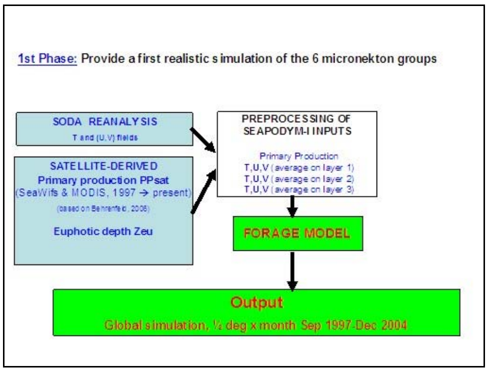

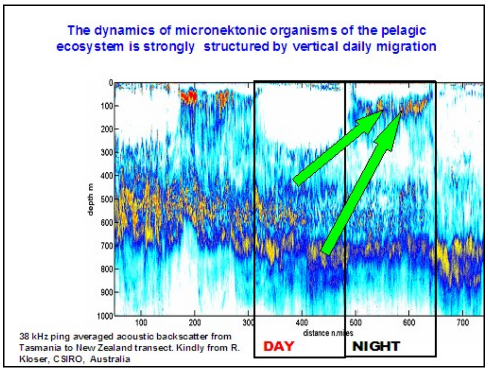

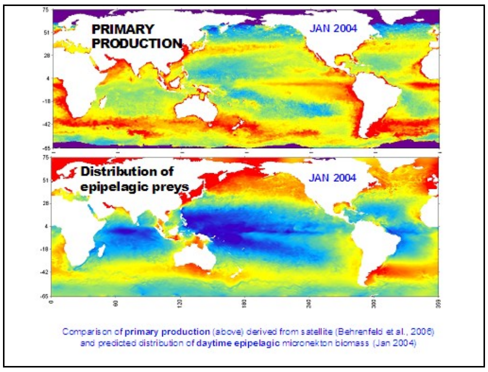

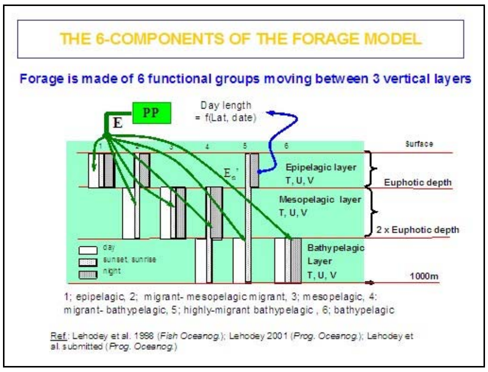

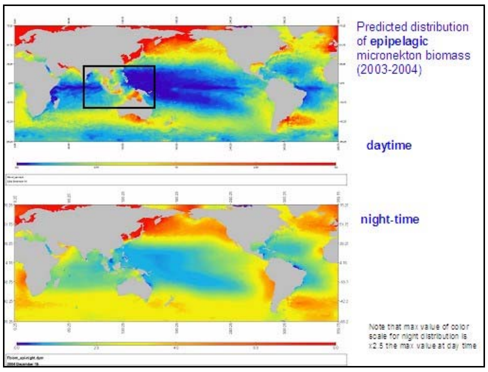

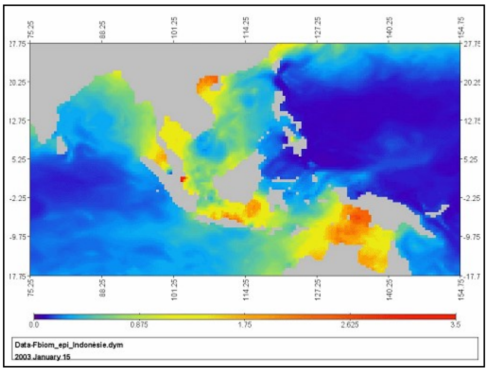
Data-Fbiom_epi_Indonesie.dym
2003 January 15

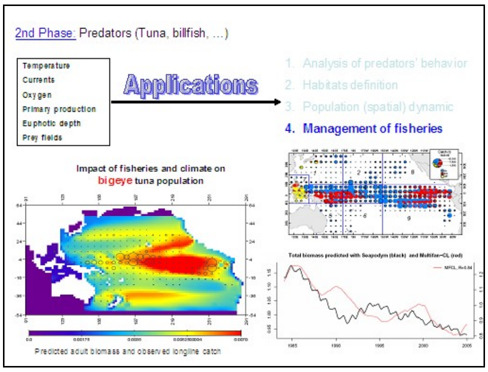
2nd Phase: Predators (Tuna, billfish, …)
Temperature
Currents
Oxygen
Primary production
Euphotic depth
Prey fields
Applications
1. Analysis of predators' behavior
2. Habitats definition
3. Population (spatial) dynamic
4. Management of fisheries
Impact of fisheries and climate on bigeye tuna population
Predicted adult biomass and observed longline catch

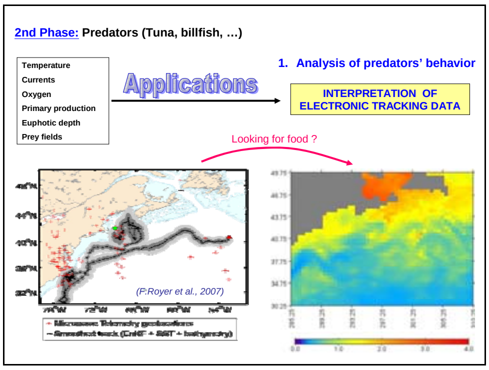
2nd Phase: Predators (Tuna, billfish, …)
Temperature
Currents
Oxygen
Primary production
Euphotic depth
Prey fields
Applications
1. Analysis of predators' behavior
INTERPRETATION OF ELECTRONIC TRACKING DATA
Looking for food ?
(P.Royer et al., 2007)

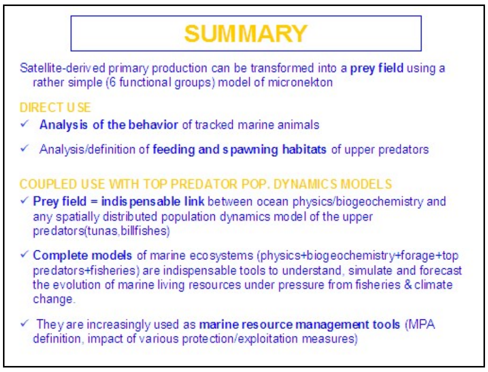
SUMMARY
Satellite-derived primary production can be transformed into a prey field using a rather simple (6 functional groups) model of micronekton
DIRECT USE
✓ Analysis of the behavior of tracked marine animals
✓ Analysis/definition of feeding and spawning habitats of upper predators
COUPLED USE WITH TOP PREDATOR POP. DYNAMICS MODELS
✓ Prey field = indispensable link between ocean physics/biogeochemistry and any spatially distributed population dynamics model of the upper predators(tunas,billfishes)
✓ Complete models of marine ecosystems (physics+biogeochemistry+forage+top predators+fisheries) are indispensable tools to understand, simulate and forecast the evolution of marine living resources under pressure from fisheries & climate change.
✓ They are increasingly used as marine resource management tools (MPA definition, impact of various protection/exploitation measures)

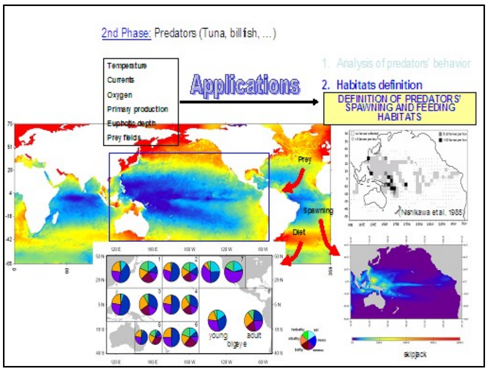
2nd Phase: Predators (Tuna, billfish, …)
Temperature
Currents
Oxygen
Primary production
Euphotic depth
Prey fields
Applications
1. Analysis of predators' behavior
2. Habitats definition
DEFINITION OF PREDATORS' SPAWNING AND FEEDING HABITATS
Prey
Spawning
Diet
Nishikawa et al., 1985
young
adult
bigeye
skipjack

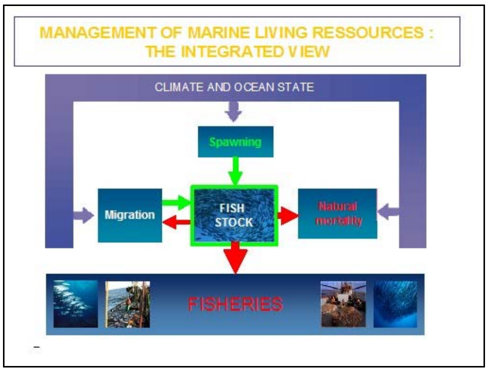
MANAGEMENT OF MARINE LIVING RESSOURCES : THE INTEGRATED VIEW
CLIMATE AND OCEAN STATE
Spawning
Migration
FISH STOCK
Natural mortality
FISHERIES

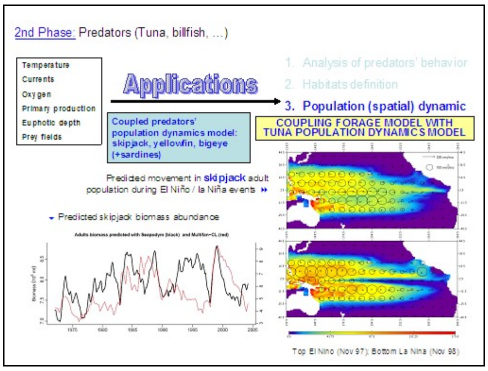
2nd Phase: Predators (Tuna, billfish, …)
Temperature
Currents
Oxygen
Primary production
Euphotic depth
Prey fields
Applications
1. Analysis of predators' behavior
2. Habitats definition
3. Population (spatial) dynamic
Coupled predators' population dynamics model: skipjack, yellowfin, bigeye (+sardines)
COUPLING FORAGE MODEL WITH TUNA POPULATION DYNAMICS MODEL
Predicted movement in skipjack adult population during El Niño / la Niña events
Predicted skipjack biomass abundance
Top El Nino (Nov 97); Bottom La Nina (Nov 98)

Application of Knowledge-Based Expert System Model for Fishing Ground Prediction in The Tropical Area

1 Muhamad Sadly, Nani Hendiarti 1, Suhendar I Sachoemar 2, Nurjannah Nurdin3, Yoke Faisal 1, Awaluddin 1

1 Center of Technology for Natural Resources Inventory (P-TISDA),
2 Center of Technology for Agro-industry,
3 Dept. of Marine, Hasanuddin University, Makassar
Agency for the Assessment and Application of Technology (BPPT)
BPPT Bldg. II, 19th Fl., Jl. M.H.Thamrin No. 8, Jakarta 10340

ABSTRACT

A geographical information system (GIS) may be viewed as a database system in which most of the data is spatially indexed, and upon which a set of procedures operate in order to answer queries about spatial entities represented in the database. Geo-study deals with answering "What", "Where", and "Why" questions. Despite the fact that GIS is a powerful tool dealing the first two questions, GIS is inferior for answering the "Why" question in geo-study (Zhang and Giardino, 1992). One of the possibility way to overcome the inferiority of GIS for answering the "Why" question of Geo-Studies is by integrating expert system in a GIS to form a Knowledge-Based Expert System GIS Model. In this study, we present the result of the application Knowledge-Based Expert System GIS Model on the prediction of the fishing ground for pelagic fish in the coastal area of Tomini Bay (Central Sulawesi) and South Sulawesi. As input data, we used and applied a series satellite data of sea surface temperature (SST), sea surface chlorophyll-*a* (SSC) and turbidity derived from Aqua MODIS in period of 2003-2005 to understand the temporal and seasonal variability of the marine environment of the study area, and identified the oceanographic phenomena, i.e. upwelling, front or eddy. To generate spatial configuration of fishing ground prediction map, we developed and integrated the result of Knowledge-Based Expert System into GIS model by using ERDAS Macro Language (EML) of ERDAS Imagine 9.0 software. To verify this result, a series of the in-situ fishing ground spots data of the study area were collected for the similar periods and location, and they were then analyzed by using a simple statistical method. The result shows that fishing ground prediction derived from Knowledge-Based Expert System GIS Model has a high accuracy level with a range of 80-90 % against the in-situ data. This result has demonstrated that the Knowledge-Based Expert System GIS Model can be applied to predict, localize and determine fishing ground spot areas in which their accuracy level will be determined by the completeness of spatial knowledge of the domain expertise and the sophistication level of the programming utilities being used.

Keywords: Remote sensing, Knowledge-based, Expert Systems, GIS, Fishing Ground

1. INTRODUCTION

It is simplest form, a geographical information system (GIS) may be viewed as a database system in which most of the data is spatially indexed, and upon which a set of procedures operate in order to answer queries about spatial entities represented in the database. Geo-study deals with answering "What", "Where", and "Why" questions. Despite the fact that GIS is a powerful tool dealing the firs two questions, GIS is inferior for answering the "Why" question in geo-study.

Expert systems, or knowledge-based systems, are branch of artificial intelligence (AI). AI is the capability of a device such as a computer to perform tasks that would be considered intelligent if they were performed by a human. An expert system is a computer program that attempts to replicate the reasoning processes of experts and can make decisions and recommendations, or perform tasks, based on user input. Knowledge Engineers (KE) construct expert systems in cooperation with problem domain experts so that the expert's knowledge is available at all times and in many places, as necessary [1,2,3,4].

On the basis of previous research concerning the design and implementation of GIS, one may infer several requirements that a GIS should satisfy, as well as several principles of design and implementation that permit the satisfaction of such requirements.

In this essay, we examine both the requirements and the associated principles, first in general terms and then in terms of a knowledge-based GIS that has been recently implemented. One possible way to use GIS for dealing with reasoning based on knowledge is by incorporating an expert system concept in a GIS.

In this study, we develop an expert system integrating with GIS for probable fishing grounds predictive model of economic pelagic fish in Tomini Bay, Central-Sulawesi using remote sensing data. The oceanographical data of Sea Surface Temperature (SST), Sea Surface Chlorophyll-a (SSC) and Turbidity in relation to the oceanographical phenomena i.e. upwelling, front and Eddy were used as input parameters of the system to generate fishing ground prediction map. These input data were than taking account into the input environmental data of the relationships established, and transforming the knowledge bases of spatial configuration in the form of IF..THEN type of production rules into macro programs written in ERDAS Macro Language (EML) of ERDAS Imagine software [5].

There appear to have been relatively few expert systems constructed, or envisioned, for oceanographic and maritime purposes. The knowledge-based expert system described below screens near real time incoming sea surface temperature, chlorophyll and turbidity data. The use of the expert system allows researchers to develop the environmental model of fishing ground prediction for further understanding of the marine environment phenomenon as a knowledge base that can be easily reconfigured [6].

2. BASIC THEORY OF SATELLITE FISHERIES OCEANOGRAPHY

The optical properties in the marine surface layer are determined by the presence of dissolved and suspended matter. Under normal conditions, visible light penetrates marine waters to a depth of tens of metres. As the concentration of the water constituents increases, i.e. the water becomes more turbid, the penetration of sunlight is reduced as a result of absorption and scattering processes. Depending on the specific characteristics of the materials present in the water, i.e. on their spectral signature, the absorption and scattering processes will vary with the wavelength of the incident radiation [7]. Multispectral observations, therefore, can be employed to estimate the nature and concentration of the water constituents. Passive sensors working in the visible wavelengths are commonly used to image water colour. Active sensors providing their own source of illumination, can also be used but only from aircraft and for sampling, rather than for imaging purposes.

The sea covers two thirds of the earth's surface. To a large extent, man is dependent on it for food species which include fish, shellfish, marine mammals, turtles, aquatic plants and algae. To exploit these resources more effectively, fishermen must catch the most fish possible while, at the same time, minimizing costs and optimizing the scheduling of their operations. Reliable environmental information is required from the scientific community for these purposes. Remote observations of the sea surface can provide a significant part of the information needed to assess and improve the potential yield of the fishing grounds. The environmental parameters most commonly measured from airborne and spaceborne sensors are as follows: surface optical or bio-optical properties (diffuse attenuation coefficient, total suspended matter, yellow substance, chlorophyll pigments and macrophytes, commonly grouped under the general term of ocean colour); surface temperature; vertical and horizontal circulation features [8]. Several remote sensing techniques can provide information regarding surface circulation features of importance in defining marine fish habitats. These include the location and evolution of frontal boundaries, upwelling areas, currents and circulation patterns in general. Optical and thermal characteristics of surface waters can be used as natural tracers of dynamic patterns.

Variations in environmental conditions affect the recruitment, distribution, abundance and availability of fishery resources. It is not possible to measure remotely the entire range of information needed to assess changes in the marine environment. Knowledge of particular conditions and processes affecting fish populations, however, may often be deduced using measurements made by remote sensors, e.g., concentration of dissolved and suspended matter, variations in primary production levels, distribution of surface isotherms, location of frontal boundaries, regions of upwelling, currents and water circulation patterns. The parameters providing information on these environmental factors may allow a forecast of fish distribution or more generally the definition of marine fish habitats [9]. These are often easier to sense remotely than the presence of fish. Estimation of a fishery resource can be assisted by the measurement of parameters which affect its distribution and abundance. Much of the research dealing with environmental effects related to fisheries are concerned with the correlation of a single parameter with the spatial and temporal distribution of fish. It is most likely, however, that fish respond to the sum total of environmental factors. Thus, it becomes necessary to correlate a large number of parameters, obtained by remote sensing techniques, with fish distribution.

3. METHODOLOGY

3.1 Knowledge-Based Expert System-GIS Development

A Knowledge-based Expert Systems GIS is defined as an integrated GIS and Expert System that is specially designed to answer the three questions of a geo-study. A module that integrates these two components is employed (Figure 1).

The GIS component is composed of two main modules that facilitate answering the "What" and "Where" questions: GIS database and spatial analysis. The expert system component is composed of two main modules for facilitating answering the "Why" question: knowledge-base and inference engine.

The knowledge-base of an expert system is built based on the result of knowledge acquisition in the form of production rules. A production rule is composed of sets of heuristics. One of the typical characteristics of heuristics is the use of IF…THEN statements that represent knowledge or guidelines through which a system may be operated.

An inference engine is a knowledge processing tool of the expert system component. Its main task is to merge facts with rules to develop or to infer or to draw conclusions about new facts. If the rules of a knowledge base relate to a specific domain or expertise, those of the inference engine pertain to more general control and search strategy for deriving inferences based on screening, filtering, and pruning mechanism.

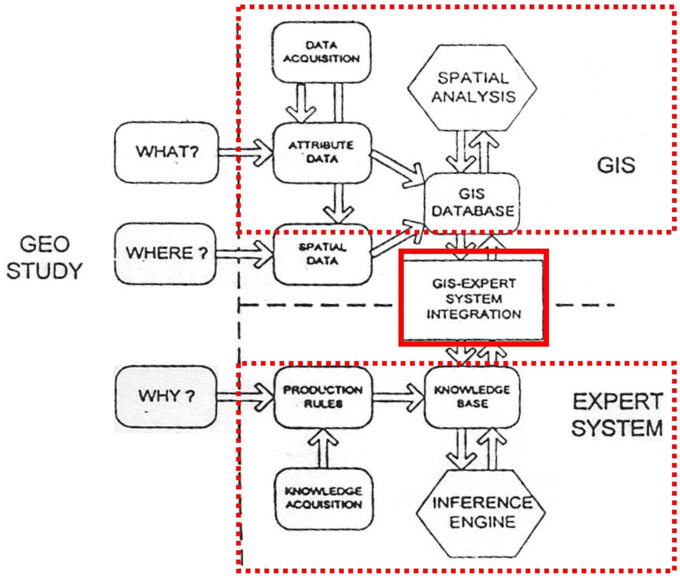

Figure 1: The elements of a knowledge-based GIS

The most important element of a knowledge-based GIS is an integration module that links the GIS spatial analysis and inference engine through GIS database and knowledge base. In this research, ERDAS Macro Language (EML) was used for the expert system processing.

3.2 Study Area and Data Acquisition

The study area was located in the coastal area of Tomini Bay, Central-Sulawesi and South Sulawesi (Figure 2). As input data, we used the Sea Surface Temperature (SST), Sea Surface Chlorophyll-a (SSC) and Turbidity data derived from MODIS satellite data of NASA. While to verify the result of Fishing Ground Prediction Model, we collect the in-situ data of fishing ground spots in both areas, and the simple statistical analysis was employed to understand the percentage of their accuracy.

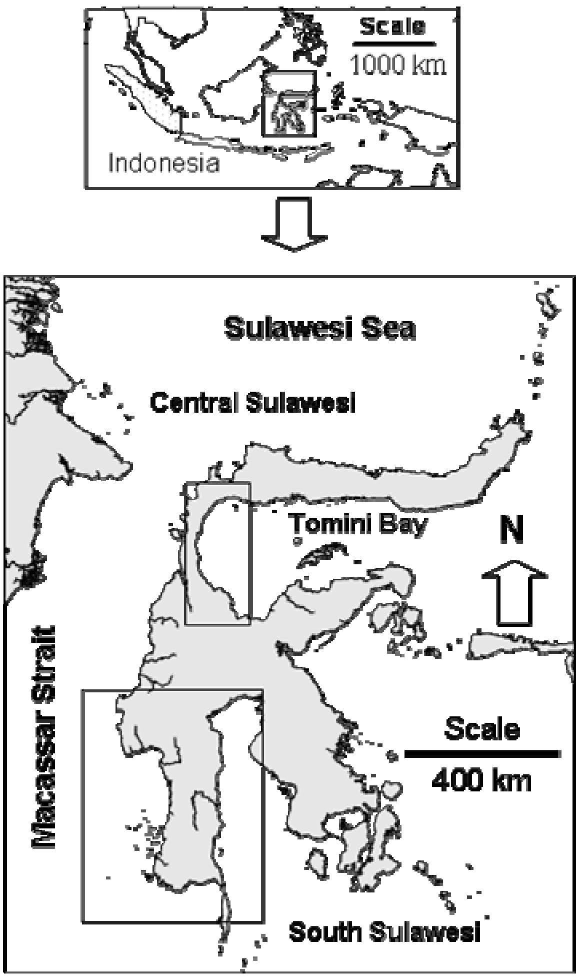

Figure 2: Study are in the coastal area of Tomini Bay (Central Sulawesi) and South Sulawesi.

3.3 Design of Knowledge-Based Expert System GIS (KBES-GIS) Fishing Ground

In this research, we used 3 (three) oceanographic parameters (SST, Chlorophyll-a, and Turbidity) as input data of the Knowledge-Based Expert System GIS Fishing Ground Model (KBES-GIS-FG) to define potential fishing ground. These parameters were then also processed to investigate and identify the oceanographic phenomena (upwelling, front, and eddy) in the study area that suspected has strong correlation with the potential fishing ground. In the application of the KBES-GIS-FG, we used the daily data of SST, Chl-a, and Turbidity images as input variables to generate the daily information of the potential fishing ground formation. The formulation process of the KBES-GIS-FG ontology is presented in Figure 3.

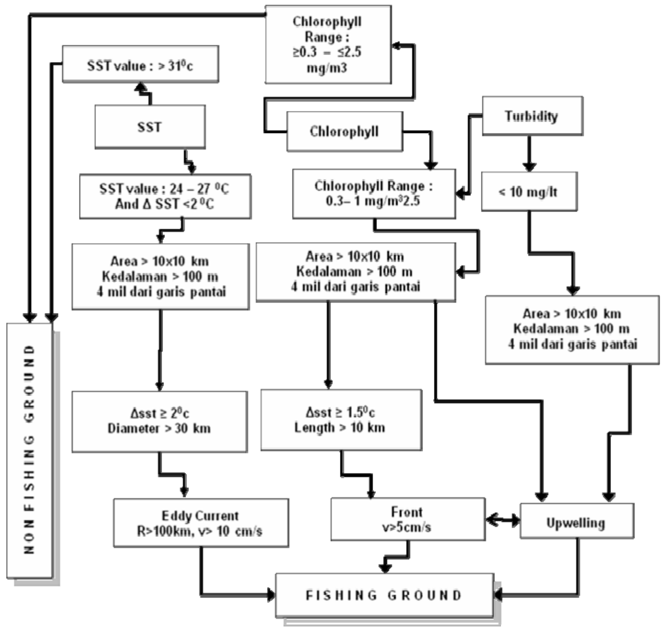

Figure 3: A representational structure of the Knowledge-Based Expert System GIS Fishing Ground Model (KBES-GIS- FG) ontology.

From the above processes, we formulated the rules to produce the fishing ground prediction modules as the expert system as described bellowed :

3.3.1 Sea Surface Temperature (SST)

- IF SST (range : 24^0c - 27^0c) with different 1.5^0c, AND diamaeter > 10km, AND located > 4 mill sea line with area 100 km^2 AND deep > 100m, THEN this location is front.
- IF front have V (speed value) = 5 cm/s, THEN this location is Fishing Ground.
- IF SST (24^0c - 27^0c) with different 2^0c, AND diameter > 30km, and located > 4 mill sea line with area 100 km^2, deep > 100m, AND different 5^0c AND length > 10km,
  THEN this location is Eddy Current.
- IF area with UPWELLING criterion,
  THEN predicted area as the Potensial Fishing
  Ground.

3.3.2 Chlorophyll

- IF Chl-a concentration in the range of 0.3 to 2.5 mg/m3, AND that area is located more than 4 mill sea line, AND deep more than 100m, AND acreage is 100km^2 , THEN Upwelling area.

- IF area is called as Upwelling, THEN Fishing Ground area.
- IF Chl-a concentration < 0.3 AND more than 2.5 mg/m^3, THEN Non Fishing Ground

3.3.3 Turbidity

- IF turbidity value less than 10mg/lt, AND located in more than 4 mil sea line, AND deep more than 100m, AND have acreage more than 100 km^2, THEN Upwelling area.
- IF the area is UPWELLING, THEN the area is Fishing Ground.
- IF turbidity have the chlorophyll concentration between 0.3 to 2.5 mg/m^3 , AND located more than 4 mill sea sea line, AND deep more than 100m, AND have the coverage area more than 100 km^2 ,THEN Upwelling.
- IF area is Upwelling, THEN the area is Fishing Ground.

3.3.4 Predictive model for Fishing Ground (A proposed cyclical modeling approach)

The modeling concept used in this research is based on the cycling model approach (as illustrated in Figure 4). This model consists of three (3) stages, as described bellow :

(a). Observation stage: to define the characteristics of fish behavior, physical condition of ocean and use the pattern recognition method to cluster fishing ground and non fishing ground.

(b). Analysis and interpretation of data (SST, Chl-a, Turbidity images.

(c). Modeling and testing/verification: using a knowledge-based expert system GIS model for fishing ground prediction.

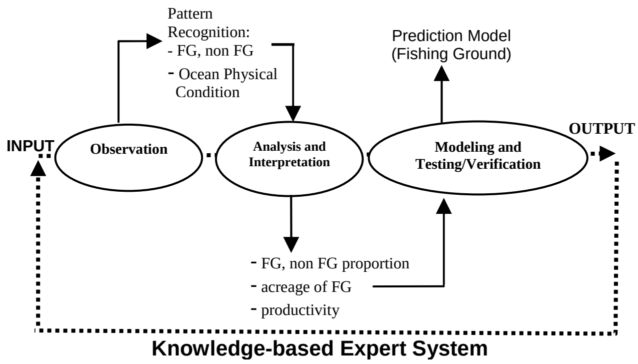

Figure.4. Prediction model of Fishing Ground. (A proposed cyclical modeling approach)

From this model, we will understand that the proven of the model performance will depend on the feedback data from the in-situ field observation and the knowledge base of the expert system in which further investigation can be carried out and adjusted to predict more accurately fishing ground events and the oceanographic phenomenon.

4. EXPERIMENTAL DESIGN

The experimental design in this research is conducted as follows:

(a). Preparation of the Knowledge-Based Expert System GIS Fishing Ground Model (KBES-GIS-FG) systems.

(b). Building the knowledge-base and parameter settings.

(c). Data preparation: Satellite data (SST, Chl-a, Turbidity), field observation data of fishing round.

(d). Pre-processing data.

(e). Run model and validate.

5. RESULTS AND DISCUSSION

The scenes result of the KBES-GIS-FG model in the coastal area of Tomini Bay (Central Sulawesi) and South Sulawesi and their statistical analysis were illustrated in Figure 5 and 6, respectively. Three (3) input data of SST, Chlorophyll-a, and Turbidity are used in the model to generate predicted potential fishing ground. The analysis processes were used the Knowledge-Base Engineer of ERDAS software.

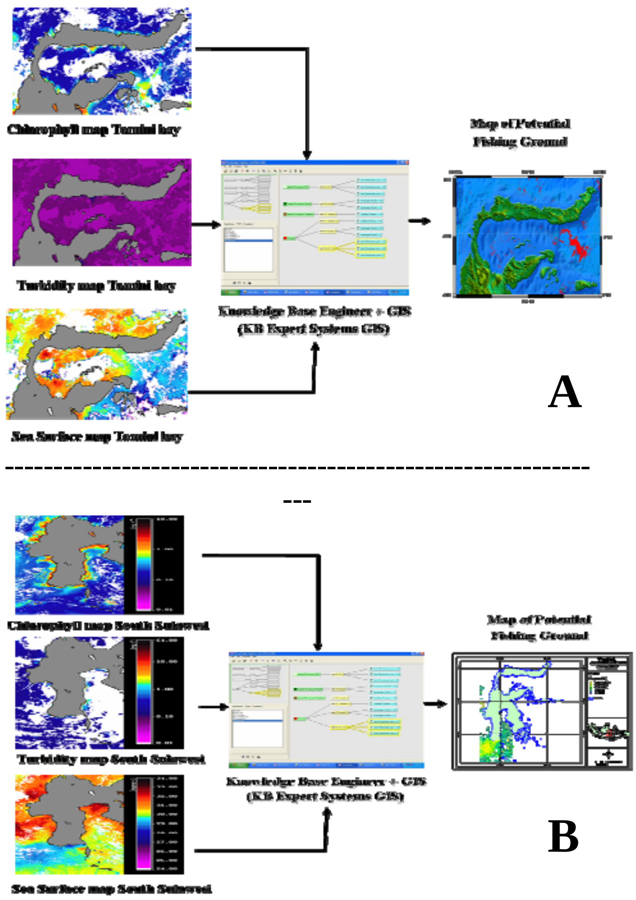

Figure.5. Fishing Ground Map produced by the KBES-GIS-FG Model in the coastal area of Tomini Bay, Central Sulawesi (A) and South Sulawesi (B)

The result in Figure 5 shows that the fishing ground map which produced from the model can be divided into two (2) categories. The first category is potential FG area that is marked by red color dots, and the second category is semi potential FG area marked by green color dots. While the black color dots is non FG area. The KBES-GIS-FG model was applied and run by considering the marine environmental information identified by three (3) parameters of daily SST, Chlorophyll-a, and Turbidity as input data. The daily and variability result of the model in generating predicted potential fishing ground area was strong depend on and governed by the level of cloud ness (cloud cover) as well as the meteorological situation. The result also shows that the potential fishing ground area was mostly concentrated in the near border (front) of the high and low concentration level of chlorophyll-a. This result indicated and well agreement with the most previous results that shows the potential fishing ground is well correspond with the area in the near border of the different water environment (front).

To understand the accuracy level of the result model, the simple statistical analysis was employed by comparing the daily result model and the daily field observation fishing ground data in the similar time of the data acquisition and observation. The result as shown in Figure 6, indicated that the average percentage of level accuracy of the model result in both areas of the coastal area of Tomini Bay, Central Sulawesi and South Sulawesi was relatively high with accuracy level of 86 %. While the daily result of the prediction model in the coastal area of Tomini Bay, Central Sulawesi and South Sulawesi is within a range of 68 % to 95 %. As mentioned above, the variability of the accuracy level of the model result in the prediction potential fishing ground seems to be strong corresponded with the cloud ness level (could cover) in which in the tropical area to be a problem. To eliminate and increase the accuracy level in the satellite data acquisition, the development of technical processes of the data satellite for the tropical area was recommended.

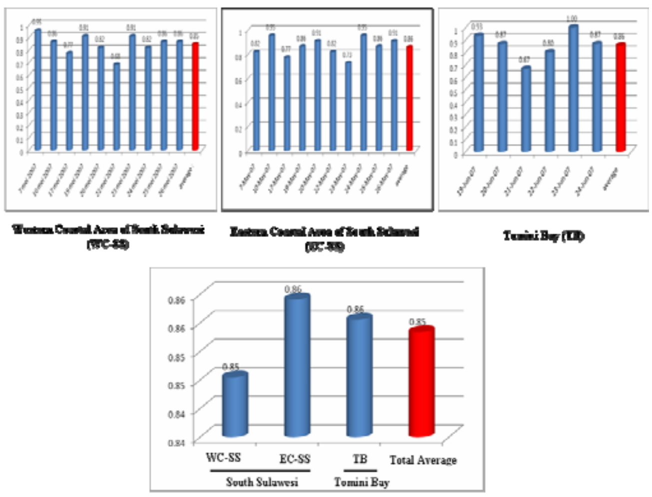

Figure 6. The statistical analysis result of the model and field data of fishing round.

6. CONCLUSIONS

In this paper, a knowledge-based expert system GIS model for prediction of fishing ground was introduced. We developed an expert system integrated with the GIS model for prediction of the potential fishing ground of the economic pelagic fish in the coastal area of Tomini Bay, Central-Sulawesi and South Sulawesi by using Sea Surface Temperature (SST), Sea Surface Chlorophyll a (SSC) and

Turbidity data derived from Modis satellite. The results demonstrated that the level of the success of implementing any knowledge based GIS model is determined by the completeness of spatial knowledge concerning the domain expertise and the sophistication level of the ERDAS macro programming. Moreover, it was found that the use of the expert system has allowed the development of fishing ground model to understand further of the ocean phenomenon in relation to the fishing ground characteristic. By using the knowledge base expert system, the prediction of fishing ground automatically would be more easy and accurate.

ACKNOWLEDGEMENT

We would like to acknowledge The Ministry of Research and Technology (KMNRT) Republic of Indonesia through the Incentive Research Program (Program Riset Insentif) for funded this research. Also we would like to thank to all members of the Center of Technology for Natural Resources Inventory (P-TISDA), BPPT for their support of the project.

REFERENCES

P. M. Atkinson and A. R. L. Tatnall, "Neural networks in remote sensing", Int. J. Remote Sensing, Vol. 18, No. 4, 1997.

Ignizio, J.P. "Introduction to Expert Systems: the development and implementation of rule-based expert system". NewYork: McGraw-Hill, Inc.

Poul Degnbol, "The Knowledge base for fisheries management in developing countries: alternative approaches and methods", Institute for Fisheries Management and Coastal Community Development, Bergen Norway Published, 2004.

James C. Hendee, "An Expert System for Marine Environmental Monitoring in the Florida Keys national Marine Sanctuary and Florida Bay", Proceedings of the Second International Conference on Environmental Coastal Regions, ed. C.A. Brebbia, Computational Mechanics ublications/WIT Press. Southampton, pp. 57-66, 1998.

Sadly, Muhamad, "Assessment and Applicfations of the *Knowledge-based Expert System* in Natural Resources Management", Technical Report P-TISDA, BPPT. 2005.

Hendiarti, N., Siegel, H., Ohde, T., 2004. Investigation of different coastal processes in Indonesian waters using SeaWiFS data, Deep Sea Research Part II 51 : 85-97. (2004)

Venegas, R., P.T. Strub, E. Beier, Letelier, T. Cowles, and A.C. Thomas, "Assessing satellite-derived variability in chlorophyll pigments, wind stress, sea surface height, and temperature in the northern California Current System", J. Geophys. Res. In Press, 2007.

Laurs, R.M. et al., "Albacore tuna catch distributions relative to environmental features observed from satellites", Deep-Sea Res., 31(9):1085–99, 1984.

Kemmerer, A.J., "Environmental preferences and behavior patterns of Gulf menhaden (Brevoortia patronus) inferred from fishing and remotely sensed data", ICLARM Conf.Proc., (5):345–70, 1980.

Vulnerability of Reef Resources to The Mariculture Industry: A Remote Sensing and Modeling Exercise

E.E. Salamante, C.L. Villanoy and L.T. David
Marine Science Institute University of the Philippines Diliman, Quezon City Philippines

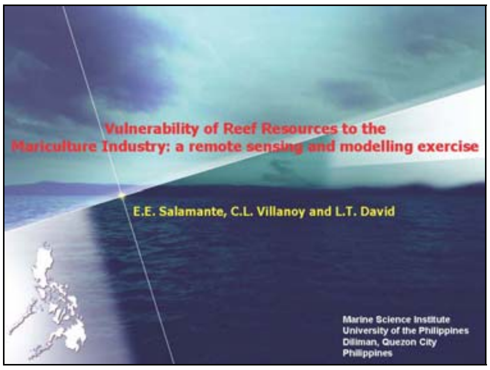

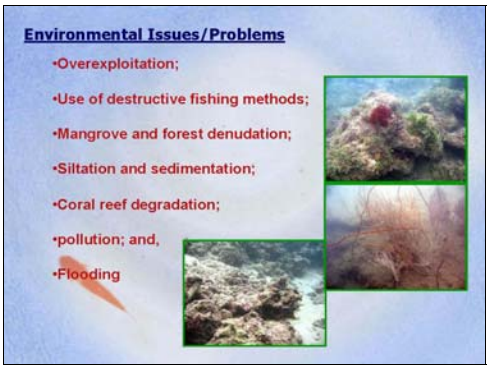

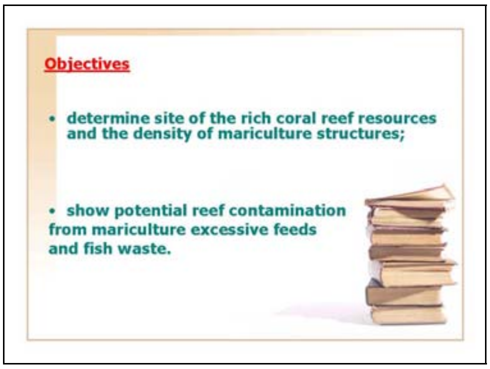

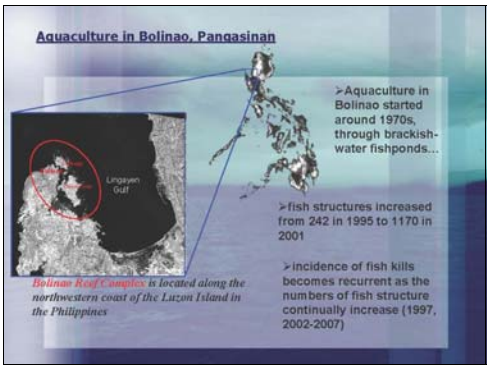

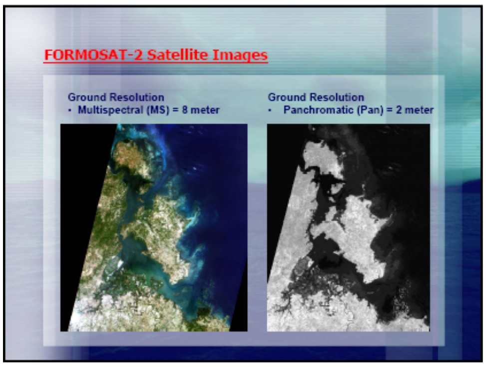

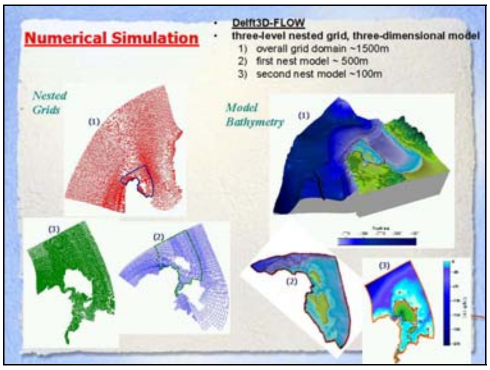

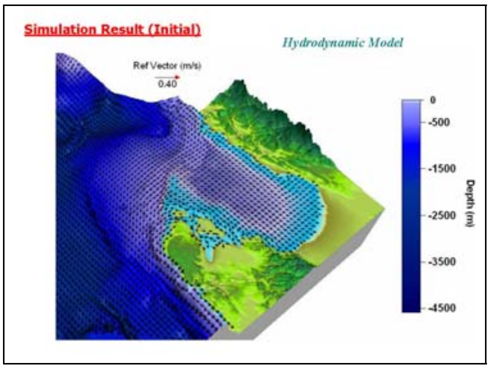
Simulation Result (Initial)
Hydrodynamic Model
Ref Vector (m/s)
0.40
0
-500
-1500
-2500
-3500
-4500
Depth (m)

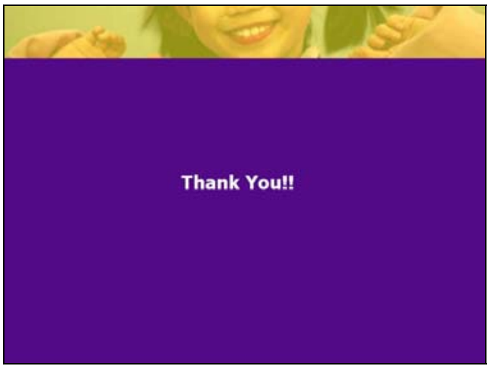
Thank You!!

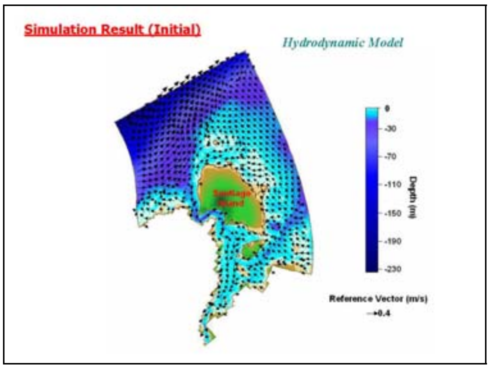
Simulation Result (Initial)
Hydrodynamic Model
0
-30
-70
-110
-150
-190
-230
Depth (m)
Reference Vector (m/s)
→0.4

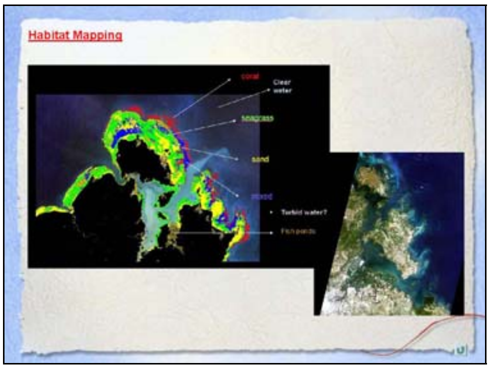
Habitat Mapping
coral
Clear water
seagrass
sand
mixed
Turbid water?
Fish ponds

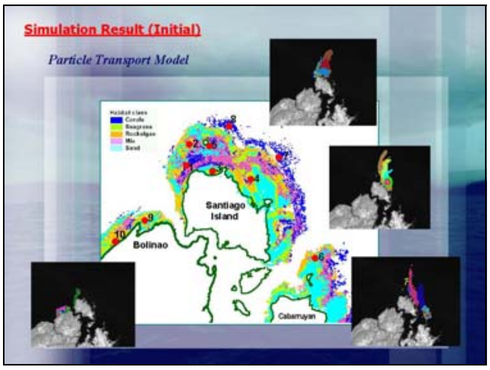
Simulation Result (Initial)
Particle Transport Model
Santiago Island
Bolinao
Cabarruyan

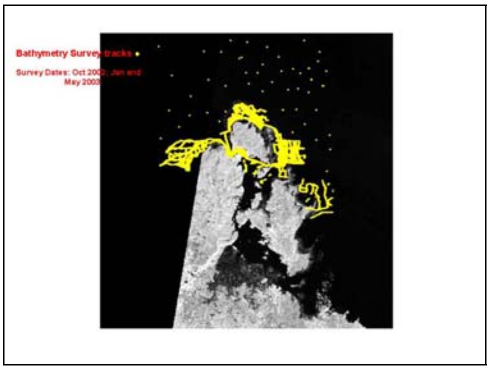
Bathymetry Survey tracks
May 2003

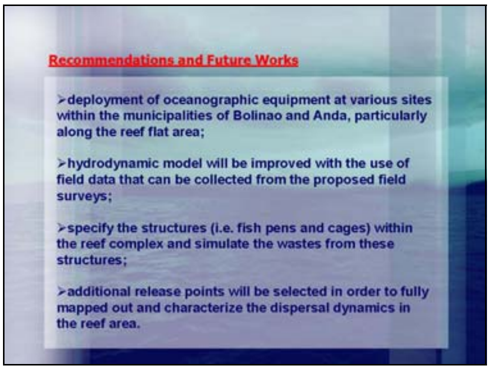
Recommendations and Future Works
➢deployment of oceanographic equipment at various sites within the municipalities of Bolinao and Anda, particularly along the reef flat area;
➢hydrodynamic model will be improved with the use of field data that can be collected from the proposed field surveys;
➢specify the structures (i.e. fish pens and cages) within the reef complex and simulate the wastes from these structures;
➢additional release points will be selected in order to fully mapped out and characterize the dispersal dynamics in the reef area.

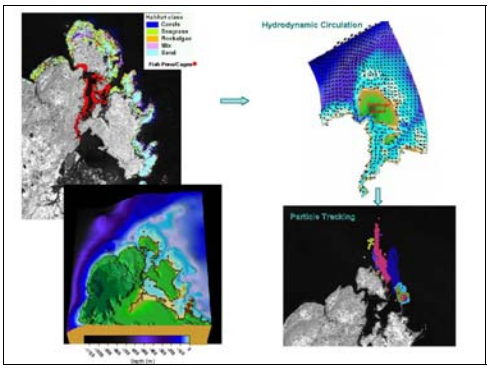
Hydrodynamic Circulation
Particle Tracking

Understanding The Abundance of Pelagic Fish in Bali Strait during Southeast Monsoon

Teja Arief & Dedy Aan Z
Institute of Marine Research and Observation (IMRO), Bali
Agency for Marine Research and Fisheries

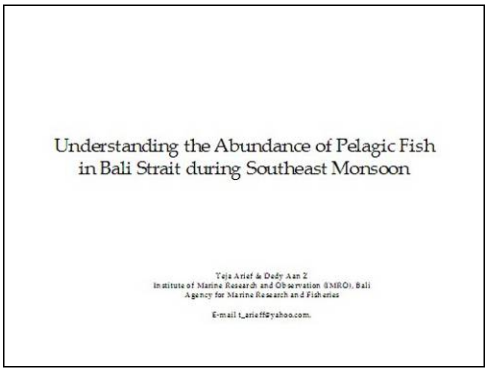

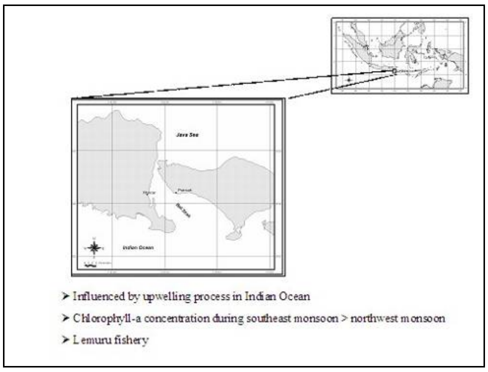

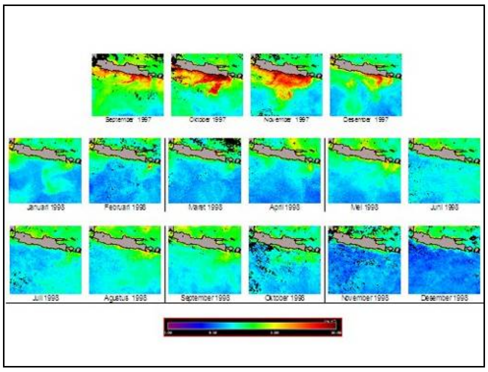

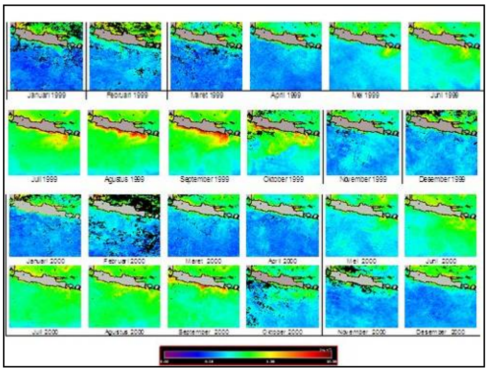

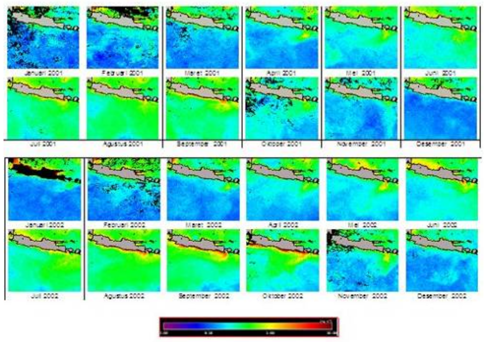

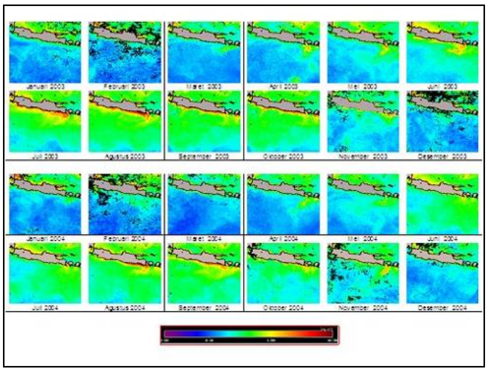

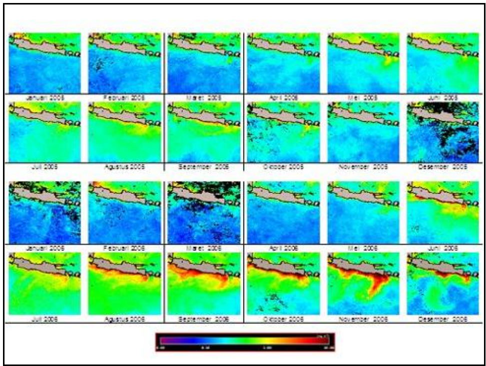

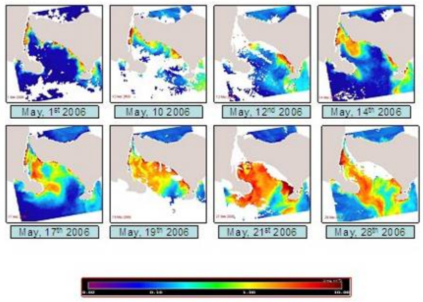

Fishermen of Bali Strait :

1. Most of them use purse seine as fishing gear
2. One day fishing methods with catch area of inner Bali strait
3. Two major group of purse seine fishermen : Muncar fishermen and Pengambengan fishermen. Muncar fishermen are largest fishermen group who operates in Bali Strait.
4. Catching activities usually being done at the good weather and at non full moon period

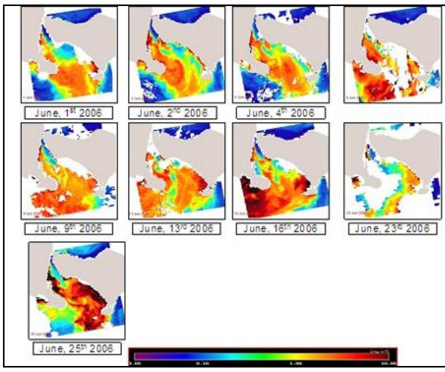

Pelagic fish commonly being captured in Bali Strait :

1. Lemuru (*Sardinella longiceps*)
2. Layang (*Decapterus* spp)
3. Tongkol (*Auxis* spp)
4. Slengseng (*Scomber australasicus*)
5. Banyar (*Ratreliger* spp)
6. Tembang (*Sardinella fimbriata*)

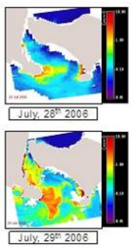

Data

1. Daily Chlorophyll-a concentration and sea surface temperature during southeast monsoon 2004-2006 derived from MODIS Aqua
2. Data processed by SeaDAS. Both dataset and software were obtained from Goddard Space Flight Center of the National Aeronautics and Space Aministration (NASA/GSFC)
3. The spatial resolution of data was 1000 m with the area coverage of 114.2 E to 115.3 E and 8.1 N to 9 N
4. The daily fishes catch along the southeast monsoon 2004 – 2006, documented in TPI Muncar, East Java, were being used as the comparison data..The data of the total fishes landed along the southeast monsoon 2004 – 2006 were not available in each day due to the bad weather and full moon period which the fishermen didn't do any catch activities.

Objective of the study

- To estimate the elapsed time from the availibility of chlorophyll-a concentration up to abundance of pelagic fish

This study acts as a preliminary step to obtain a better understanding of pelagic fishes abundance pattern in Bali Straits and also as a part of efforts to assist the fishermen on determining the pelagic fishes catch area with the aid from oceanographic satellite data.

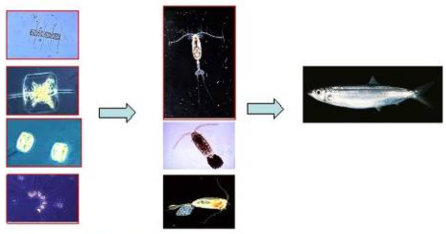

Simple Food Chain of Sardine (Csirke, 1977)

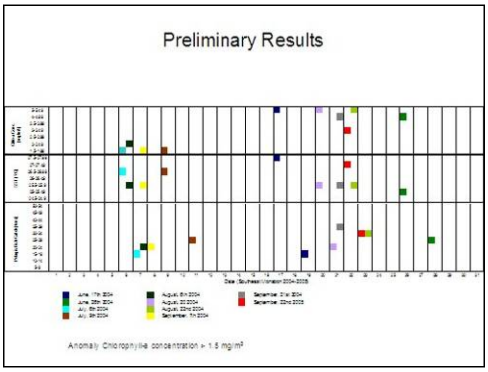
Preliminary Results
Anomaly Chlorophyll-a concentration > 1.5 mg/m³


Matur Suksma

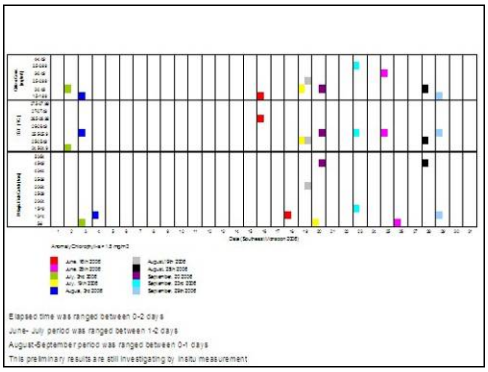
Elapsed time was ranged between 0-2 days
June- July period was ranged between 1-2 days
August-September period was ranged between 0-1 days
This preliminary results are still investigating by insitu measurement

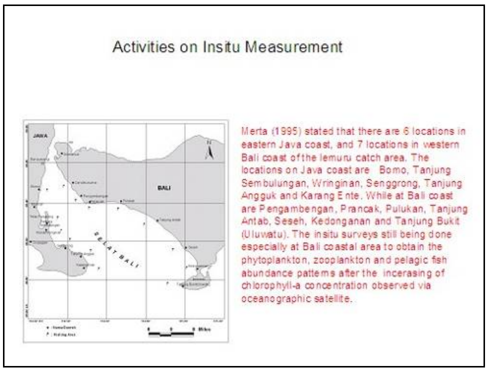
Activities on Insitu Measurement
JAVA
BALI
Merta (1995) stated that there are 6 locations in eastern Java coast, and 7 locations in western Bali coast of the lemuru catch area. The locations on Java coast are Bomo, Tanjung Sembulungan, Wringinan, Senggrong, Tanjung Angguk and Karang Ente. While at Bali coast are Pengambengan, Prancak, Pulukan, Tanjung Antab, Seseh, Kedonganan and Tanjung Bukit (Uluwatu). The insitu surveys still being done especially at Bali coastal area to obtain the phytoplankton, zooplankton and pelagic fish abundance patterns after the incerasing of chlorophyll-a concentration observed via oceanographic satellite.

Remote Sensing Application for Fisheries

Dr. Aryo Hanggono
Agency for Marine and Fishery Research, Ministry of Marine Affairs and Fisheries

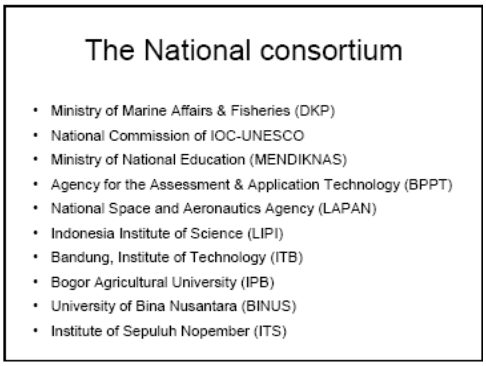

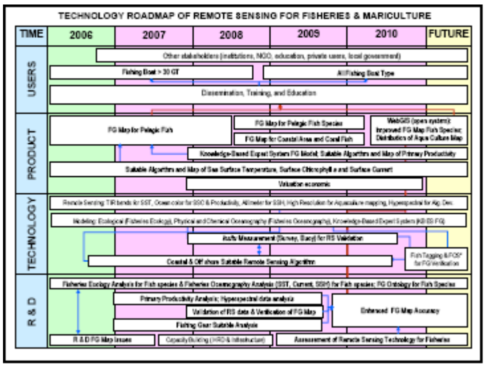

R & D PROGRAMS

- Fisheries Ecology Analysis for Fish species
- Fisheries Oceanography Analysis (SST, SSC, SSHA) for Fish Species
- Fishing Ground Ontology for Fish Species
- Primary productivity analysis
- Hyperspectral data analysis
- Validation of Remote Sensing Data
- Verification of Fishing Ground Map
- Fishing gear suitable analysis
- Assessment of remote sensing technology for fisheries
- Enhanced Fishing Ground Map Accuracy
- Capacity Building (HRD & Infrastructure)

TECHNOLOGICAL ASSESSMENT

- Coastal & off shore suitable remote sensing algorithm
- In-situ measurement (survey, buoy) for remote sensing data validation
- Modeling: fisheries ecology, fisheries oceanography (physical & chemical oceanography)
- Knowledge-based expert system
- Remote sensing data assessment: TIR bands for SST, ocean color for SSC & productivity, altimeter for SSH, high resolution for aquaculture mapping, hyper spectral for algorithm development
- Fish tagging and Fishery Observing System (FOS) for fishing ground validation

PRODUCTS

- Economic valuation
- Suitable algorithm and map of SST, SChl-a, SCC
- Knowledge-based expert system of fishing ground model
- Suitable algorithm and map of primary productivity
- Fishing ground map for pelagic fish species
- Fishing ground map for coastal area and coral fish
- Web GIS (open system)
- Improves fishing ground map of fish species
- Distribution of aquaculture map

USERS

- Dissemination, training and education
- Fisheries company
- Other stakeholders: research institutions, fishing port authority, NGO, education institutions, private users, local government


LAUT KITA
terima kasih

Appendix I : Agenda of APEC SAKE-2 Workshop

November 5, 2007 (R. Komisi Utama BPPT Lt. 3)

08:30	Registration	
09:00	**Opening session** 1. Report by Local Organizer (Director of PTISDA BPPT: Dr. Yusuf S. Djajadihardja) 2. Introduction on SAKE activities (Prof. Cho-Teng Liu) 3. Welcome Speech (Lead Shepherd APEC MRC WG: Prof. Dr. Indroyono Soesilo) 4. Opening Remark (Chairman of BPPT: Prof. Said D. Jenie) 5. Group Picture	
10:00	Coffee break	
10:30	**Session A: Monitoring of coastal ecosystem** (Chair: Prof. CC Kao)	
	1. Mapping of inland and underwater habitats with satellite images, VNU – Vietnam (Dr. Nguyen P. Khu)	A-1
	2. Reef Connectivity: a Study of Larval Dispersal in Sulu Sea, UP - Philippine (Prof. Cesar Villanoy)	A-2
	3. Mapping of coastal ecosystem condition and its water quality aroujind the Thousand Island of North Jakarta, BPPT - Indonesia (Mr. Yudi Wahyudi)	A-3
	4. A remote sensing investigation on seasonal variations of river discharges and their influences to marine environmental changes over Jakarta Bay, BPPT - Indonesia (Dr. Nani Hendiarti)	A-4
	5. Application of ocean color remote sensing for monitoring and mapping total suspended matter: a case study in the East China Sea, Nagoya University / BPPT – (Dr. Eko Siswanto)	A-5
	6. Using remote sensing to study the coastline change from typhoon and coastal erosion at Ban Laem Sing, Upper Gulf of Thailand, CU – Thailand, (Prof. Absornsuda Siripong)	A-6
12:30	Lunch	
13:30	**Session B: Hyperspectral mapping on natural resources** (Chair: Dr. M Sadly)	
	1. Coastal water monitoring and algorithm development for hyperspectrum sensor, TUIS –Japan (Prof. Ichio Asanuma)	B-1
	2. Development of mangrove spectral library, BPPT – Indonesia (Mr. Hartanto Sanjaya)	B-2

	3. Land Cover Classification of Fordata Island, BPPT - Indonesia (Ms. Marina Frederik)	B-3
	4. Observation of sea surface temperature and chlorophyl-a concentration along Southern Vietnam Sea using ocean color remote sensing, VNU – Vietnam (Dr. Nguyen Phi Khu)	B-4
14:40	**Session C: Mapping & mitigation of marine pollution** (Chair: Prof. A. Siripong)	
	1. A Multi-scale detection technique for anomaly on ocean surface using optical satellite images, NCU, Chinese Taipei (Prof. L.Y. Chang)	C-1
	2. Simulation of spilled oil in Seribu Islands waters, ITB - Indonesia (Prof. Safwan Hadi)	C-2
15:20	Coffee Break	
15:40	**Session D: Field verification on coastal ecosystem mapping** (Chair: Prof. C. Villanoy)	
	1. Optical Properties of Inorganic Suspended Solids and their Influence on In-water Algorithm of Ocean Color Remote Sensing in Coastal Turbid Waters, Chulalongkorn Univ. – Thailand (Prof. Absornsuda Siripong)	D-1
	2. Identification of groundtruthing needs for the extended use of satellite imagery in nearshore habitat mapping – Indonesia (Dr. Karen von Juterzenka)	D-2
	3. Assesment of Formosat satellite imagery for coastal ecosystem mapping in West Banten, Indonesia, BRKP – Indonesia (Mr. Syamsul B. Agus)	D-3
	4. Integration of satellite application and computational tool for marine conservation area design, BROK – BRKP (Mr. Elvan Ampou)	D-4

November 6, 2007 (R. Komisi Utama BPPT Lt. 3)

09:00	**Session E: Operational oceanography** (Chair: Prof. Safwan Hadi)	Page
	1. Satellite monitoring of fishing vessels as a tool to localize and estimate the fishing activity, CLS – France (Dr. Philippe Gaspar)	E-1
	2. Operational Oceanography for the Eastern Indian Ocean, BPPT – Indonesia (Dr. Fadli Syamsudin)	E-2
	3. Data Buoy for the Operational Oceanographic Observation (Prof. Chia Chuen Kao)	
	4. Sea surface temperature changes in Indonesian seas correlation with El Nino, La Nina and Indonesian through flow phenomenon, BRKP – Indonesia (Mr. B. Realino)	E-3
	5. Typhoon swell freak wave hindcasting, NTU (Dr. Nai Kuang Liang)	E-4
	6. Monitoring of Marine Resources in Indonesia's Small Outer Islands (Case: Manterawu Island, North Sulawesi), BROK – Indonesia (Mr. Dendy Mahabror)	E-5
10:45	Coffee break	
11:05	**Session F: Marine energy assessment** (Chair: Mr. Berny A. Subki)	
	1. Renewable ocean energy for the APEC region, NTU (Prof. Nai Kuang Liang)	F-1
	2. The energy of Taiwan Current, NTU (Prof. Cho-Teng Liu)	F-2
11:50	Lunch	
12:50	**Session G: Fishery and mariculture** (Chair: Mrs. Frida S.)	
	1. Coupling 3-D models of ocean physics and biogeochemistry to fish population dynamics to monitor marine living resources in a context of global change, CLS – France (Dr. Philippe Gaspar)	G-1
	2. Application of Knowledge-Based Expert System Model for Fishing Ground Prediction in the Tropical Area, BPPT – Indonesia (Dr. Muhamad Sadly)	G-2
	3. Vulnerability of reef resources to the mariculture industry: a remote sensing and modeling exercise, UP – Philippines (Dr. Salamante)	G-3
	4. Understanding the abundance of pelagic fish in Bali Strait during southeast monsoon, BROK – Indonesia (Mr. Teja Arief)	G-4
14:20	**Panel discussion of technology roadmap on remote sensing application in Indonesia** (Chair: Dr. Aryo Hanggono) 1. Presentation of Roadmap for Marine and Fishery application (BRKP) 2. Panel Discussion	
15:00	Coffee Break	

15:20	**Panel discussion on SAKE project report** and announcement of next SAKE meeting (Chair: Prof. Cho-Teng Liu)
16:00	**Summary and closing remarks** Dr. Aryo Hanggono, Director of Research Center for Marine Technology BRKP

Nov. 7-8, Technical Tour:

Field verification of satellite images near Tanjung Lesung, Banten (about 4-hour drive southwest of Jakarta)

Appendix II: Summary of Panel Discussion

Panel members: Dr. Aryo Hanggono, Dr. Nani Hendiarti, Prof. Cesar Villanoy and Prof. Cho-Teng Liu

Summary:

We are grateful to BPPT and BRKP in organizing this SAKE-2 workshop successfully. This is the major activity of SAKE 2007 project. The number of participating scientists, number of countries that these scientists came from, the number of presented papers, and the depth of research results are all unprecedented in SAKE and all OMISAR projects.

SAKE 2008 proposal has been approved by APEC MRCWG, and by APEC Budget Allocation Committee. About 8 proposals submitted to MRCWG in April, only two proposals were funded by APEC, and SAKE 2008 is one of them.

The Steering Committee of SAKE 2008 project will work closely with participating scientists to acquire more Formosat-2 images to meet their needs of research. The next meeting of Steering Committee will be hosted by Dr. Khu in Viet Nam

The next SAKE workshop is planned at Manado, Indonesia. Wish you all join us and present your study in the application of satellite images.

As shown in the welcome speech by Dr. Indroyono, corals are sensitive to global climatic changes. Nearly 50% of world corals were bleached in the last El Nino. Because it is a breeding ground of most marine species, and its biodiversity is the largest in all marine ecosystems, mapping coral communities in the global oceans and monitoring coral health are important to the conservation of marine resources. Working with Coral Triangle Initiative will be the first goal of the new proposal that is a follow-up of SAKE 2008 project. The new proposal to APEC Marine Resource Conservation Working Group will be drafted from now to February 2008.

The second goal of the new proposal will be the monitoring of oil spill in operational mode. This will assist the assessment of damages in near-real time fashion, the prediction of the movement of oil patches, and the allocation of the limited resources for mitigating disaster and for reducing damages to marine resources.

Proceedings of SAKE-2 Workshop
The Second APEC SAKE Workshop on "Satellite Application on Fishery and Coastal Ecosystem (SAFE)"
SAKE is APEC-sponsored project "Satellite Applications on Knowledge-based Economy"

Published for APEC Marine Resource Conservation Working Group
APEC Project No.: MRC 05/2007

Prepared by
Prof. Chia Chuen Kao
Coastal Ocean Monitoring Center (COMC)
National Cheng Kung University
Tainan, Chinese Taipei
Tel/Fax: +886-6-209-8850 / +886-209-8853
http:/sol.oc.ntu.edu.tw/sake/index.htm

Produced for
Asia-Pacific Economic Cooperation Secretariat
38 Heng Mul Keng Terrace Singapore 119616
Tel:(65)6891-9600; Fax:(65)6891-9690
e-mail:info@apec.org website:www.apec.org
©(2008) APEC Secretart
APEC#208-MR-04.2